NOTICE: This document contains information of a preliminary nature and is not intended for release. It is subject to revision or correction and therefore does not represent a final report.

S03120100-TRT10015
ORNL/TM-2026/4604

Oak Ridge National Laboratory Second Target Station Target and MRA Maintenance Dose Rates

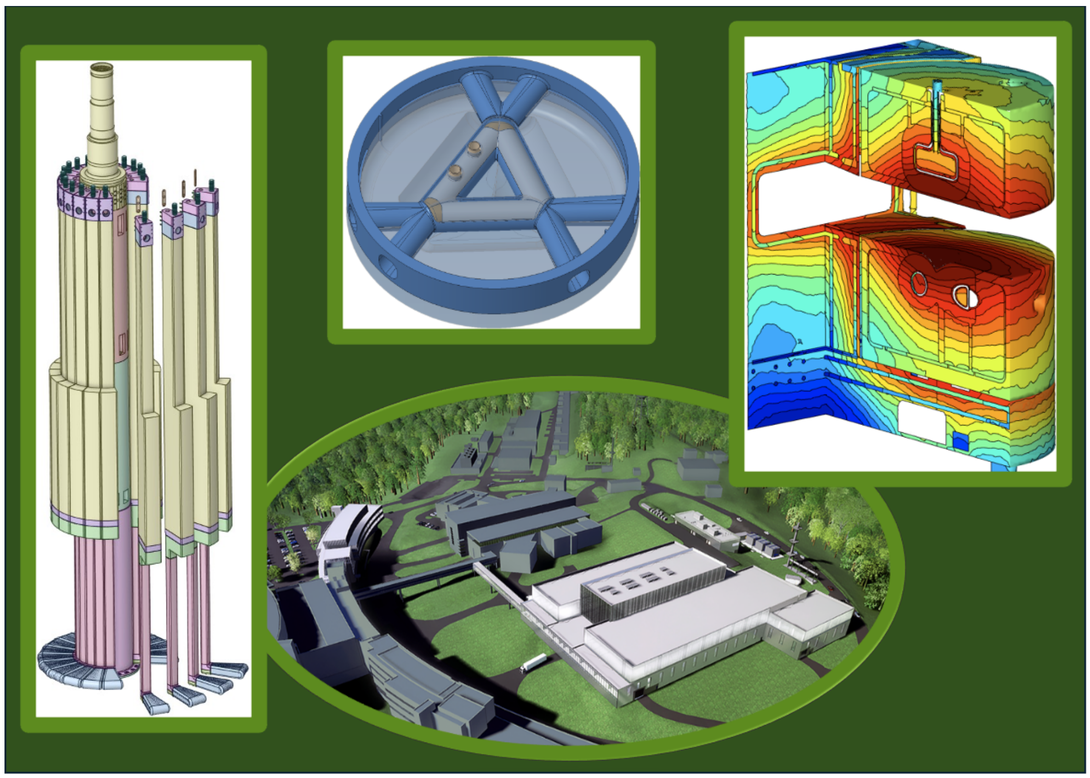

Tucker McClanahan, Ph.D.

August 2026

Draft. Document has not been reviewed and approved for public release.

Revision Date: 2026-07-14 14:17

OAK RIDGE National Laboratory

ORNL IS MANAGED BY UT-BATTELLE LLC FOR THE US DEPARTMENT OF ENERGY

Draft. Not approved for public release.

The only OFFICIAL COPY of this document is the on-line electronic version in ORNL's document management application. Before using a printed copy, verify that it is the most current version.

DOCUMENT AVAILABILITY

Online Access: US Department of Energy (DOE) reports produced after 1991 and a growing number of pre-1991 documents are available free via https://www.osti.gov/.

The public may also search the National Technical Information Service's National Technical Reports Library (NTRL) for reports not available in digital format.

DOE and DOE contractors should contact DOE's Office of Scientific and Technical Information (OSTI) for reports not currently available in digital format:

US Department of Energy
Office of Scientific and Technical Information
PO Box 62
Oak Ridge, TN 37831-0062
Telephone: (865) 576-8401
Fax: (865) 576-5728
Email: reports@osti.gov
Website: https://www.osti.gov/

This report was prepared as an account of work sponsored by an agency of the United States Government. Neither the United States Government nor any agency thereof, nor any of their employees, makes any warranty, express or implied, or assumes any legal liability or responsibility for the accuracy, completeness, or usefulness of any information, apparatus, product, or process disclosed, or represents that its use would not infringe privately owned rights. Reference herein to any specific commercial product, process, or service by trade name, trademark, manufacturer, or otherwise, does not necessarily constitute or imply its endorsement, recommendation, or favoring by the United States Government or any agency thereof. The views and opinions of authors expressed herein do not necessarily state or reflect those of the United States Government or any agency thereof.

S03120100-TRT10015
ORNL/TM-2026/4604

Second Target Station Project

Oak Ridge National Laboratory
Second Target Station Target and MRA Maintenance Dose Rates

Tucker McClanahan, Ph.D.

August 2026

Prepared by
OAK RIDGE NATIONAL LABORATORY
Oak Ridge, TN 37831
managed by
UT-Battelle LLC
for the
US DEPARTMENT OF ENERGY
under contract DE-AC05-00OR22725

Draft. Not approved for public release.
The only OFFICIAL COPY of this document is the on-line electronic version in ORNL's document management application. Before using a printed copy, verify that it is the most current version.

Approvals

Second Target Station Target and MRA Maintenance Dose Rates		ISSUE DATE: August 2026
PREPARED BY Tucker McClanahan, Ph.D.	PROJECT Second Target Station	DOCUMENT NUMBER: S03120100-TRT10015

	Signature/Date					
	Rev. 00	Date	Rev. 01	Date	Rev. 02	Date
STS Technical Director						
STS Target Systems Lead						
STS Neutronics Group Lead						
Lead Engineer						
Technical Reviewer						
Primary Author						

Revision	Description
00	Initial Release
01	Updated for Final Design

Draft. Not approved for public release.
The only OFFICIAL COPY of this document is the on-line electronic version in ORNL's document management application. Before using a printed copy, verify that it is the most current version.

CONTENTS

LIST OF FIGURES

Draft. Not approved for public release.
The only OFFICIAL COPY of this document is the on-line electronic version in ORNL's document management application.
Before using a printed copy, verify that it is the most current version.

LIST OF TABLES

ABBREVIATIONS

MRA	Moderator Reflector Assembly
ORNL	Oak Ridge National Laboratory
SNS	Spallation Neutron Source
STS	Second Target Station
TDR	Target Drive Room
TVP	Target Viewing Periscope

Draft. Not approved for public release.
The only OFFICIAL COPY of this document is the on-line electronic version in ORNL's document management application.
Before using a printed copy, verify that it is the most current version.

EXECUTIVE SUMMARY

This report presents a comprehensive analysis of radiation exposure for five distinct configurations of the Oak Ridge National Laboratory (ORNL) Spallation Neutron Source (SNS) Second Target Station (STS) target system during remote handling operations. The analyses focus on target segment and moderator reflector assembly (MRA) removal, evaluating dose rate fields at various stages of the process. The report assesses radiation dose rates for different maintenance scenarios, including the removal of target segments and MRA components, to inform the design of special equipment and planning of corresponding operations. The results aim to support the safe and efficient operation of the STS target system, while also providing a foundation for future evaluations of total dose to an individual worker during the maintenance events. Furthermore, this analysis demonstrates compliance with all applicable requirements listed in Section 2, and provides dose rate data to support the fulfillment of requirements that cannot be fully evaluated without maintenance timing sequences and worker location information.

Draft. Not approved for public release.
The only OFFICIAL COPY of this document is the on-line electronic version in ORNL's document management application.
Before using a printed copy, verify that it is the most current version.

1 SCOPE

This report presents an in-depth analysis of dose rate fields for five distinct configurations of the Oak Ridge National Laboratory (ORNL) Spallation Neutron Source (SNS) Second Target Station (STS) target system. The analyses are conducted at two time points: 8 hours after beam incidence (three configurations) and two weeks after beam incidence (two configurations). These simulations support the planning and engineering of remote handling operations for target segment and moderator reflector assembly (MRA) removal.

The five configurations examined in this report detail various stages of the removal process, allowing for the evaluation of radiation exposure during different phases of maintenance. The first configuration represents the as-operated condition, with all shielding in place, enabling verification of hands-on maintenance capabilities for target drive components and components within the target drive room (TDR). In contrast, the second configuration assumes the removal of the target segment core vessel shield block, a single target segment, and the deployment of the core vessel gamma gate shielding arm, while maintaining the core vessel gamma gate in a closed position.

The third, fourth, and fifth configurations are evaluated after two weeks of last beam-on-target and are designed to support MRA removal. The third configuration simulates the removal of a third target segment, taking into account that two adjacent segments have been already removed. In this scenario, the target is positioned for the removal of the third segment, the core vessel gamma gate remains closed, one gamma gate shielding arm is deployed, and the removable target segment core vessel shield block has been removed. However, one of the voids created by the removal of a target segment remains unmitigated.

The fourth configuration captures the scenario where the hydrogen and water transfer pipes stemming from the top of the MRA are about to be cut for their removal. This configuration includes the removal of the MRA removable shield block, both core vessel tent hatches, three target segments, and the deployment of all three gamma gate arms. The hatch in the target drive room ceiling is open to the high bay. To assess which scenario minimizes dose to pipe-cutting workers, two sub-configurations are evaluated: one with the hole caused by the removal of three target segments located on the downstream end of the target and another with the hole on the upstream end.

The fifth configuration details the dose rate field when the MRA is fully removed and the hole where the MRA was located is empty. This configuration is similar to the fourth, but with the MRA removed.

This report documents the computed dose rate fields for these configurations, along with the methodologies employed in their calculation. The results aim to inform the design of remote handling special equipment and the planning of corresponding operations, ultimately contributing to the safe and efficient operation of the STS target system.

This report shows that the requirements 1-4 from Section 2 are satisfied by the current layout and design, and provides dose rate information that will allow evaluation of requirements 5-8 when details of the maintenance operations will become available.

Draft. Not approved for public release.
The only OFFICIAL COPY of this document is the on-line electronic version in ORNL's document management application.
Before using a printed copy, verify that it is the most current version.

2 ACCEPTANCE CRITERIA

The requirements evaluated in this report are as follows:

1. Effective dose rates in the target drive room in nominal configuration shall be less than 5 mrem/hr after 8 hours after last beam-on-target [1].
2. Requirement 1774- Cool Down Time [2]
   - "In operating configuration of the target assembly and core vessel, the drive components shall be at or below 100 mrem/hr on contact within 8 hours of cessation of the beam."
3. Requirement S.03.06-7125: Shielding for Target Segment Removal and Installation [3]
   - "Vessel Systems shall allow for hands-on maintenance at the top of the target segment with the target removable shield block removed."
4. Requirement S.03.04-10944: MRA Utilities Dose Rate Requirement [4]
   - "The dose rates at 30 cm from the MRA hydrogen transfer line connection and water line connections shall be 100 mrem/hour or less after MRA operation and decay time of 8 hours to allow for hands on replacement of these connections with the target station in nominal operating configuration with the exception of the removal of the Core Vessel MRA hatch."

Requirements that are supported but not evaluated are as follows:

5. Requirement S.03.10.04-10938–Personnel Safety (for target segment maintenance) [5]
   - "A single worker shall not receive more than 600 mrem (TED) while performing a single target segment removal and replacement operation."
6. Requirement S.03.10.04-10943–Personnel Safety (for target drive maintenance) [6]
   - "A single worker shall not receive more than 1000 mrem (TED) while performing a target drive removal and replacement operation."
7. Requirement S.03.10.05-10942–Personnel Safety (for MRA maintenance) [7]
   - "A single worker shall not receive more than 1000 mrem (TED) while performing a MRA removal and replacement operation."
8. Requirement S.03.10.03-10940–Personnel Safety (for PBW or TVP) maintenance [8]
   - "A single worker shall not receive more than 1000 mrem (TED) while performing either a PBW or TVP removal and replacement operation."

3 ASSUMPTIONS AND LIMITATIONS

The main assumptions associated with the generation of the target system's decay gamma sources detailed in McClanahan's paper are also applicable to this report [9]. The decay gamma sources for the various components within the target system are calculated using neutron fluxes and spallation products computed assuming a 700 kW, 1.3 GeV proton beam resulting in $3.36{\times}10^{15}$ protons per second incident on the target in a nominal 60 cm^2 beam area. These neutron fluxes and spallation products were used to generate decay gamma sources assuming an operational year is defined as 2500 hours of beam on, 1880 hours beam off, 2500 hours beam on, and 1880 hours of beam off.

Draft. Not approved for public release.
The only OFFICIAL COPY of this document is the on-line electronic version in ORNL's document management application.
Before using a printed copy, verify that it is the most current version.

The target is assumed to have been operated for 10 years, the MRA for 6 years, the proton beam window (PBW) for 3 years, the target viewing periscope (TVP), target station shielding (TSS) and the core vessel shielding for 40 years.

The hands-on requirement for Requirement 3 in Section 2 are assumed to mean 100 mrem/hr at 30 cm from an accessible surface unless stated otherwise. This assumption is supported by the operational experience at SNS.

4 METHODOLOGY AND MODELS

Two general methodologies are utilized in the analysis detailed in this report. The first general methodology is applied to generate the decay gamma sources described in Section 4.1, and the second general methodology is used in the transport of the decay gamma sources to calculate dose rate maps as described in Section 4.2.

4.1 GENERATION OF DECAY GAMMA SOURCES

The basis of the methodology for generating the decay gamma sources for the components of the target system is detailed in McClanahan's paper [9]. MCNP® Version 6.2 with ADVANTG Version 3.2.0 along with CINDER2008 from the AARE Version 1.0 package are used in the methodology workflow in McClanahan's paper [10, 11, 12]. Further improvements in the methodology have been implemented in this report by using conservative flux and reaction rate values, and by rigorously monitoring flux convergence in each cell.

For the transmutation calculations with CINDER2008, the fluxes and high-energy reaction rates were taken at the upper bounds of the 95% confidence interval of the Monte Carlo simulations. This was accomplished by adding two times the absolute uncertainty to the average values of fluxes and high-energy reaction rates.

The energy-integrated flux for each cell was evaluated against a 5% relative error threshold. If the energy-integrated flux was found to be more than the threshold error, the cell was added to a list of other delinquent cells. The list of delinquent cells was then used to generate another round of neutron flux and high-energy reaction rates calculation by setting the motivating tally in ADVANTG for only the delinquent cells. This process was repeated until the desired level of convergence was achieved for a vast majority of the cells with a few cells left to be manually evaluated. Figures 1 & 2 show examples of the flux and flux plus 2σ uncertainty. Figure 1 shows a very well converged energy differential neutron flux in a piece of thin tantalum in the target foot. The overall ratio of the energy-integrated neutron flux and the plus 2σ uncertainty neutron flux in Figure 1 is 1.002 whereas the corresponding overall ratio in Figure 2 is 1.118. Even though the energy-integrated neutron flux spectrum in Figure 2 is converged to below 0.7%, adding 2σ uncertainty to every energy bin and integrating over energy yields a 12% increase in overall flux in that cell.

Draft. Not approved for public release.
The only OFFICIAL COPY of this document is the on-line electronic version in ORNL's document management application.
Before using a printed copy, verify that it is the most current version.

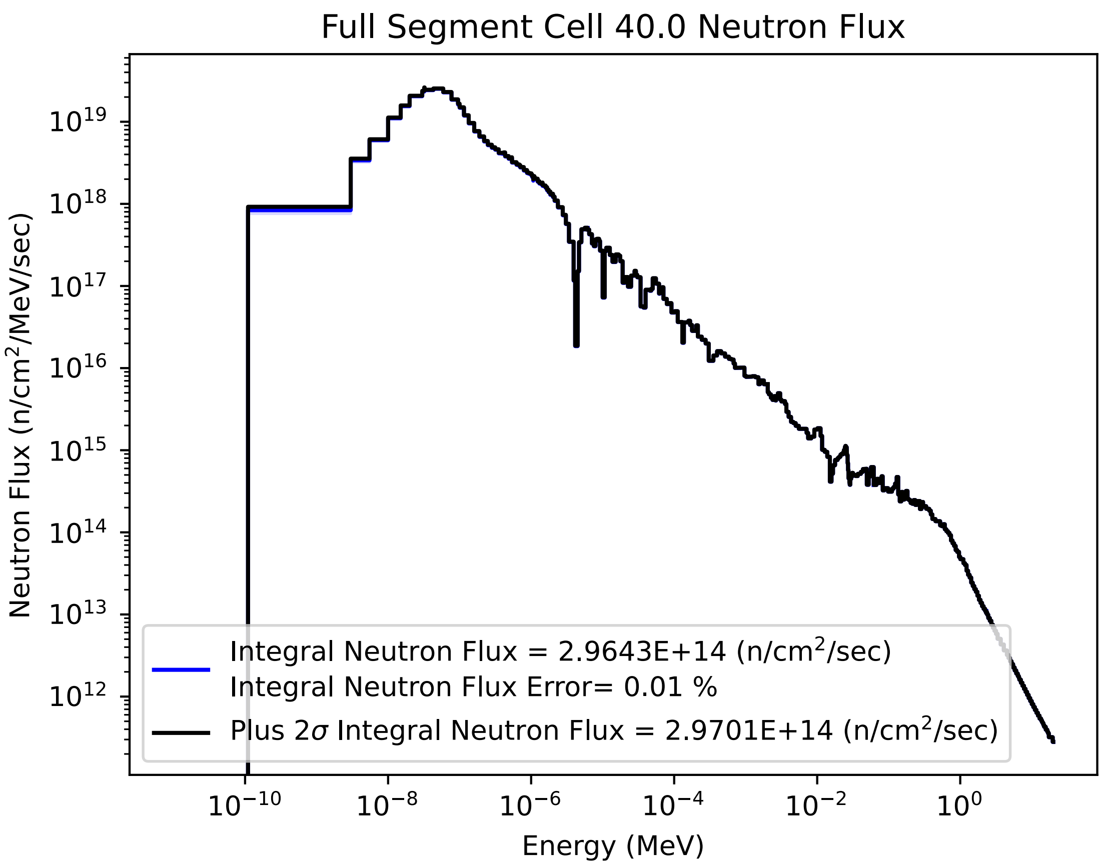

Figure 1. The energy differential neutron flux in target wheel cell number 40 containing a thin layer of tantalum showing the flux in blue and the flux plus 2σ uncertainty in black.

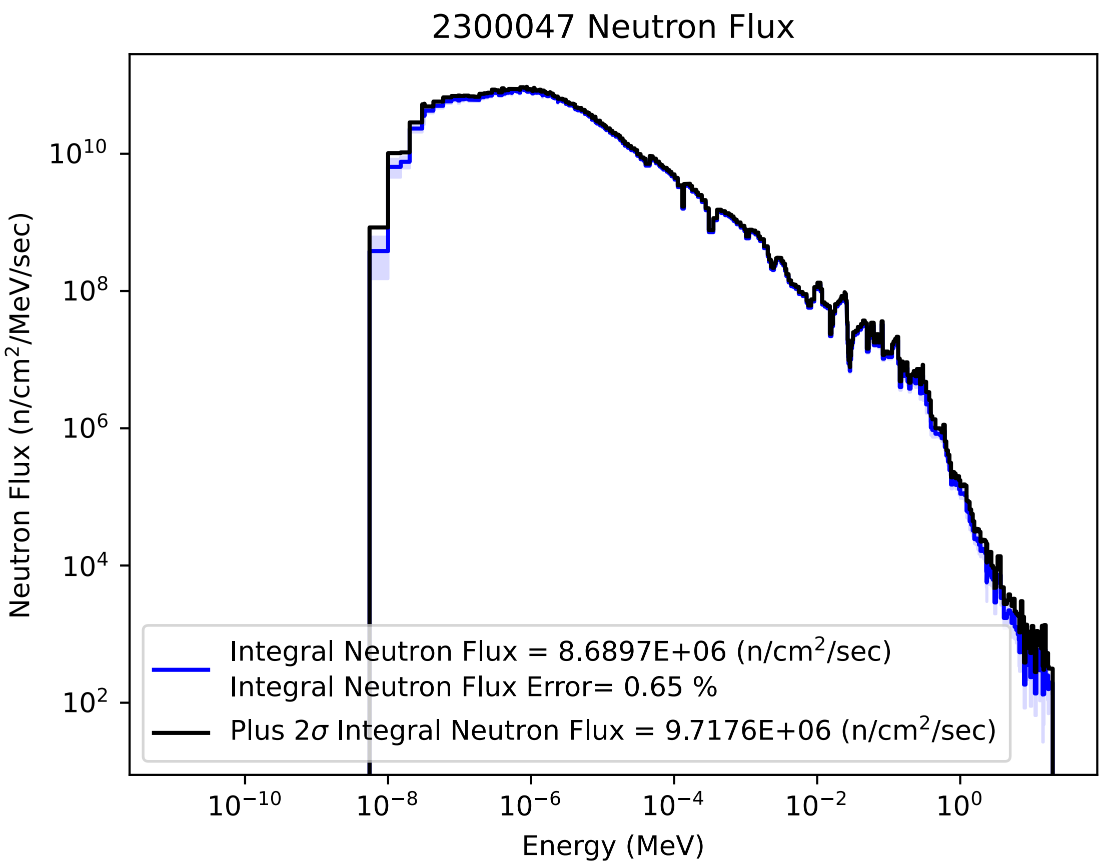

Figure 2. The energy differential neutron flux in target crown cell number 47 containing a piece of stainless steel 316L showing the flux blue and the flux plus 2σ uncertainty in black.

Draft. Not approved for public release.
The only OFFICIAL COPY of this document is the on-line electronic version in ORNL's document management application.
Before using a printed copy, verify that it is the most current version.

During operation, the process water cooling the target and other components becomes activated, generating ^{17}N in the coolant. As the water flows through the system, it transports the ^{17}N from its origin within the core vessel shielding, where prompt neutron flux is high, to areas with significantly lower prompt neutron flux, such as the target drive room. In this region, the decay neutrons emitted by ^{17}N in the water coolant contribute substantially to the overall neutron flux, often rivaling or even exceeding the prompt streaming neutron flux. As a result, the target drive room piping and target crown assemblies are subject to an additional neutron flux source in the activation calculations.

4.2 TRANSPORT OF DECAY GAMMA SOURCES

Various components of the methodology for transporting the decay gamma sources to compute dose rate maps in the target drive room of the STS are detailed in the sections below. Section 4.2.1 describes the geometry used in the decay gamma transport in the five configurations of the STS target system. Section 4.2.2 details the isotopic composition of the materials used in the geometry. Section 4.2.3 shows the decay gamma sources used to compute the decay dose rate maps. Section 4.2.4 describes the two methods used to transport the sources to the target drive room. Section 4.2.5 includes details on the variance reduction used to streamline the Monte Carlo particle transport calculation, and Section 4.2.6 describes the tallies used to capture the results from the Monte Carlo or discrete ordinates solutions. Section 4.2.7 describes the post processing scripts used to view the dose rate maps.

4.2.1 Geometry

Five configurations of the geometry are analyzed in Section 5 and are shown below. Figure 3 shows the nominal geometry of the STS target system with all shielding and components in place where the major systems of the STS have been identified. This geometry was also used to calculate the neutron fluxes and high-energy reaction rates discussed in Section 4.1. Figure 3 is cut along the proton beam, 1.01 cm away from the proton beam as to not cut through the 10 mm gaps between core vessel (CV) shield blocks. This geometry is used to calculate the decay dose maps after 8 hours of decay to confirm hands-on maintainability of the target crown and confirm hand-removal of water lines at the top of the target segment vertical stave (elevation of 500 cm above beam center in Figure 3).

Draft. Not approved for public release.
The only OFFICIAL COPY of this document is the on-line electronic version in ORNL's document management application.
Before using a printed copy, verify that it is the most current version.

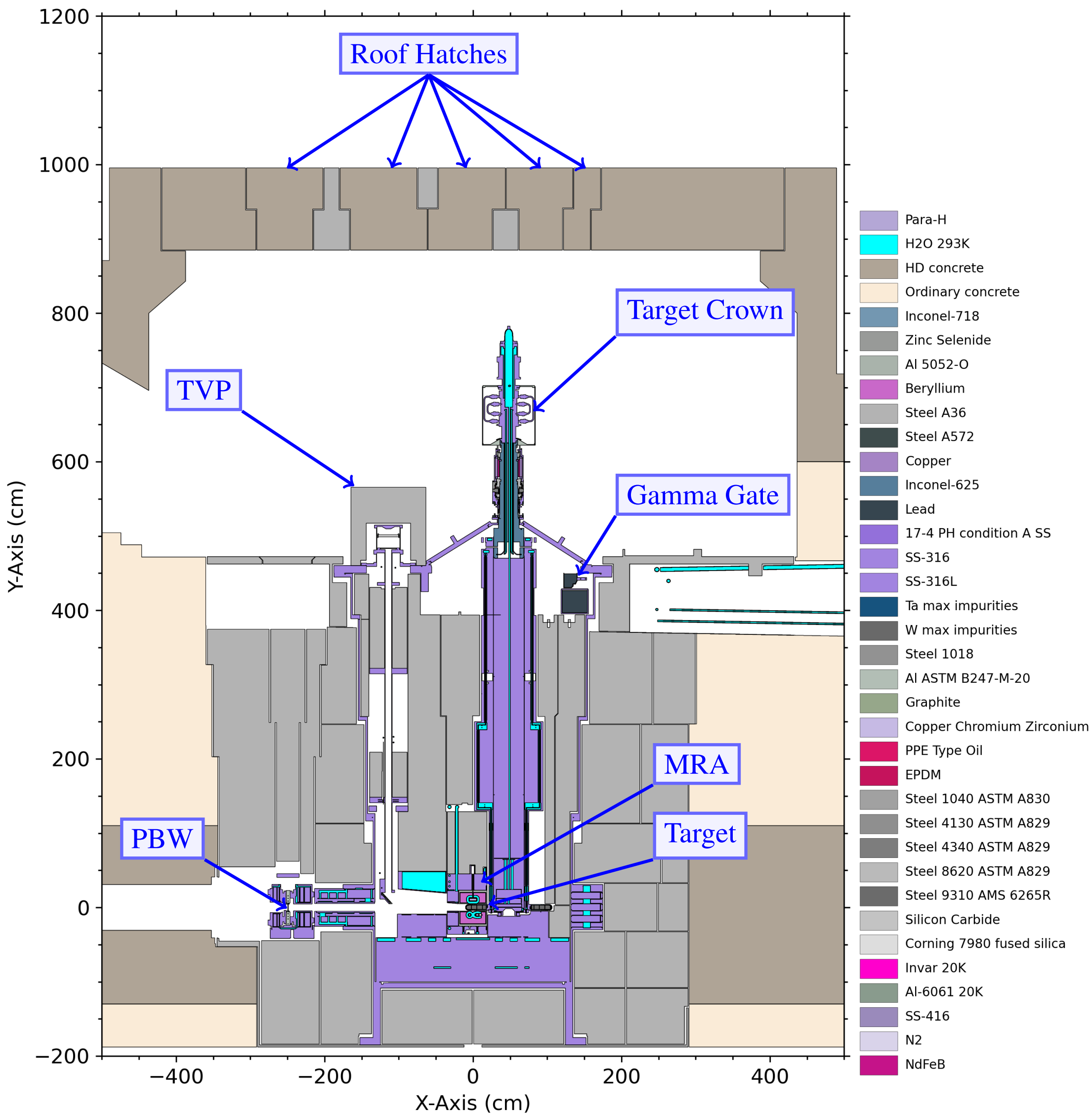

Figure 3. Cross section view of the geometry of the nominal configuration with all of the shielding in place along the proton beam (Z=1.01 cm).

Figure 4 shows a cross section view of the STS target system in the segment removal configuration with a target segment removed, the lead gamma gate is deployed, and the removable target segment access shield block removed. Figure 5 shows a plan view of the segment removal configuration at an elevation 426 cm above the proton beam. The detail view contained within Figure 5 shows the gamma gate arm deployed into the open spot vacated by the removal of a single target segment.

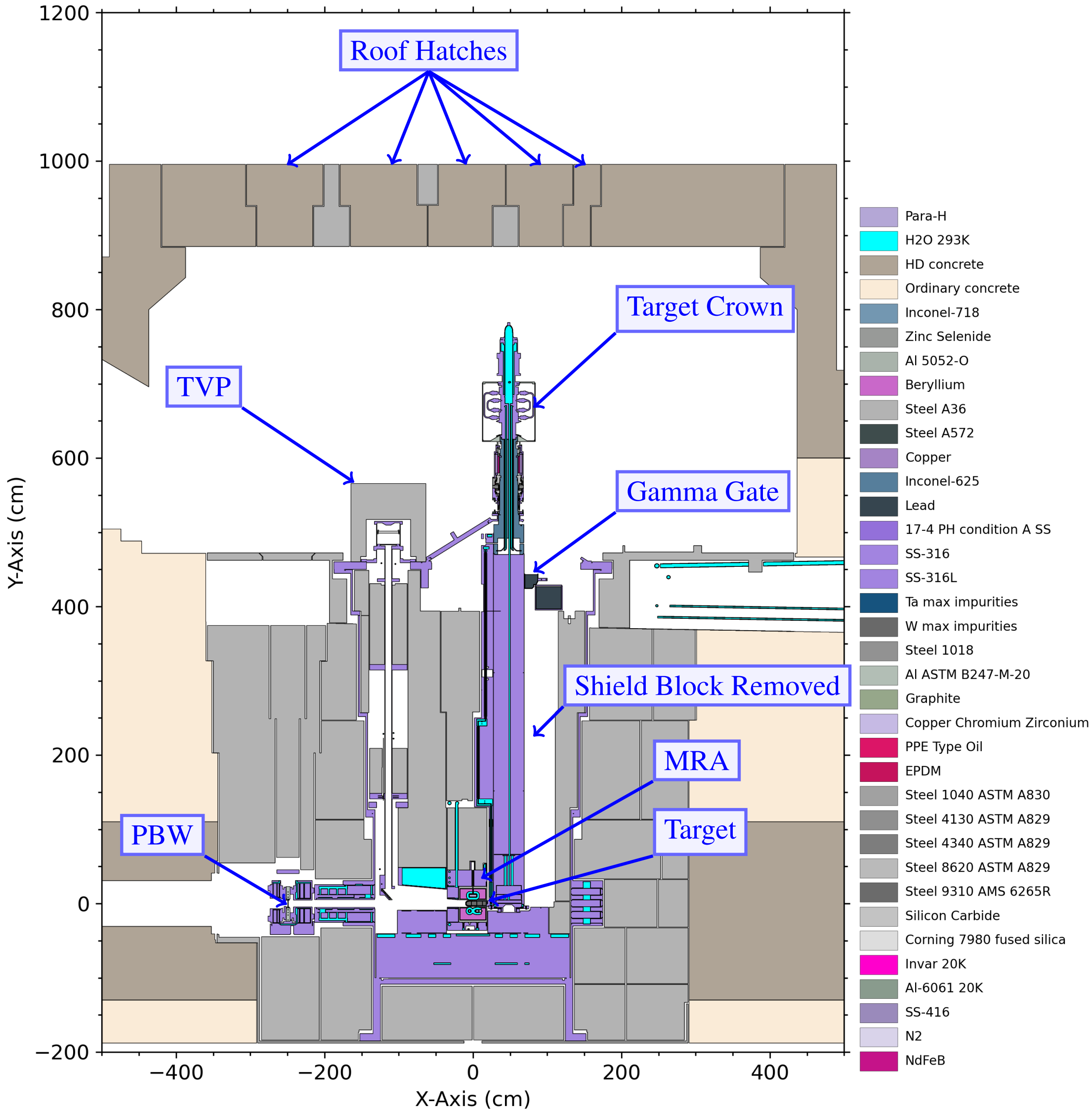

Figure 4. Cross section view of the geometry of the single target segment removed configuration with the CV target segment removable shield block removed and the gamma gate deployed the proton beam (Z=1.01 cm).

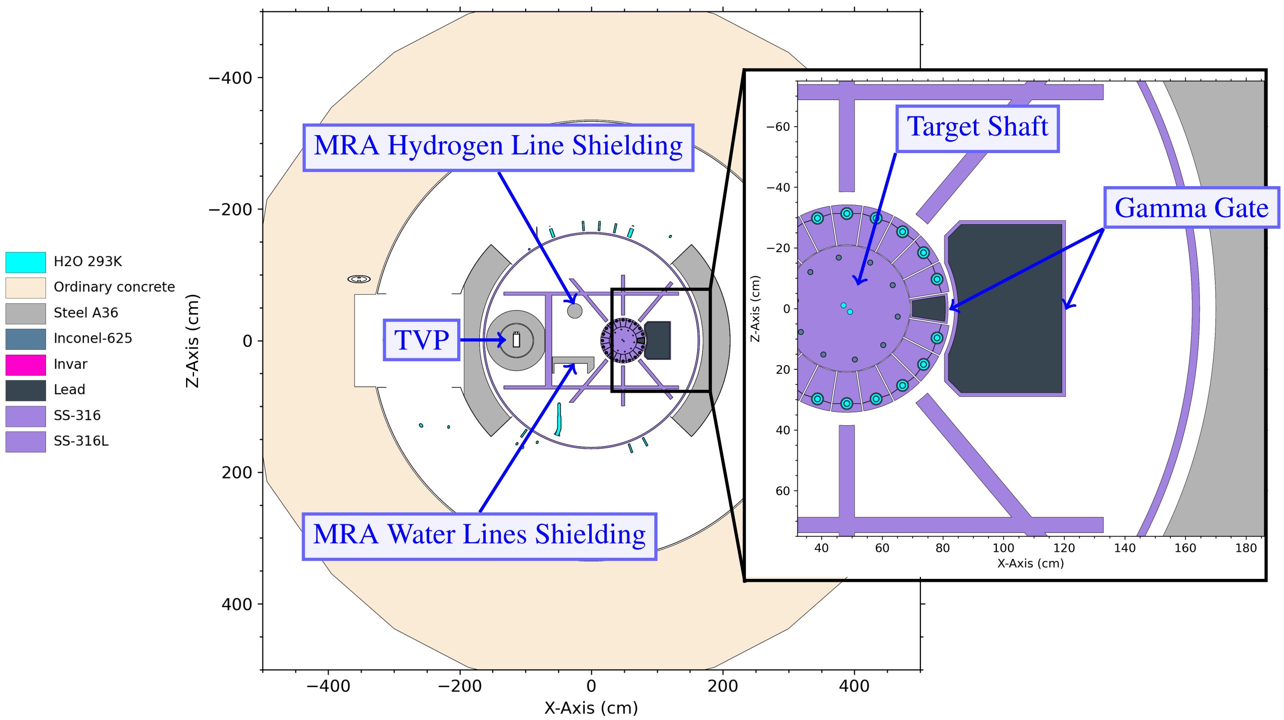

Figure 5. Plan view of the geometry of the single target segment removed configuration with the CV target segment removable shield block removed and the gamma gate deployed viewed 426 cm above the proton beam (Y=426 cm).

Figures 6 & 7 show the third configuration used to calculate the dose rate field during the removal of a third target segment after two have been removed. In this scenario, the target is positioned for the removal of the third segment, the core vessel gamma gate remains closed, one gamma gate shielding arm is deployed, and the removable target segment core vessel shield block has been removed. However, one of the holes created by the removal of one of the two target segments remains unmitigated, as shown in Figure 7.

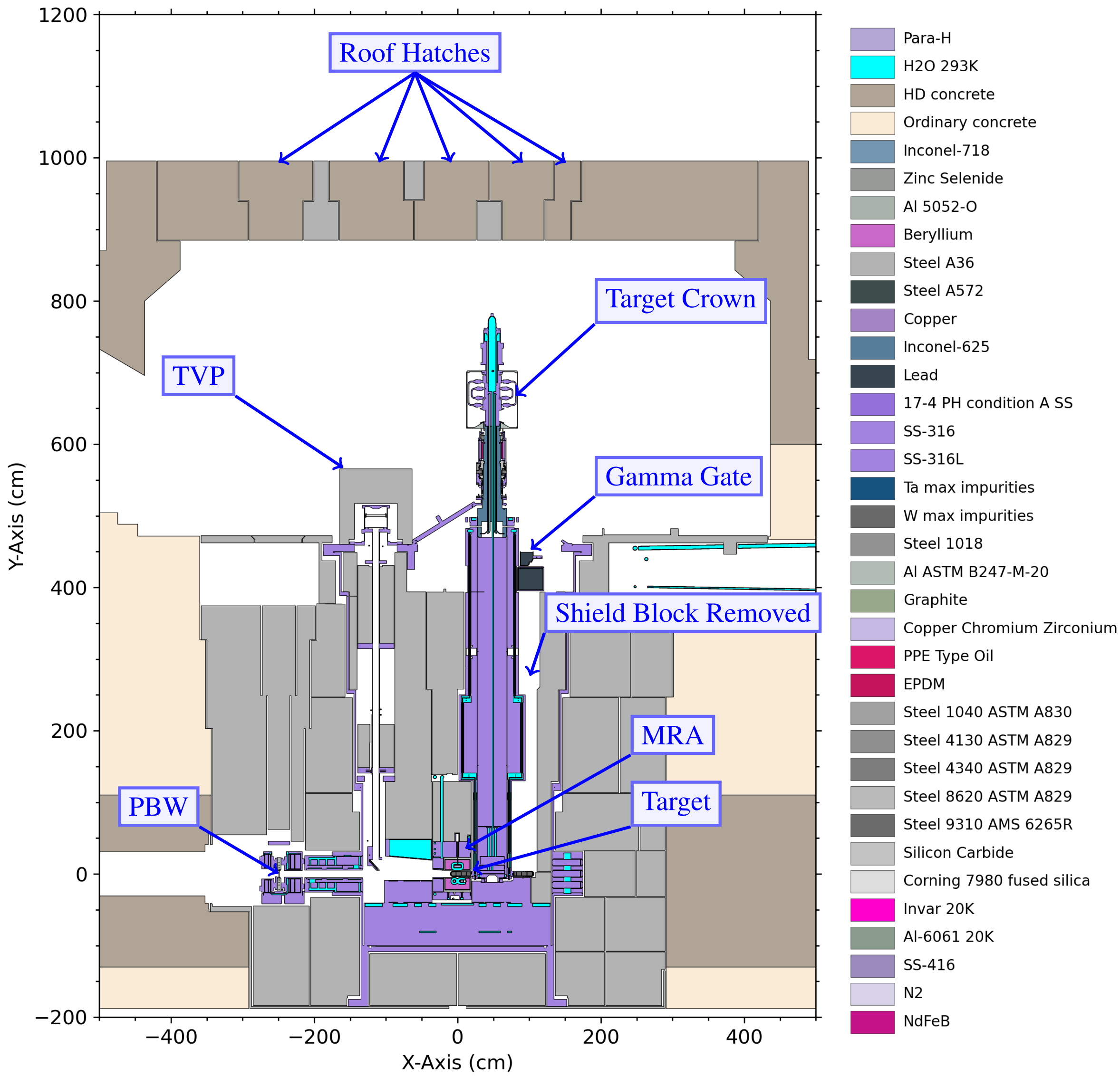

Figure 6. Cross section view of the geometry of the two segments removed configuration with the CV target segment removable shield block removed and the gamma gate deployed along the proton beam (Z=1.01 cm).

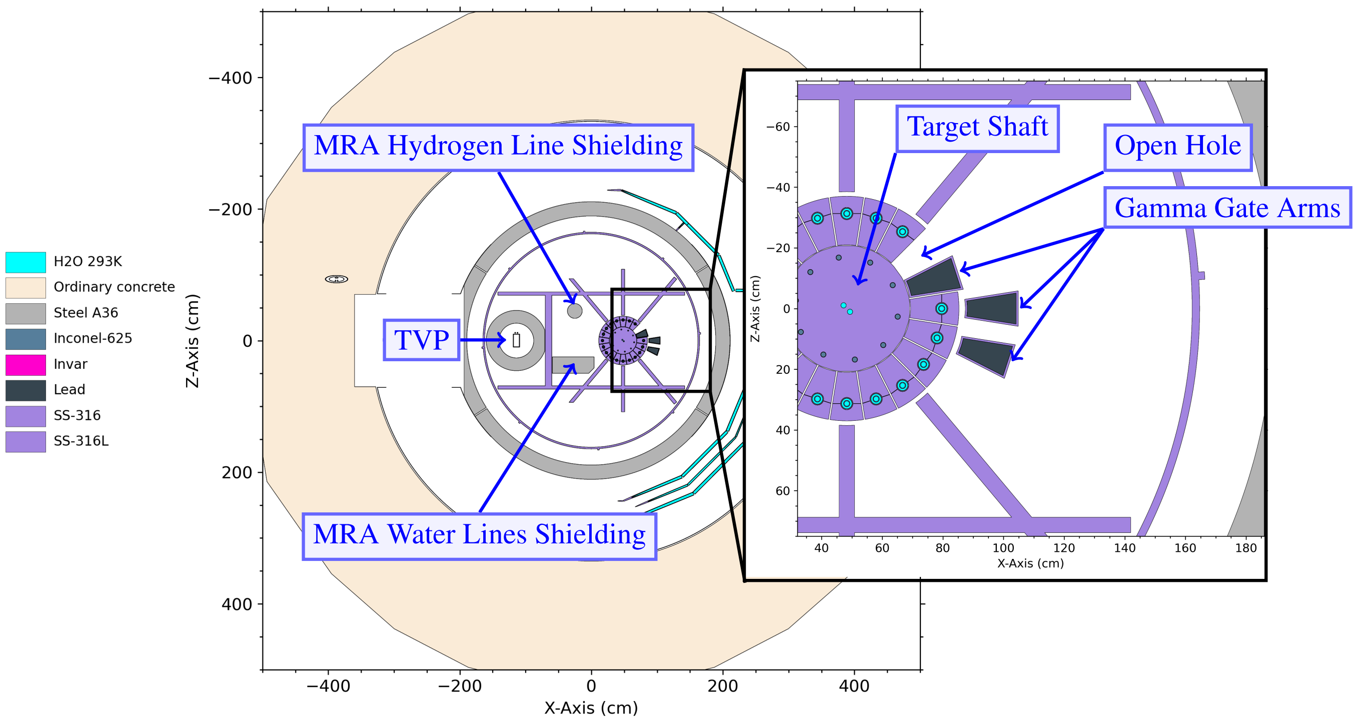

Figure 7. Plan view of the geometry of the two target segments removed configuration with the CV target segment removable shield block removed and the gamma gate deployed viewed at 438 cm above the proton beam (Y=438 cm).

Figures 8, 9,10, & 11 show the fourth configuration that captures the scenario where the hydrogen and water transfer pipes stemming from the top of the MRA are about to be cut for their removal. This configuration includes the removal of the MRA removable shield block, both core vessel tent hatches, three target segments, and the deployment of all three gamma gate arms. The hatch in the target drive room ceiling is open to the high bay. To assess which scenario minimizes dose to pipe-cutting workers standing in either the target drive room or high bay areas, two sub-configurations are evaluated: one with the hole caused by the removal of three target segments located on the downstream end of the target shaft and another with the hole on the upstream end. Figures 8 & 9 show the configuration where the three target segment holes are located downstream of the target.

Draft. Not approved for public release.
The only OFFICIAL COPY of this document is the on-line electronic version in ORNL's document management application.
Before using a printed copy, verify that it is the most current version.

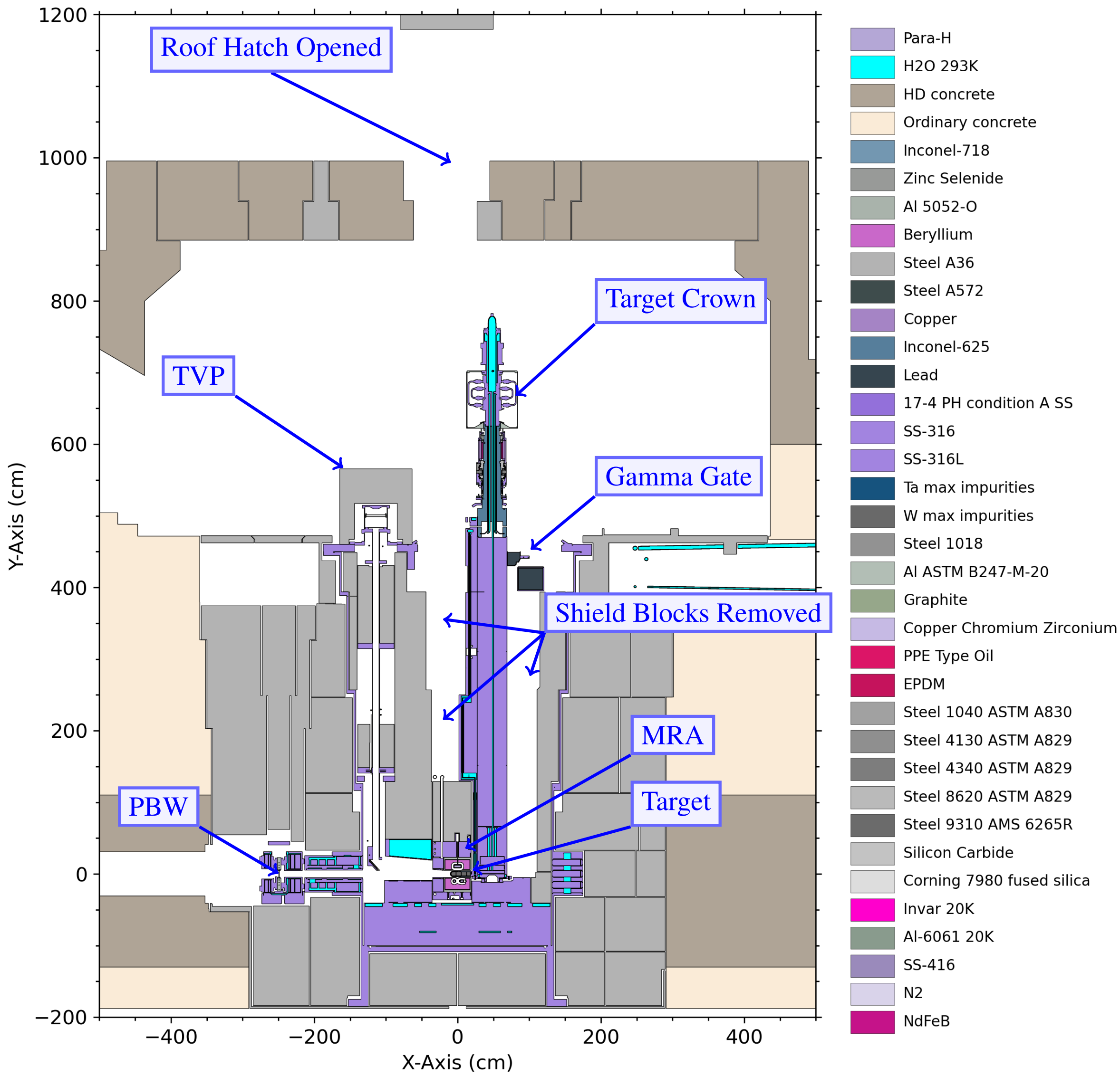

Figure 8. Cross section view of the geometry of the MRA pipe cutting configuration with the CV target segment removable shield block removed, and the MRA removable shield block removed, and the gamma gate deployed viewed at 1.01 cm away from the proton beam (Z=1.01 cm).

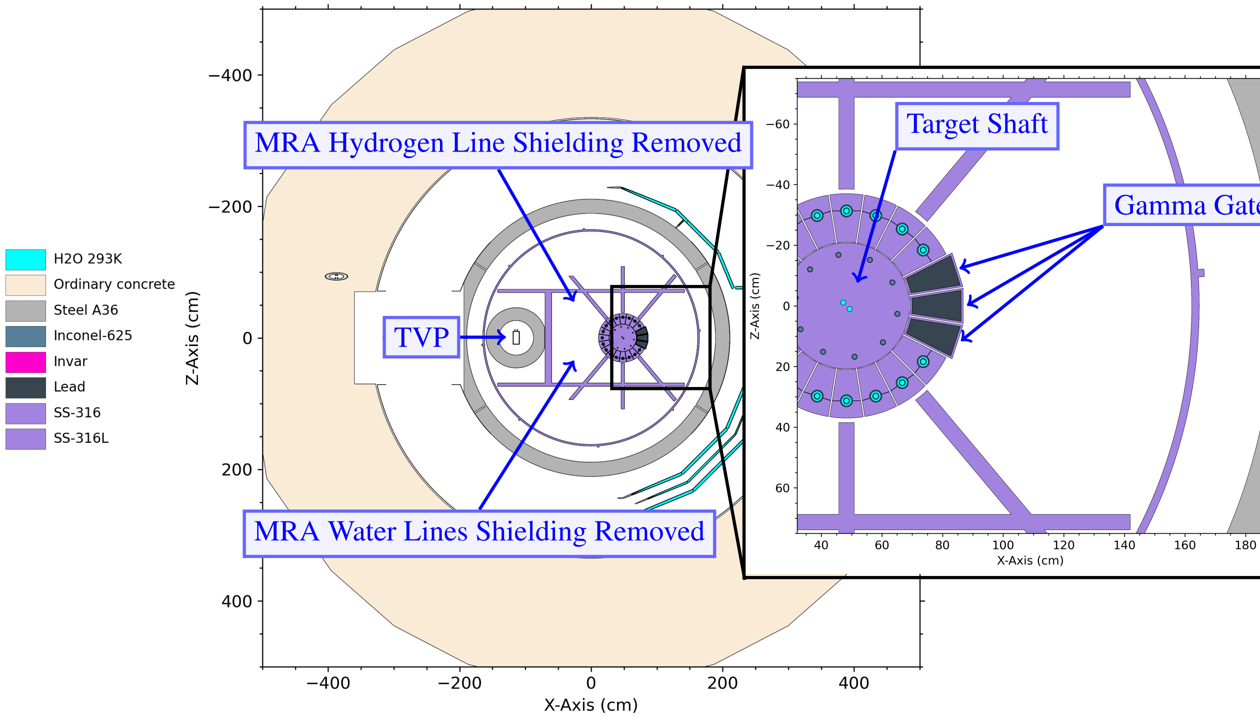

Figure 9. Plan view of the geometry of the MRA pipe cutting configuration with the CV target segment removable shield block removed, and the MRA removable shield block removed, and the gamma gate deployed viewed at 438 cm above the proton beam (Y=438 cm).

Figures 10 & 11 show the configuration where the three target segment holes are located upstream of the target. Figure 10 shows a detail view of the hole generated by the removal of the target segments located along the MRA and the MRA supplemental shielding. Figure 11 shows a plan view of the hole left by removing three target segments and the MRA removable shield block viewed 350 cm above the proton beam elevation.

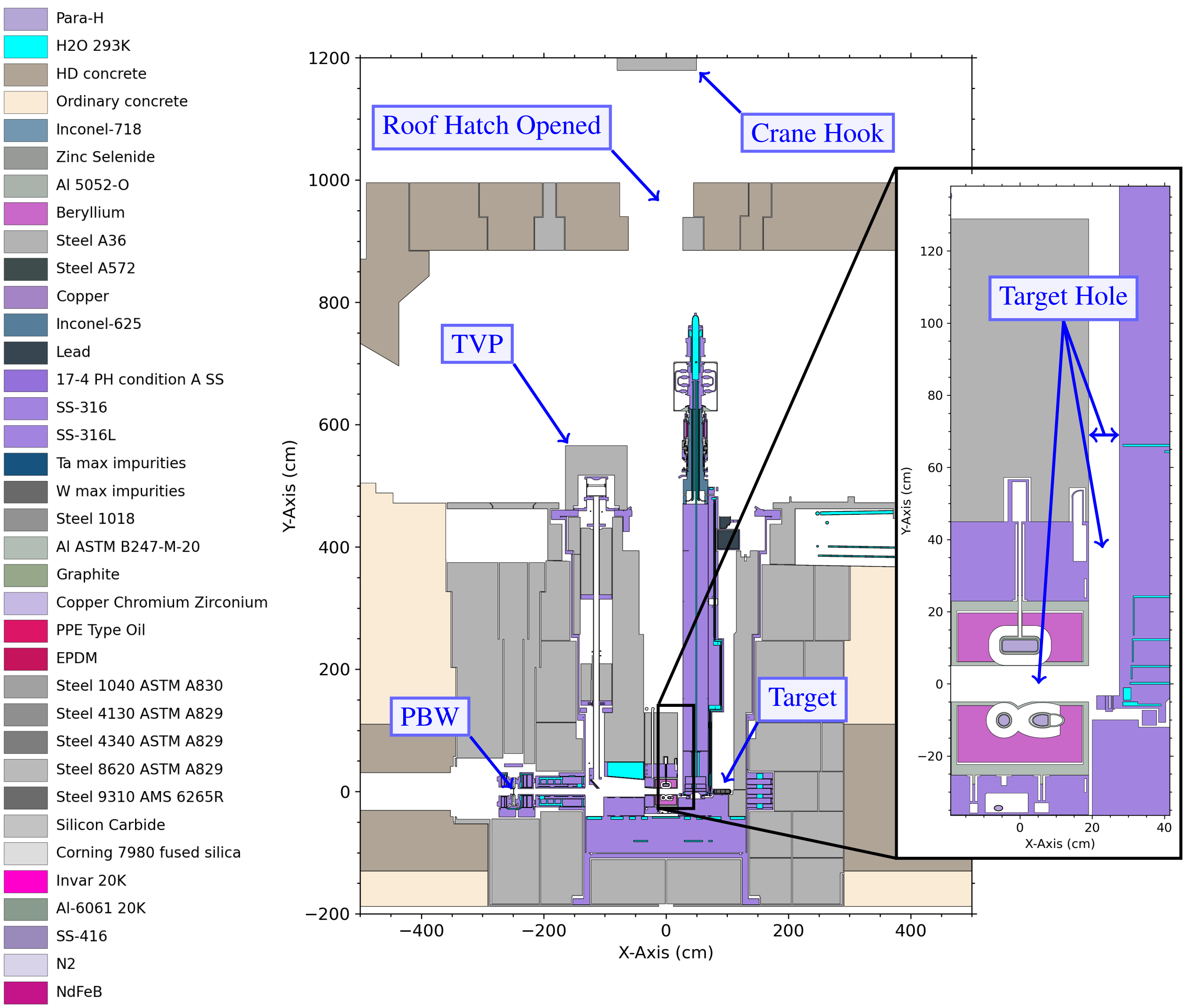

Figure 10. Cross section view of the geometry of the MRA pipe cutting configuration with the CV target segment removable shield block removed, and the MRA removable shield block removed, and the gamma gate deployed viewed at 1.01 cm away from the proton beam (Z=1.01 cm).

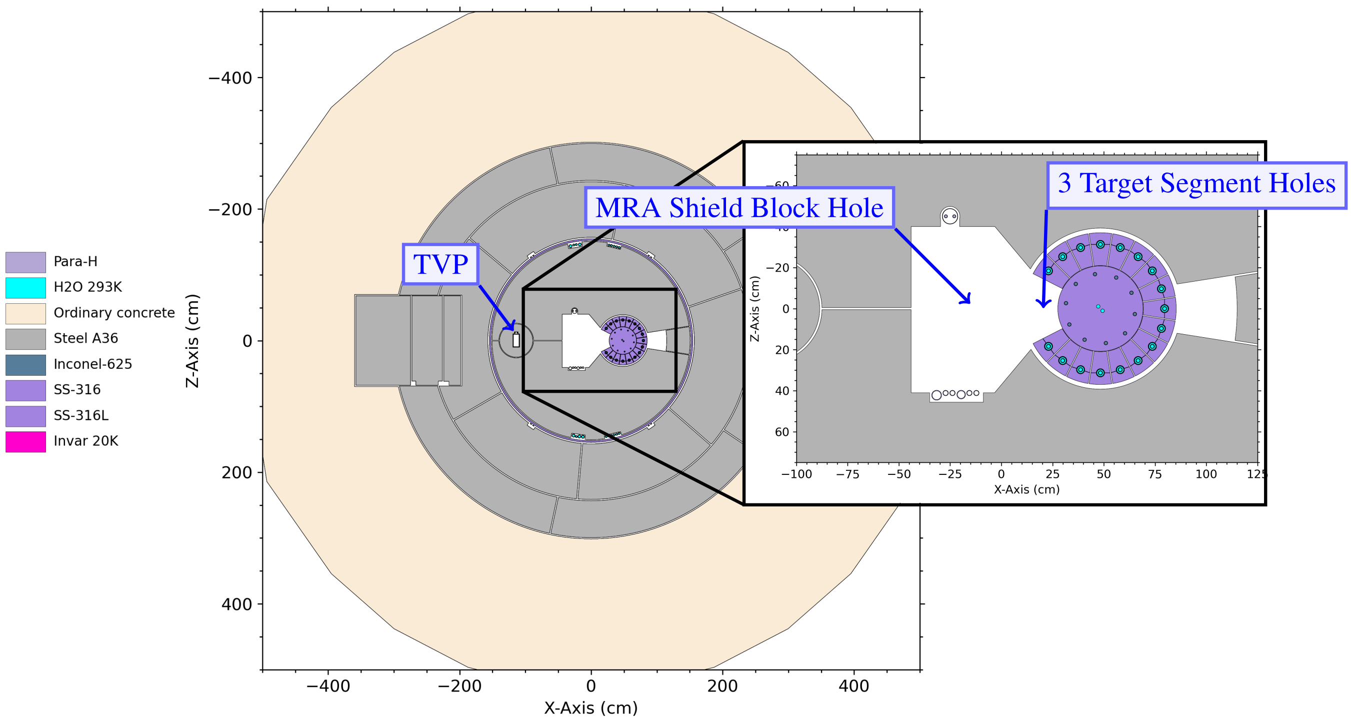

Figure 11. Plan view of the geometry of the MRA pipe cutting configuration with the CV target segment removable shield block removed, and the MRA removable shield block removed, and three target segments removed viewed at 350 cm above the proton beam (Y=350 cm).

Figure 12 illustrates the fifth configuration, where the MRA has been completely removed, along with three target segments. In this scenario, the crane block is lowered to its operational position, as indicated in the figure, to facilitate maintenance activities that will take place during the MRA removal. With the crane block in this lowered position, the radiation scattering off the block back into the TDR is more intense compared to when the block is located in a higher position in the high bay.

Draft. Not approved for public release.
The only OFFICIAL COPY of this document is the on-line electronic version in ORNL's document management application.
Before using a printed copy, verify that it is the most current version.

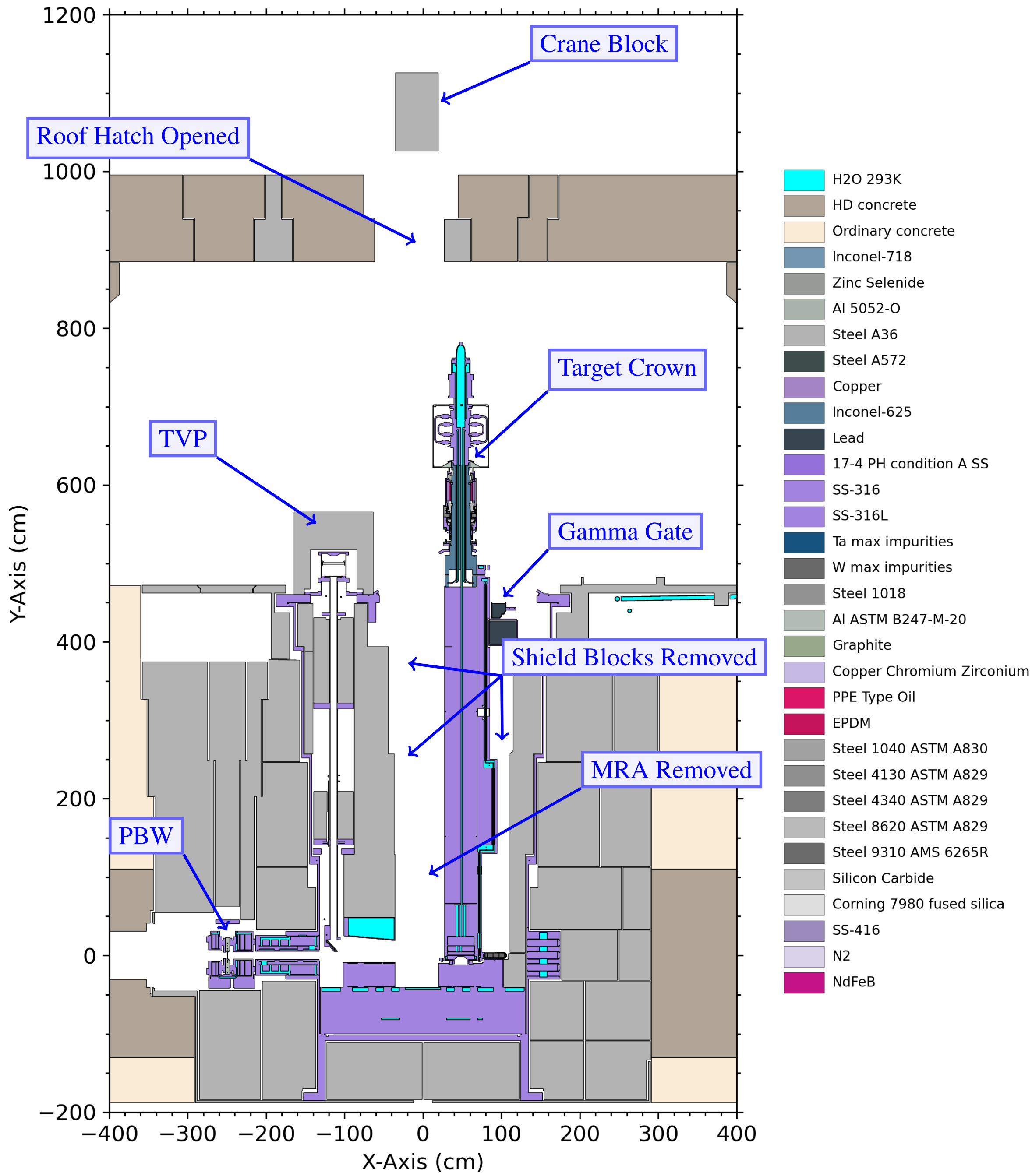

Figure 12. Cross section view of the geometry of the MRA removed configuration with the CV target segment removable shield block removed, and the MRA and MRA removable shield block removed, and the gamma gate deployed viewed at 1.01 cm away from the proton beam (Z=1.01 cm).

Draft. Not approved for public release.
The only OFFICIAL COPY of this document is the on-line electronic version in ORNL's document management application.
Before using a printed copy, verify that it is the most current version.

4.2.2 Materials

The materials used in the analysis described in this report are detailed in tables included in Appendix D. During the Monte Carlo transport runs where the photon dose rates are tallied, ENDF/B-VII.1 cross sections are used and the 27n19g multigroup library as a part of the ADVANTG 3.2.0 code package is used in the discrete ordinates transport calculations [13, 11].

4.2.3 Decay Gamma Source

The decay gamma source intensities calculated using the methodology described in Section 4.1 are shown in the figures of this section. Figures 13-15 show sources used in configurations 1-3 after 8 hours of decay since last beam on target. Figures 16-18 show sources used in configurations 4-5 after 2 weeks of decay since last beam on target. The most intense sources of decay gammas are the target wheel, MRA, and the core vessel shielding located in close proximity to the MRA. The major components of the STS target system have been subdivided to spatially resolve the decay gamma source. If a space is white in the figures, that region's decay gamma source term was not included in the analysis of this report.

Draft. Not approved for public release.
The only OFFICIAL COPY of this document is the on-line electronic version in ORNL's document management application.
Before using a printed copy, verify that it is the most current version.

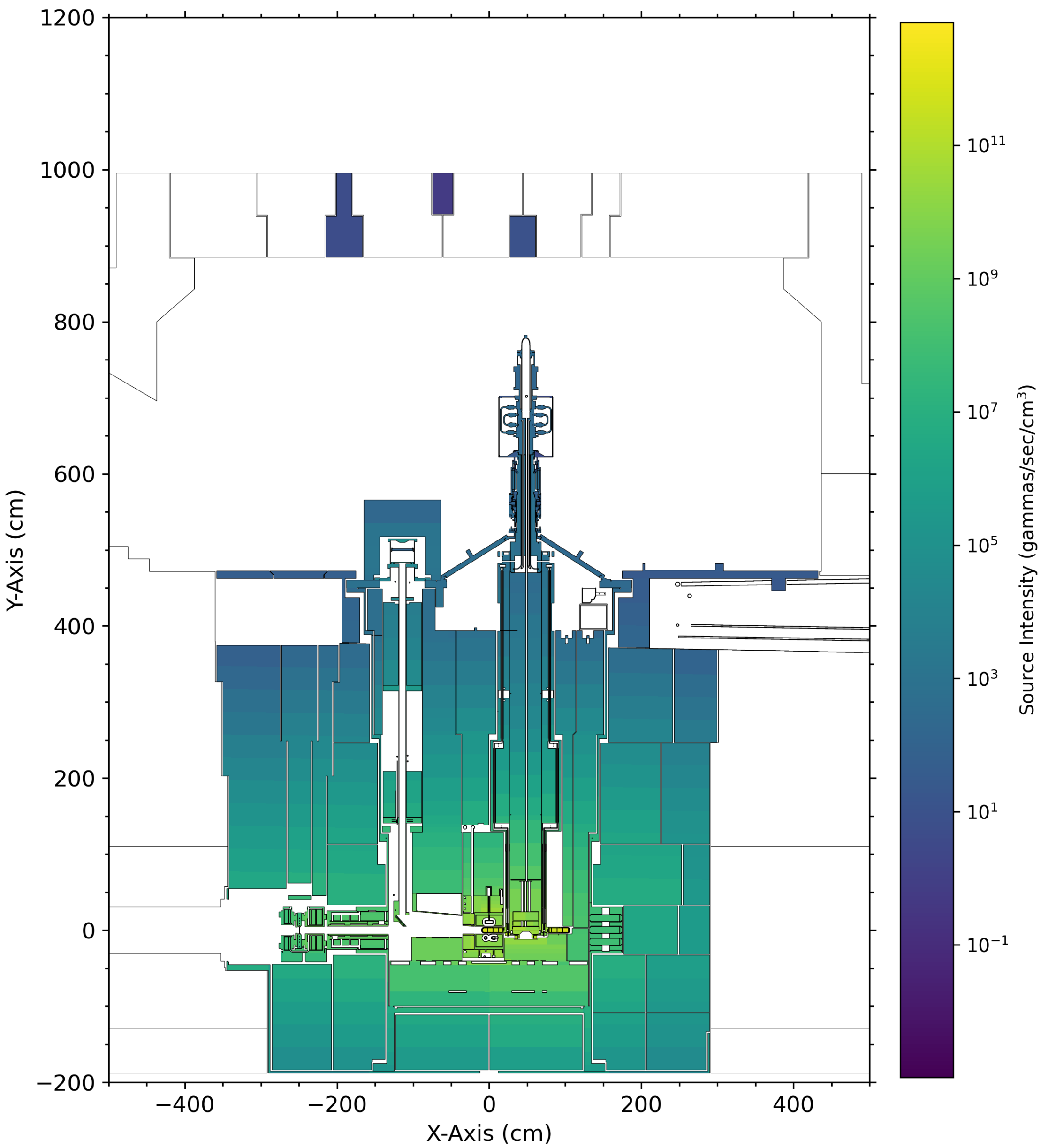

Figure 13. Cross section view of the decay gamma source intensity after 8 hours of decay for the STS target system configuration 1.

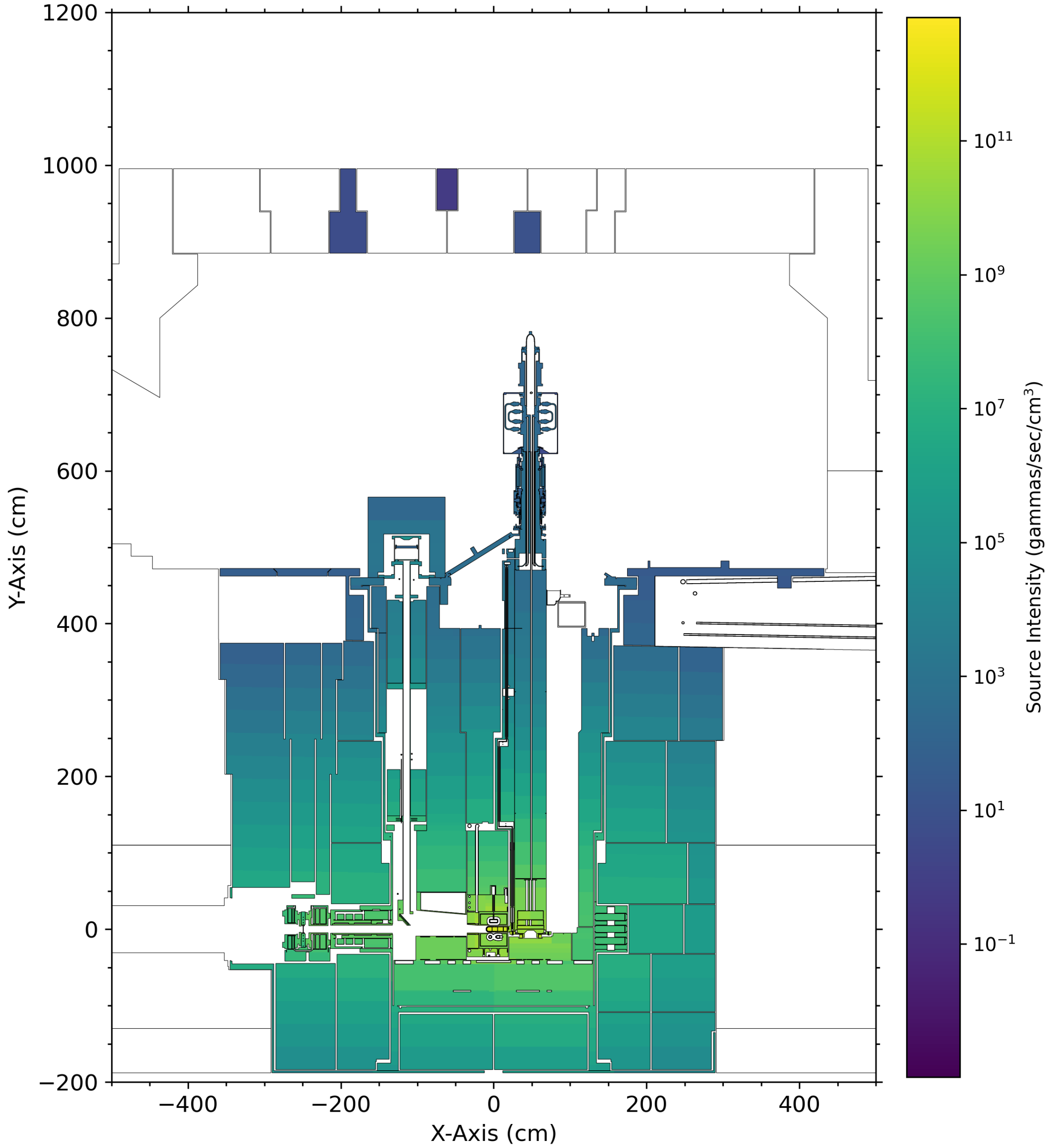

Figure 14. Cross section view of the decay gamma source intensity after 8 hours of decay for the STS target system configuration 2.

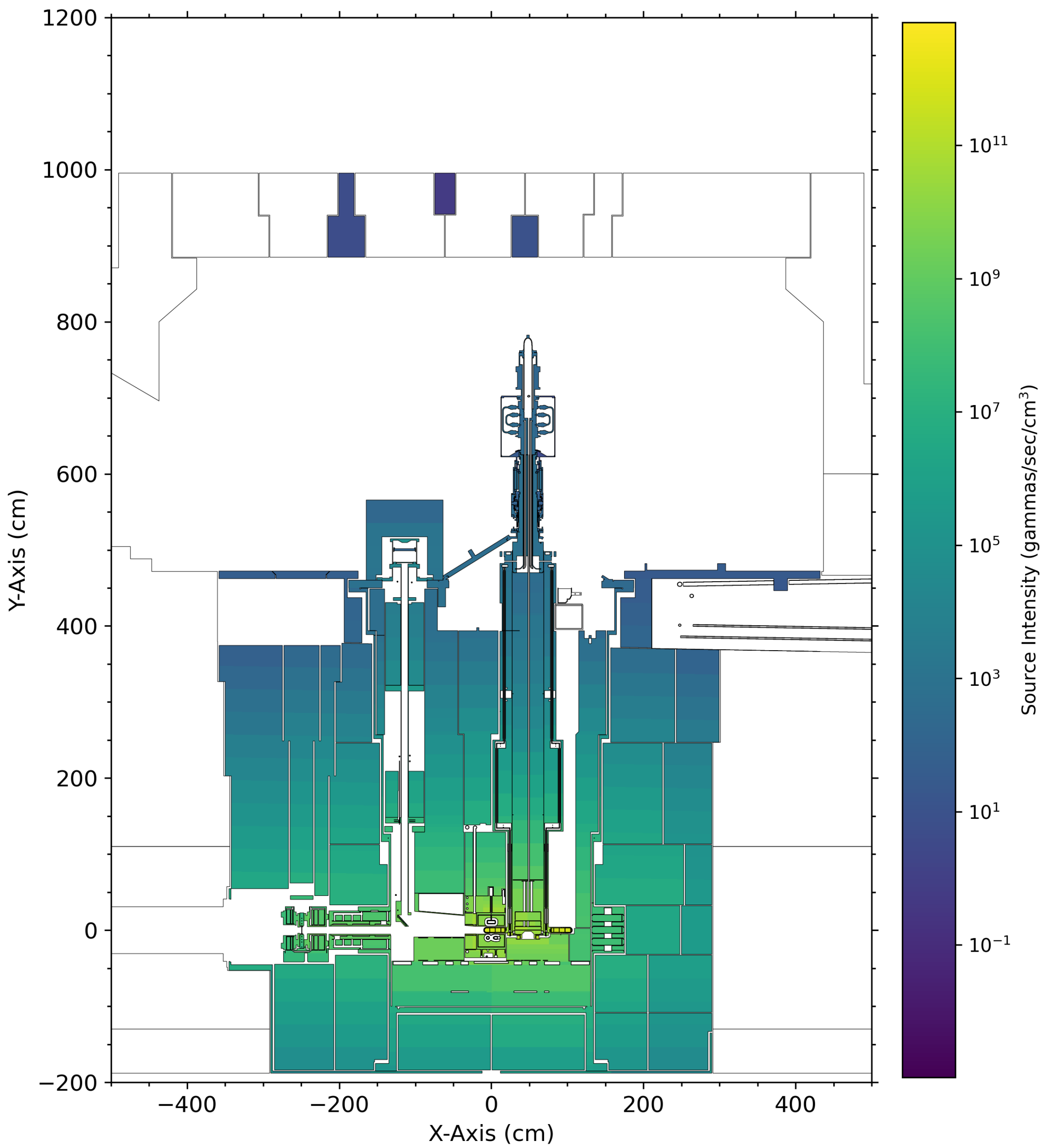

Figure 15. Cross section view of the decay gamma source intensity after 8 hours of decay for the STS target system configuration 3.

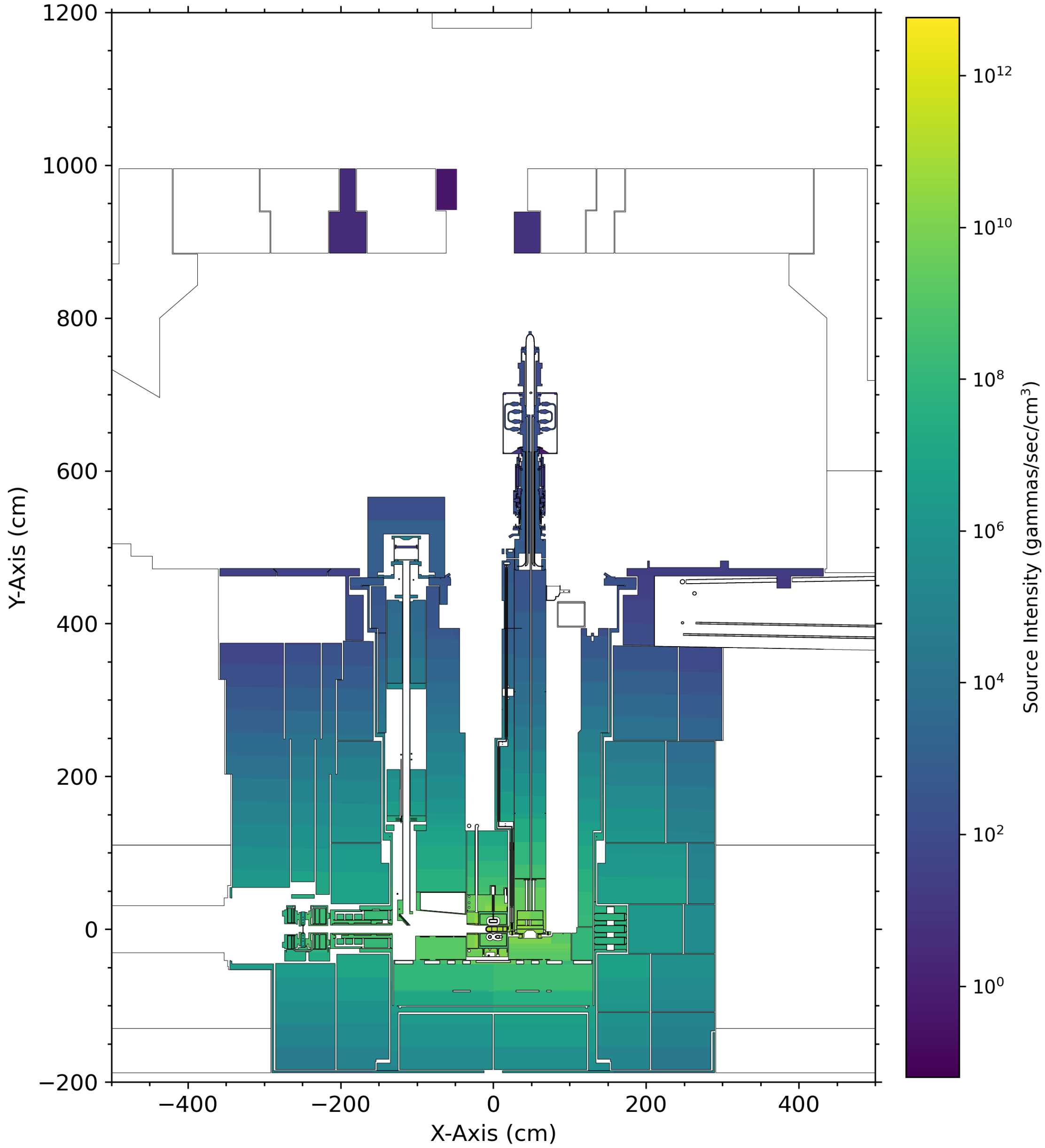

Figure 16. Cross section view of the decay gamma source intensity after 2 weeks of decay for the STS target system configuration 4.

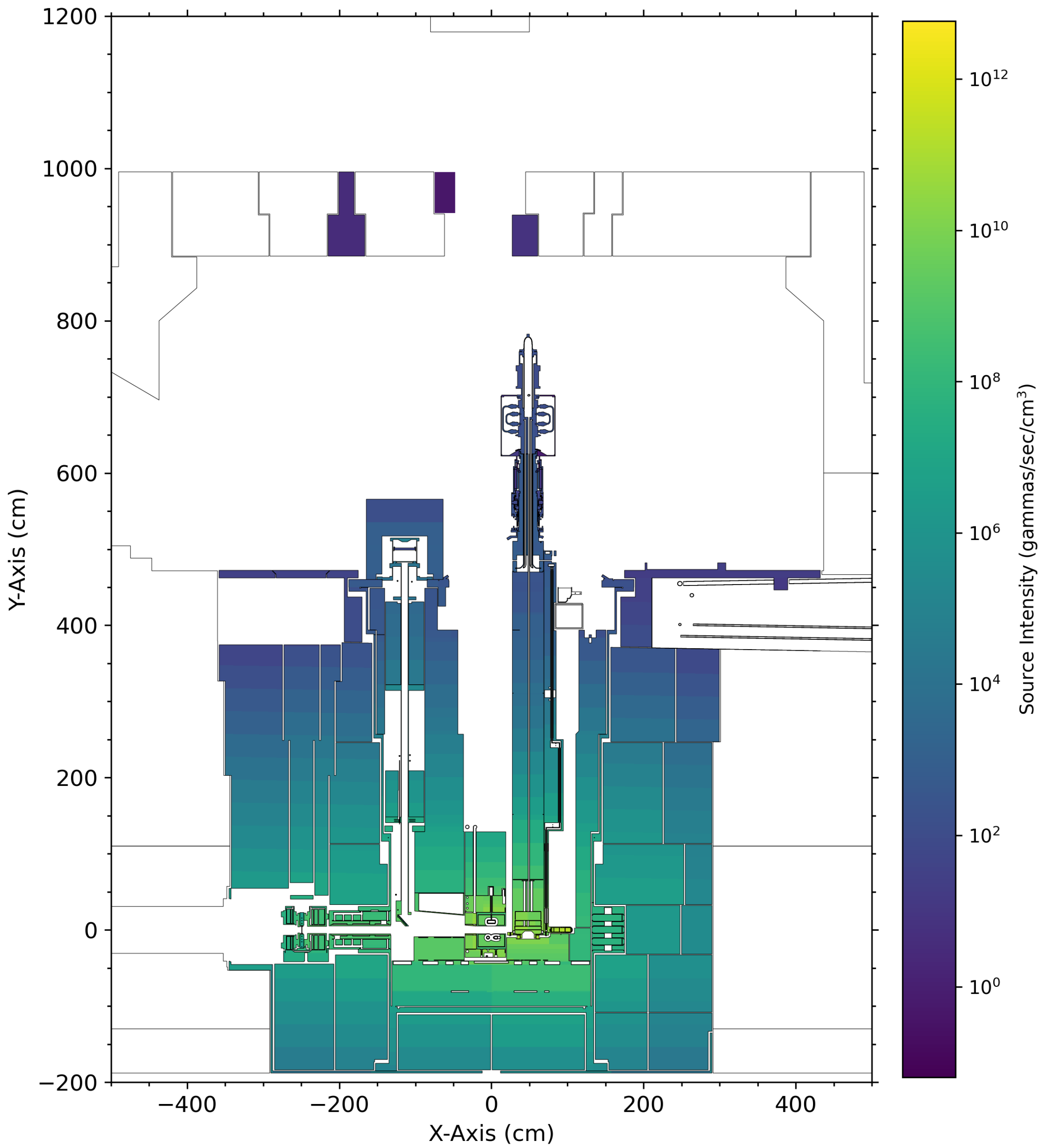

Figure 17. Cross section view of the decay gamma source intensity after 2 weeks of decay for the STS target system configuration 4a.

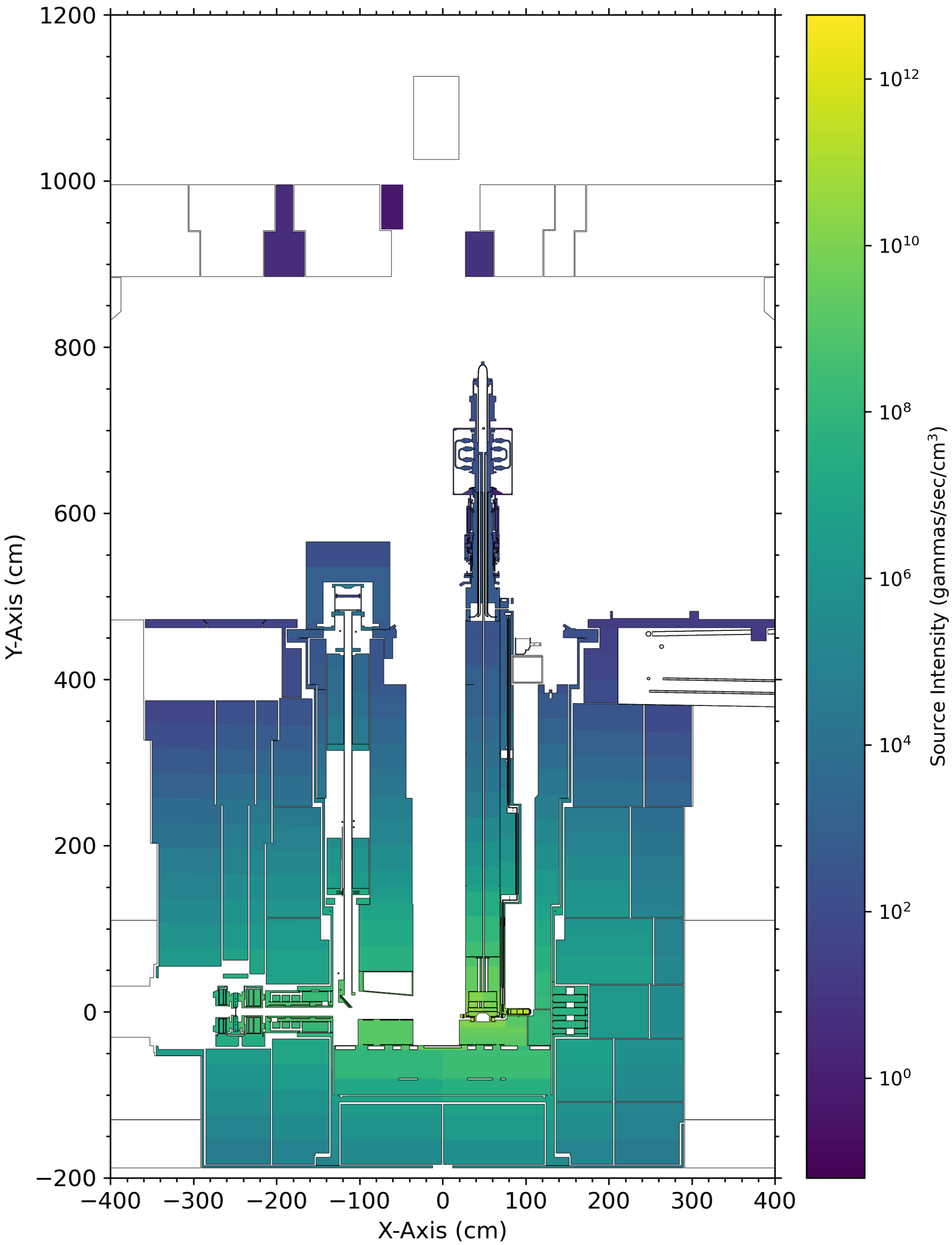

Figure 18. Cross section view of the decay gamma source intensity after 2 weeks of decay for the STS target system configuration 5.

4.2.4 Particle Transport

The residual gamma sources were created for a total of 14,991 geometry cells. The sources were then divided into 83-87 groups based on total source intensity in each cell for each geometric configuration. For each group of sources, a separate radiation transport simulation was performed. Finally, the dose rate distributions of the many runs were merged to obtain the final dose rate maps. Most of the results shown in Section 5 show the discrete ordinates transport solutions to the decay gamma dose from Denovo [11]. Only one case in the results section includes Monte Carlo results from MCNP®. MCNP® Code Version 6.2.0 is used to transport the decay gamma sources for the one case shown in Section 4.2.3 to the target drive room and high bay areas and tally photon dose rates as discussed in Section 4.2.6[12]. Weight windows are applied as a variance reduction technique to expedite convergence in the regions of interest and the details of the weight window generation are discussed in Section 4.2.5. The discrete ordinates solutions shown in Section 5 were generated separately from the weight windows using a finer resolution mesh and higher Pn order. The quadrature set used in the Denovo runs was generated by Joel Risner and is a midpoint Gauss quadrature set with 26 polar angles and 166 total angles per octant based on quadrature studies carried out by I.K. Abu-Sumays [14]. The spatial rectilinear grid used in the Denovo discrete ordinates calculation covered the spatial extent of the geometry and had a resolution of approximately 3 X 2 X 3 cm in the extent of the core vessel and target drive room. With some mesh resolution refinements around key gaps and pertinent features, the resulting mesh is between 49-90 million mesh elements. Outside of the core vessel and target drive room, the resolution is coarse (>10 cm). The discrete ordinates calculates utilized the 27n19g cross section library, a Pn order of 3 with a diagonal transport correction and a step characteristic discretization. The discrete ordinates solutions prove to be in good agreement with the Monte Carlo solution.

4.2.5 Variance Reduction

ADVANTG 3.2.0 was used to produce variance reduction parameters in the form of weight windows and source biasing to aid in the timely convergence of the tallies discussed in Section 4.2.6. The tally-of-interest in the ADVANTG run was a mesh tally that covered the full extent of the target drive room for all configurations. The quadrature set used in the ADVANTG run is described in Section 4.2.4. The spatial rectilinear grid used in the Denovo discrete ordinates calculation for ADVANTG covered the spatial extent of the geometry and had a resolution of approximately 5 X 10 X 5 cm in the extent of the core vessel and target drive room resulting in 14 million mesh elements. Outside of the core vessel and target drive room, the resolution was coarse (>10 cm). The weight windows generated with this spatial grid were then collapsed in ADVANTG by a factor of 2. A few of the runs required use of the cesaro transport correct while the majority of the runs were successful with a diagonal transport correction.

4.2.6 Tally Details

The photon effective dose rates are tallied with volume-averaged flux mesh tallies in the MCNP® calculation modified by dose energy and dose function (DE/DF) cards. The DE/DF cards applied the photon flux to effective dose conversion factors shown in Table E.1 of Appendix E with logarithmic interpolation of energy [15]. Post processing scripts described in Section 4.2.7 apply the dose response function shown in Table E.1 with energy logarithmically interpolated to the photon fluxes calculated with Denovo.

4.2.7 Post Processing

A Python script was written to combine the photon effective dose from 87 discrete ordinate runs for each configuration. This script loads in the forward flux file from each Denovo run, applies the dose response function described in Section 4.2.6, sums all runs, and produces a total effective photon dose rate map. The same script also loads each meshtal file from each MCNP® run, sums the mesh tallies, and propagates the uncertainties to generate a total effective photon dose rate map along with an uncertainty map. The geometry, source intensity, and dose plots are generated using the RTPlotter Python suite of tools developed by Joel Risner and Wouter de Wet.

5 ANALYSIS AND RESULTS

This section presents the results of the dose rate field analyses for the five target system configurations described in Section 4.2.1. The following subsections provide detailed descriptions of the calculated dose rates and radiation fields for each configuration, including comparisons with relevant requirements and limits. The results are organized by configuration, with each subsection focusing on a specific scenario and highlighting key findings and observations.

The dose rates shown in this report are photon dose rates only. The contribution to the total effective dose rate from photoneutrons in configurations 1-3 and 5 to the regions of interest is minimal. Configuration 4 is the only configuration where photoneutrons may significantly contribute to the dose rates in the target drive room.

All of the figures included in this section are colored according to the definitions of posted areas at ORNL [16]. The lowest level corresponds to a generally accessible area where dose rates are below 0.25 mrem/hr. The next highest level shows the extents of a controlled area where the dose rates are between 0.25 and 2.0 mrem/hr. A radiological buffer area (RBA) is represented by the zone between 2.0 and 5.0 mrem/hr. The zone of the figures between 5 and 100 mrem/hr represent the extents of a radiation area (RA). A high radiation area (HRA) is represented by the zone between 100 mrem/hr and 500 rem/hr. The highest zone shown in the figures shows the extents of a very high radiation area (VHRA) with dose rates greater than 500 rem/hr.

5.1 CASE 1: NOMINAL CONFIGURATION DOSE RATES

The results discussed in this section show the dose rates after 8 hours of decay for the nominal configuration of the STS target system. The nominal configuration consists of all core vessel shield blocks in place and all target system components are in operational positions. The figures in this section confirm compliance with the requirement stating the target drive room in nominal configuration shall be less then 5 mrem/hr after 8 hours of decay, Requirement 1774, and Requirement S.03.04-10944.

Figure 19 shows the decay dose rates as calculated with the discrete ordinates method described in Section 4.2.4 in a cross section view along the proton beam. Figure 19 shows a very high radiation area exists deep within the core vessel shielding surrounding the target segment wheel and MRA, and is inaccessible to personnel. The high radiation area is mostly buried in the core vessel shielding except for the area within the TVP shielding in the target drive room, but is nevertheless inaccessible to personnel. The dose rates in the target drive room are maximally a RBA (2-5 mrem/hr) due to the radiation around the TVP shield block and above the core vessel tent hatch over the MRA. Figure 19 shows that the area around the target drive assembly is largely a controlled area.

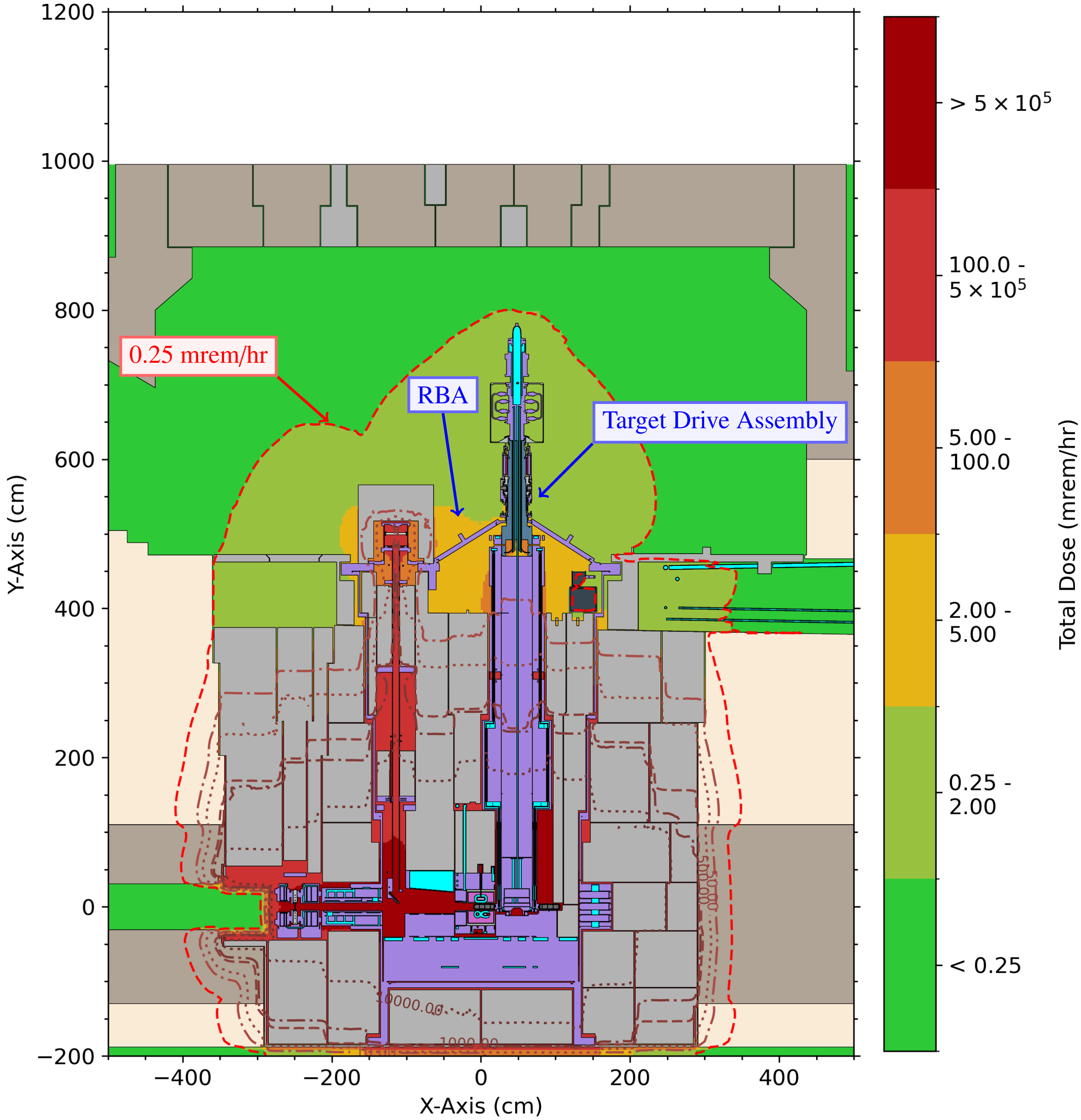

Figure 19. Cross section view of the discrete ordinates photon effective dose rate solution after 8 hours of decay in the target drive room and STS target system for the nominal configuration.

Figure 20 shows a plan view of the discrete ordinates dose rates at an elevation of 20 cm above the top of the core vessel shielding (415 cm above proton beam). The plan view in Figure 20 is taken at a working elevation if personnel are working under the target drive room floor elevation. Most of the accessible area underneath the core vessel lid is a radiation buffer area except for the region within 20 cm of the target.

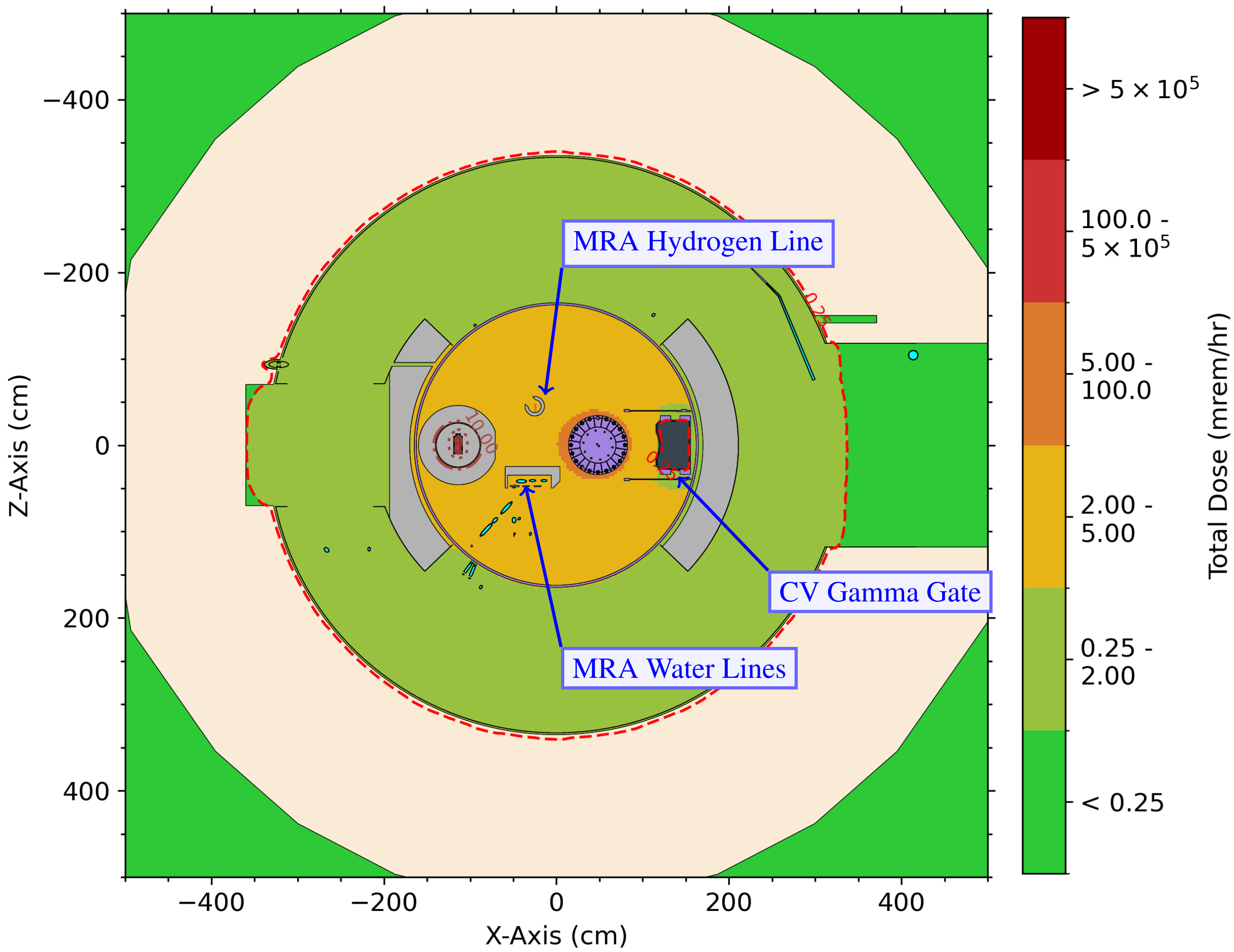

Figure 20. Plan view at a working elevation just below the target drive room floor (415 cm above beam center) of the discrete ordinates photon effective dose rate solution after 8 hours of decay in the target drive room for the nominal configuration.

Figure 21 shows a plan view of the discrete ordinates dose rates at an elevation of 20 cm above the target drive room floor (500 cm above proton beam). The only accessible radiation area is around the target assembly. Most of rest of the area directly over the core vessel shielding is a controlled area with the exception of the area surrounding the TVP, where the region is a radiation buffer area. The region of the target drive room outside of the core vessel is could be a generally accessible area based on dose rate. Figure 22 shows an elevation view of the dose rate field cut perpendicular to the proton beam, through the center of the TVP. The radiation emanating from the opening in the TVP causing the radiation area extends out past the opening by < 50 cm.

Draft. Not approved for public release.
The only OFFICIAL COPY of this document is the on-line electronic version in ORNL's document management application.
Before using a printed copy, verify that it is the most current version.

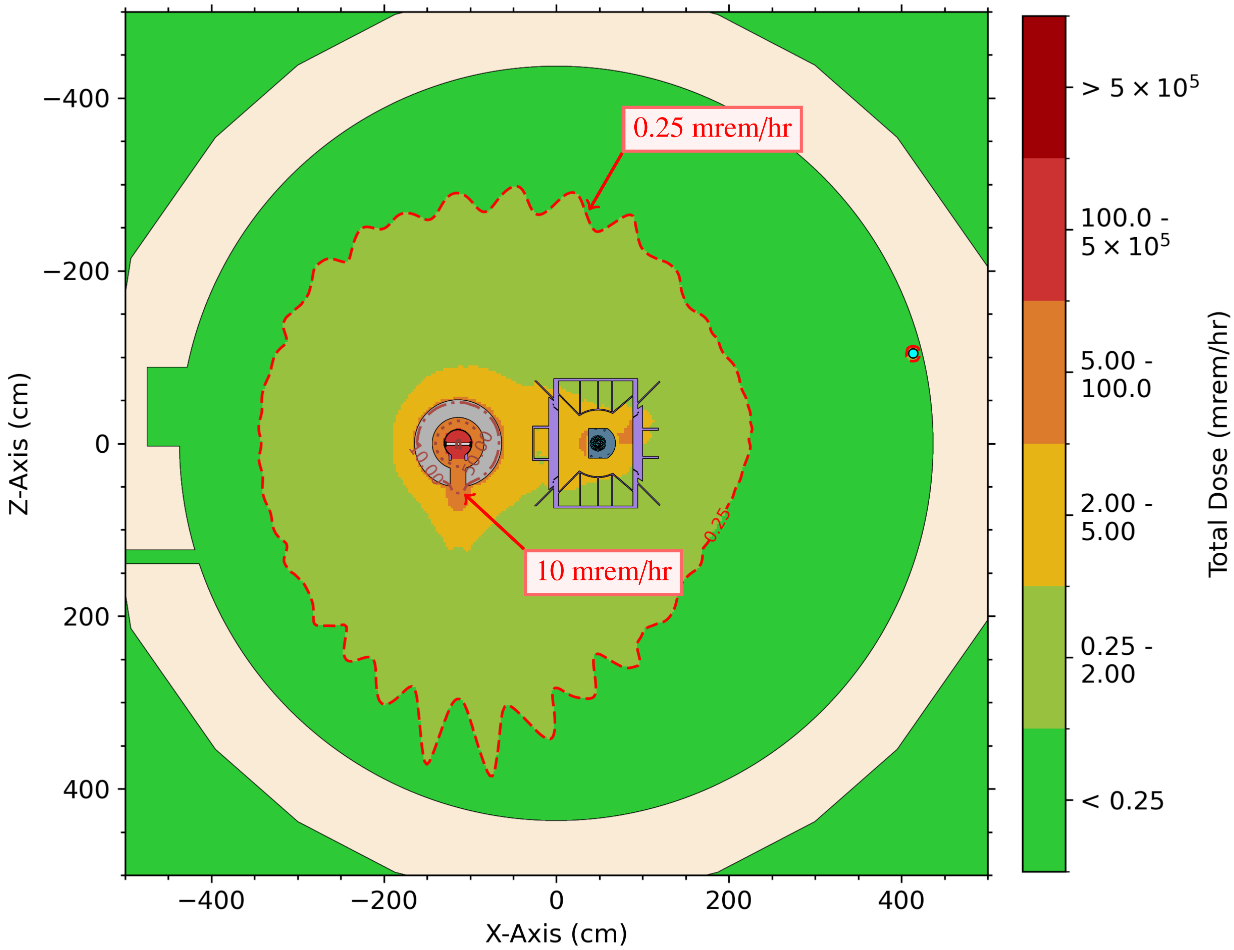

Figure 21. Plan view at 20 cm above the elevation of the target drive room floor (500 cm above beam center) of the discrete ordinates photon effective dose rate solution after 8 hours of decay in the target drive room for the nominal configuration.

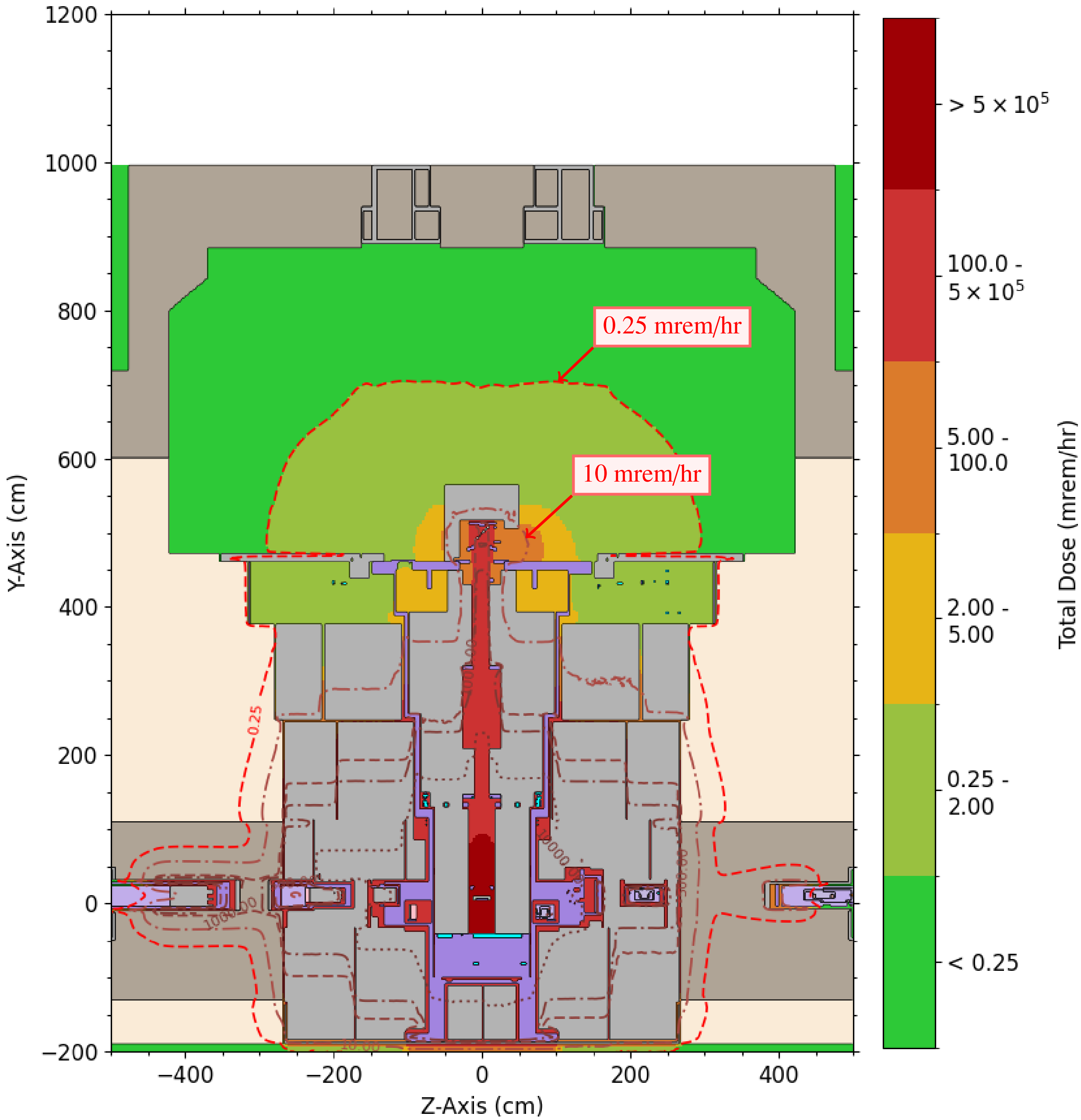

Figure 22. Elevation view at -113.9 cm upstream of the target through the center of the TVP of the discrete ordinates photon effective dose rate solution after 8 hours of decay in the target drive room for the nominal configuration.

5.2 CASE 2: SINGLE TARGET SEGMENT REMOVED

The results discussed in this section show the dose rates after 8 hours of decay for the configuration where a single target segment is removed, the lead gamma gate is deployed and the removable target segment access shield block is removed. The figures shown in this section confirm compliance with Requirement S.03.06-7125.

Figure 23 shows the decay dose rates as calculated with the discrete ordinates method described in Section 4.2.4 in a cross section view along the proton beam for the target segment removal configuration. The dose rate map shown in Figure 23 supports maintenance operations occurring above the lead gamma gate while the segment has been removed. Due to gaps between the core vessel gamma gate and the target assembly, radiation areas are present in human occupiable spaces where the highest dose in these areas does not exceed 50 mrem/hr except for a very small space located at the bottom of the gamma gate. The RA extends up the target drive showing that during hands on maintenance activities of the target drive in this configuration, the workers will have to enter a RA. The 10 mrem/hr contour is shown and labeled in Figure 23. The RBA shown in yellow in Figure 23 extends up into the target drive room 1.2 m.

Draft. Not approved for public release.
The only OFFICIAL COPY of this document is the on-line electronic version in ORNL's document management application.
Before using a printed copy, verify that it is the most current version.

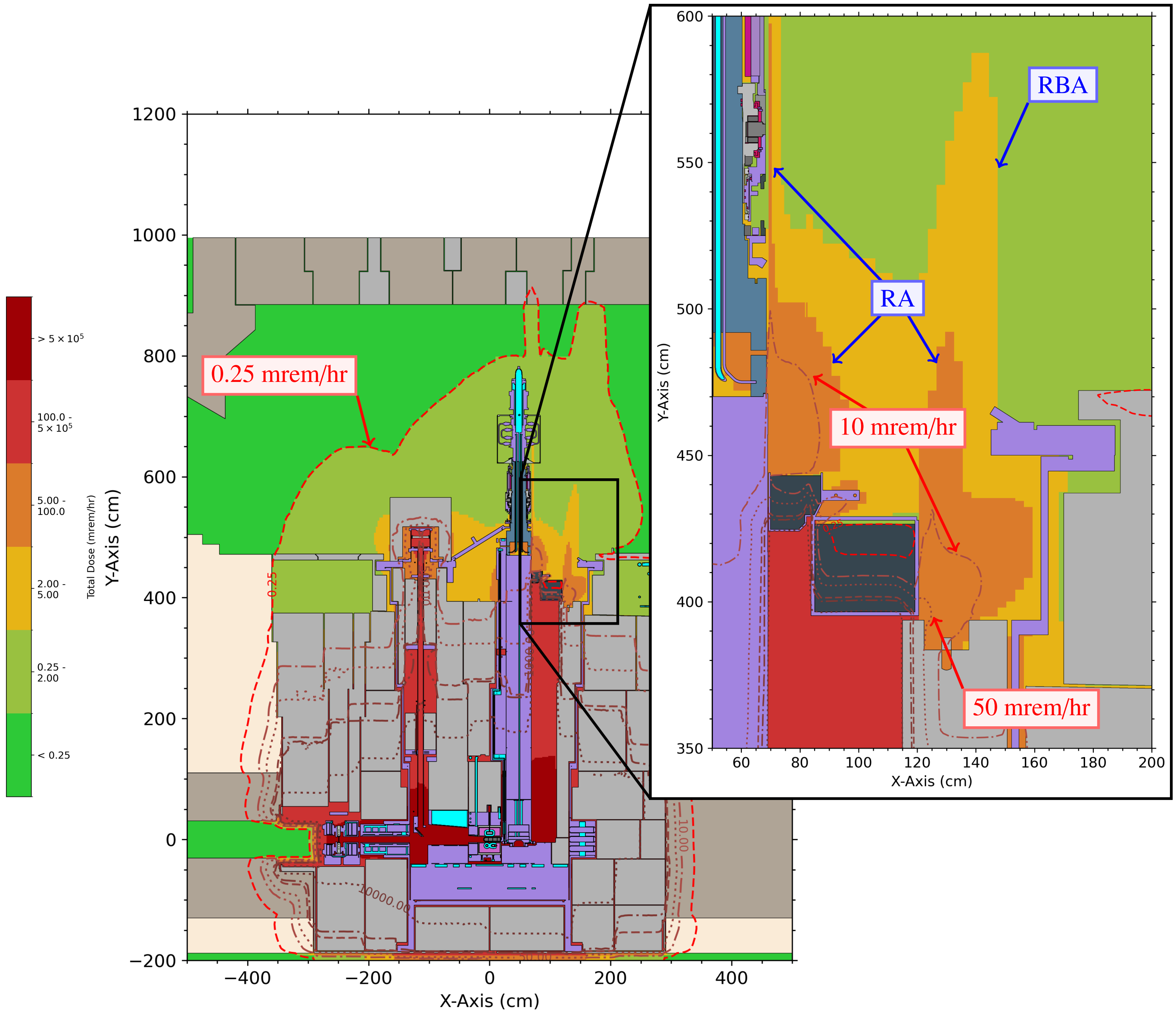

Figure 23. Cross section view of the discrete ordinates photon effective dose rate solution after 8 hours of decay in the target drive room and STS target system for the target segment removal configuration.

Figure 24 shows a plan view of the working area at an elevation of 455 cm above the proton beam. This elevation corresponds to the elevation of the target segment water seals that may have to be a part of hands-on maintenance. The high radiation area is present in between two segments but is overall very thin in the plan view.

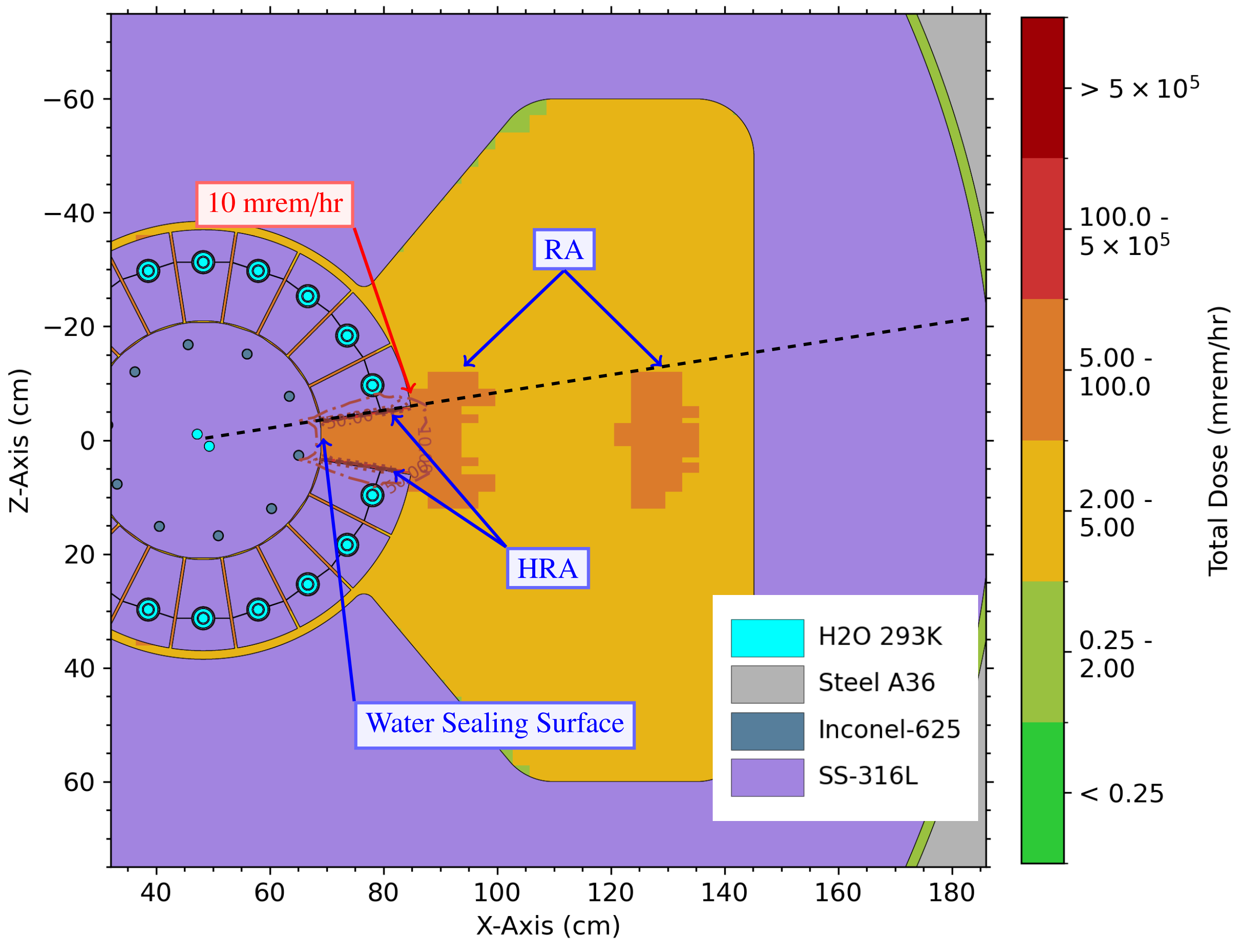

Figure 24. Plan view at the working height at an elevation of 455 cm above the proton beam of the discrete ordinates photon effective dose rate solution after 8 hours of decay in the target drive room and STS target system for the target segment removal configuration.

The high radiation areas shown in Figure 24 are near where hands-on maintenance may be required to the water sealing surface of the target segment to the target crown. Figure 25 shows a slice through the thin high radiation area (along the black dashed line shown in Figure 24) showing the extents of the radiation area in height and distance from the target shaft.

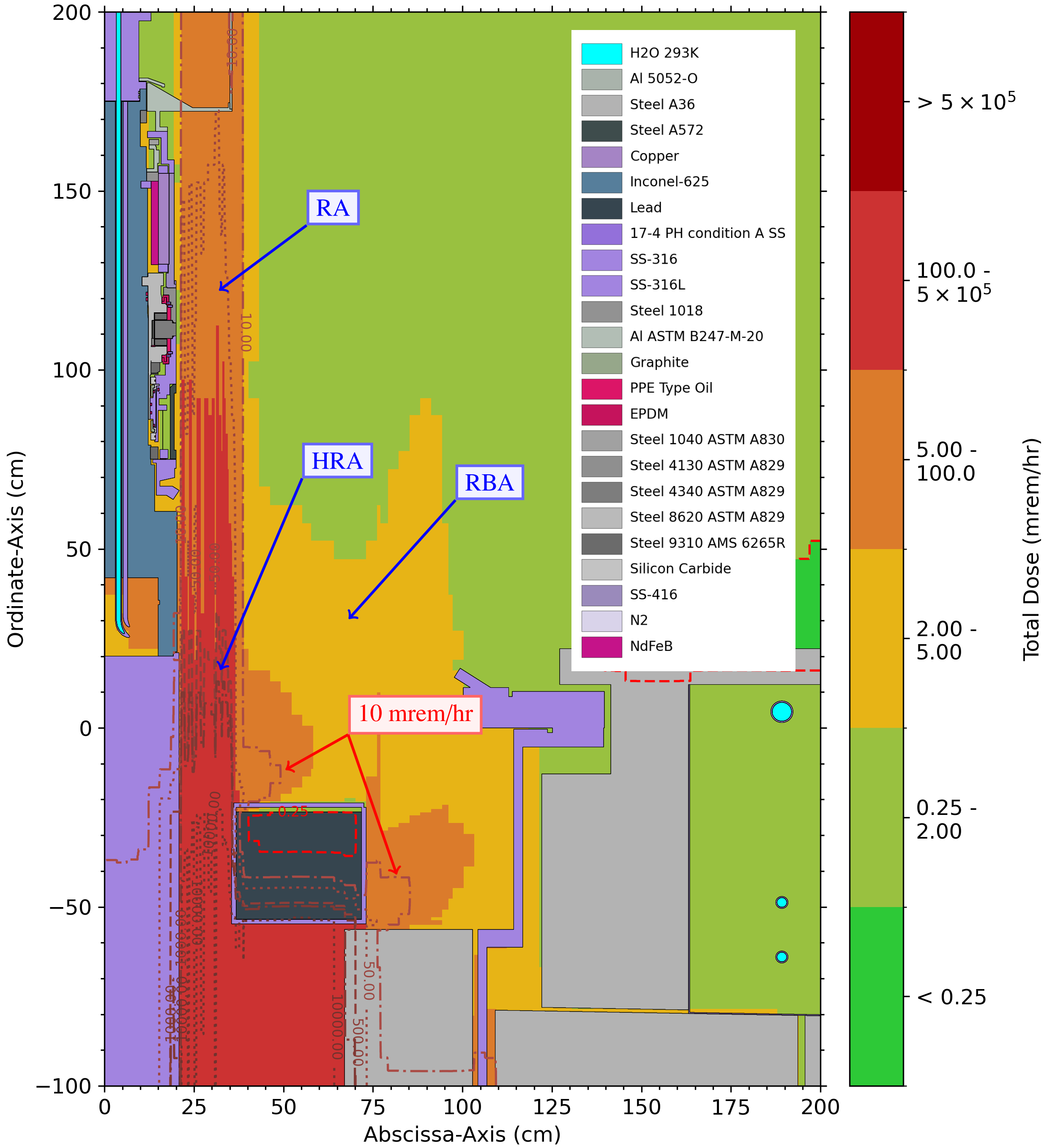

Figure 25. View through the high radiation area in the gap between the gamma gate and target segment of the discrete ordinates photon effective dose rate solution after 8 hours of decay in the target drive room and STS target system for the target segment removal configuration.

5.3 CASE 3: THIRD TARGET SEGMENT REMOVAL

The results presented in this section correspond to the configuration where two target segments have been removed and the third target segment is positioned for removal, after 2 weeks of decay. In this scenario, the core vessel gamma gate is closed with one gamma gate shielding arm deployed, and the removable target segment access shield block has been removed. The figures shown in this section confirm compliance with Requirement S.03.06-7125.

Figure 26 illustrates the calculated decay dose rate field using the discrete ordinates method (Section 4.2.4) in a cross-sectional view along the proton beam axis for this third target segment removal configuration. The orange-colored radiation area in Figure 26 is primarily attributed to the unmitigated opening in the target assembly, resulting from the removal of a target segment located two positions away from the current removal position. Notably, dose rates exceeding 50 mrem/hr are present in accessible areas of the target drive room.

A plan view at an elevation of 1 m above the target drive room floor is shown in Figure 27. The radiation area and high-radiation area depicted in Figure 27 are concentrated around the target shaft and downstream of the target. However, Figure 27 also exhibits ray effects, which are artifacts of the discrete ordinates method used for calculating decay gamma dose rates. These ray effects will be mitigated in future calculations using Monte Carlo methods, providing a more accurate representation of the radiation field.

Draft. Not approved for public release.
The only OFFICIAL COPY of this document is the on-line electronic version in ORNL's document management application.
Before using a printed copy, verify that it is the most current version.

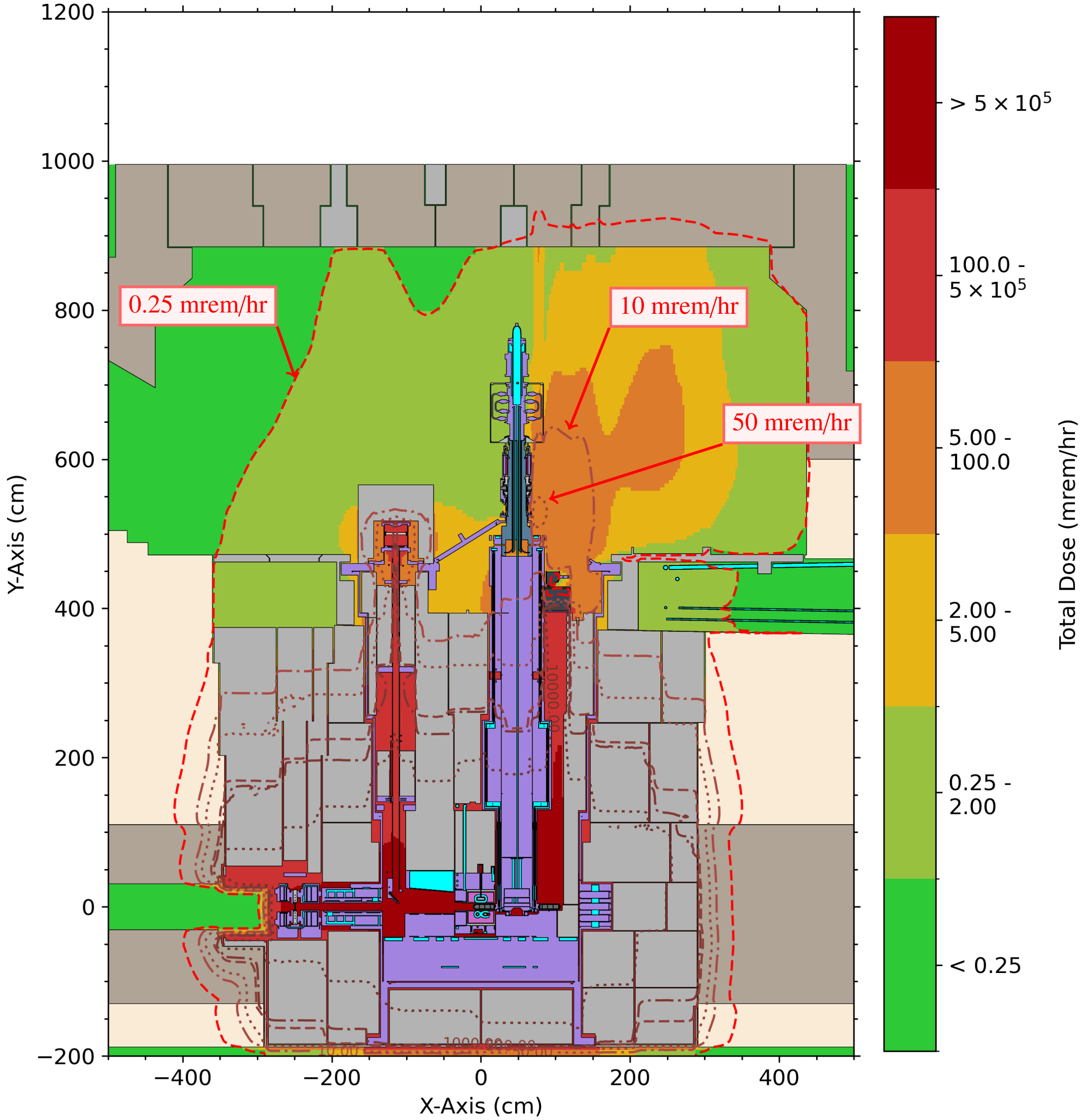

Figure 26. Cross section view of the discrete ordinates photon effective dose rate solution after 2 weeks of decay in the target drive room and STS target system for the third target segment removal configuration.

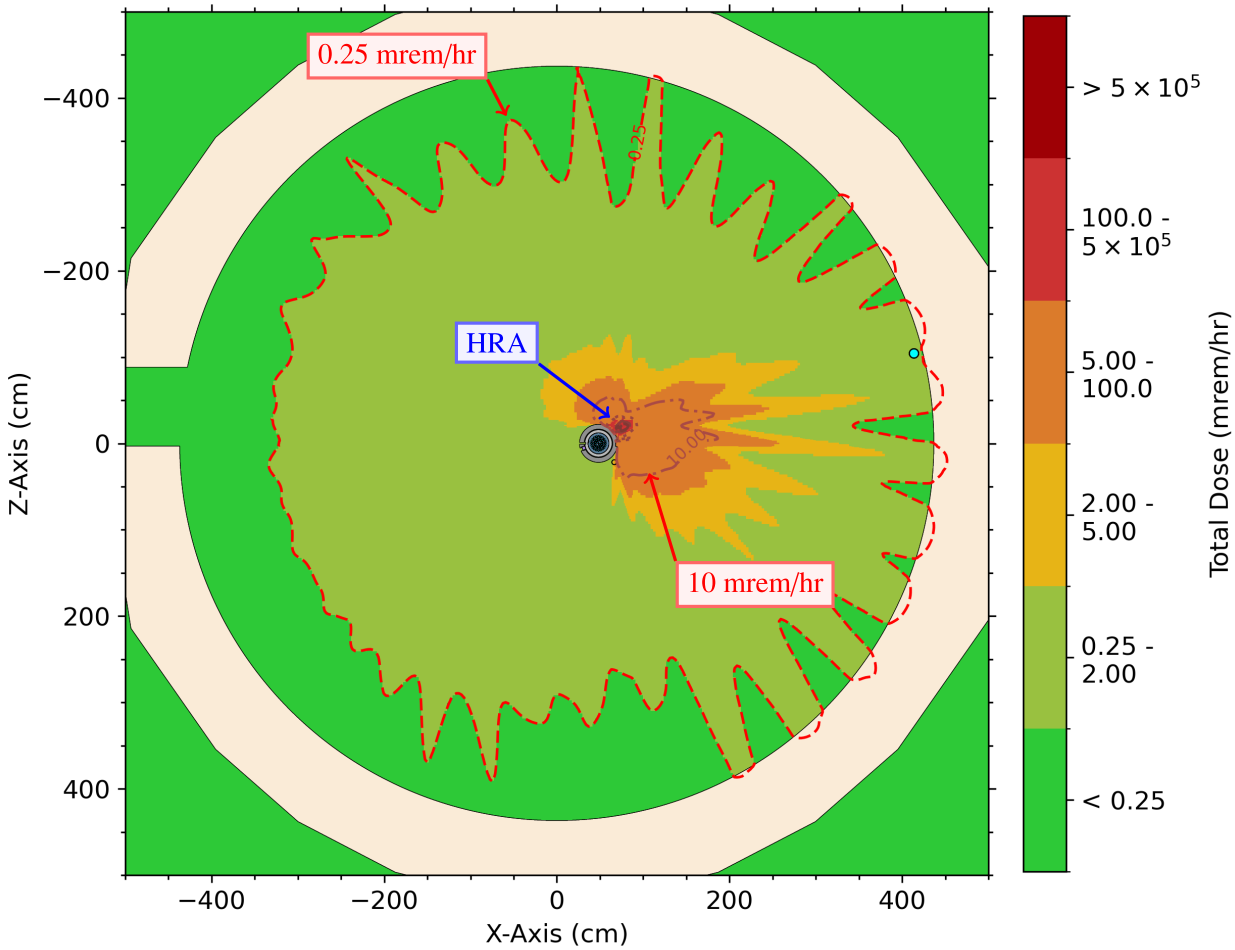

Figure 27. Plan view 1 m above the TDR floor of the discrete ordinates photon effective dose rate solution after 2 weeks of decay in the target drive room and STS target system for the third target segment removal configuration.

Figure 28 presents a detailed view of the target drive room downstream of the target assembly in a cross-sectional view along the proton beam axis. The radiation area is observed to extend more than 2 m from the target shaft, while the radiation buffer area (yellow) extends beyond 3 m. Although Figure 28 shows a cross-section along the proton beam, it is notable that the primary source of radiation streaming into the target drive room is the unmitigated opening left by the removal of the first target segment, which is not shielded by the core vessel gamma gate.

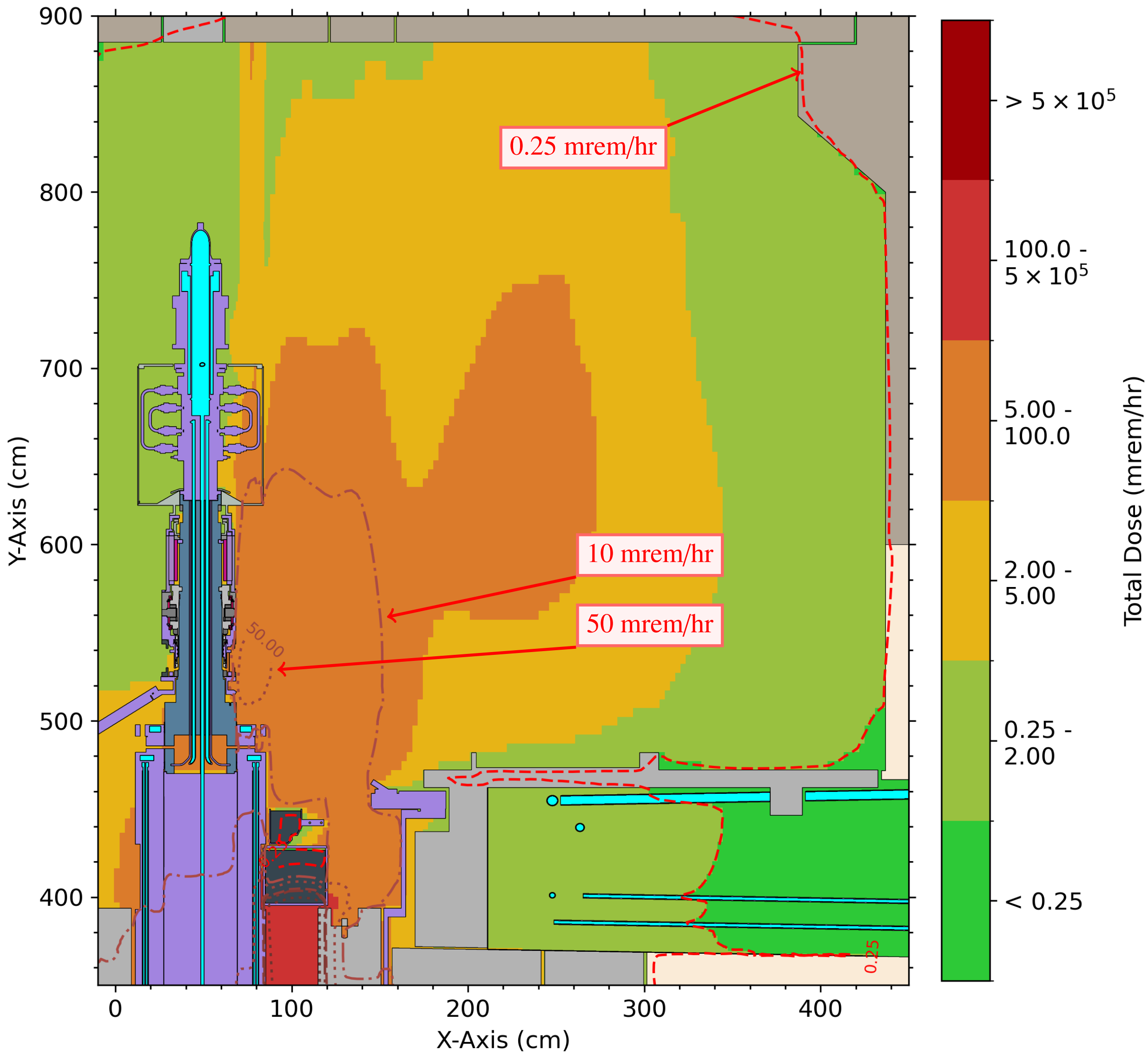

Figure 28. Cross section view of the discrete ordinates photon effective dose rate solution after 2 weeks of decay in the target drive room and STS target system for the third target segment removal configuration zoomed in on the downstream region of the target drive room.

To further investigate this phenomenon, Figures 29 and 30 provide a closer examination of the radiation streaming through the hole. Figure 29 displays a plan view of the residual dose rates at an elevation of 438 cm above the proton beam axis, highlighting the gamma gate arm configuration. The high-radiation area (red) indicates that the current design of the gamma gate does not effectively mitigate the radiation streaming through the open hole left by the removal of the first target segment. A cross-sectional view along the black dashed line in Figure 29 is presented in Figure 30.

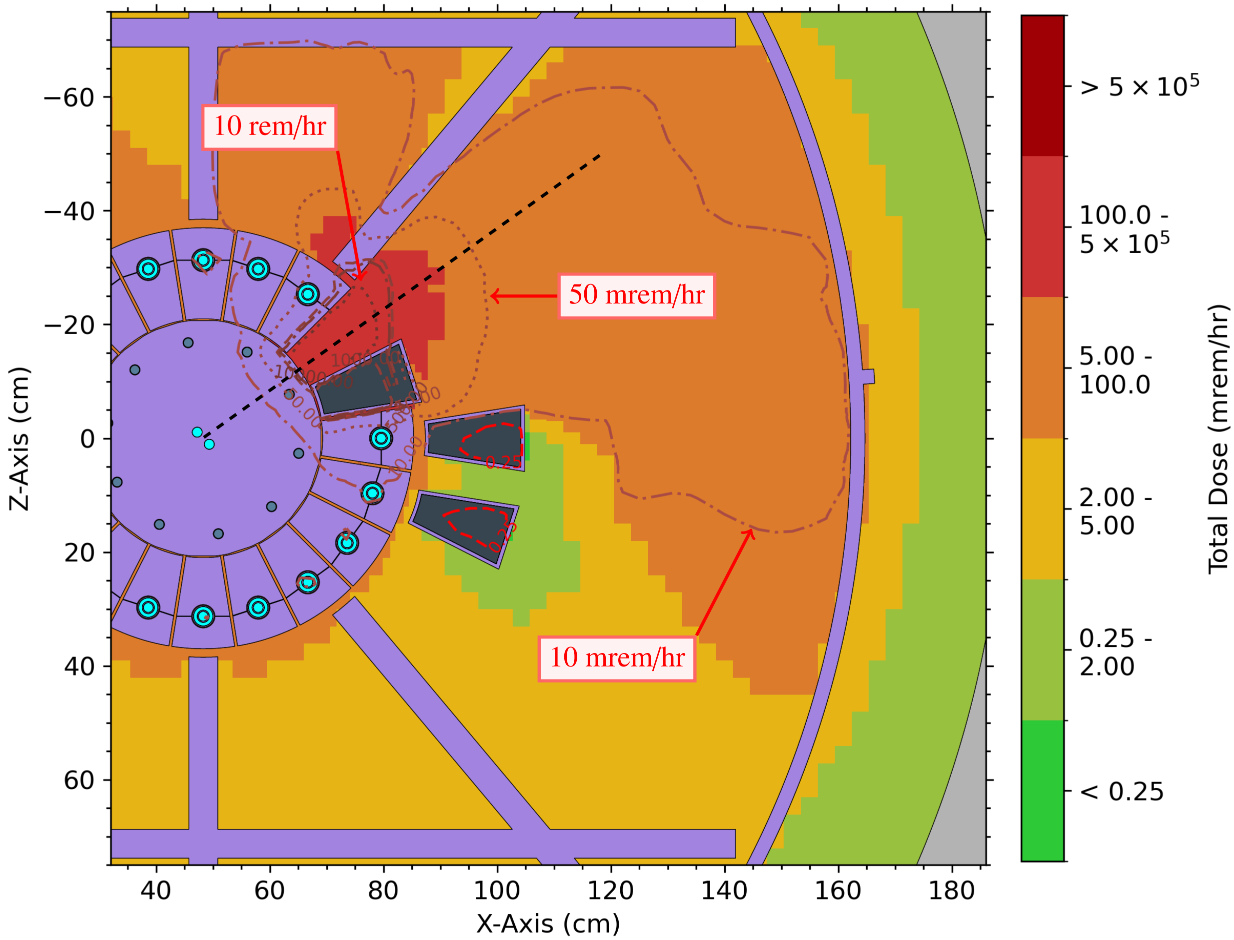

Figure 29. Plan view at 438 cm above the proton beam of the discrete ordinates photon effective dose rate solution after 2 weeks of decay in the target drive room and STS target system for the third target segment removal configuration zoomed in on the downstream region of the target drive room.

Figure 30 illustrates the vertical extent of the high-radiation area, which reaches up to the roof of the target drive room. Despite the core vessel lid covering this region, it provides minimal shielding against the radiation streaming through the open hole. The plot's origin is set at the midpoint of the target shaft (abscissa axis) and floor level of the target drive room (ordinate axis). Notably, the high-radiation area remains within 30 cm radially from the target drive shaft, while the radiation area extends out to more than 70 cm beyond the surface of the target shaft. These findings emphasize the importance of accounting for this significant radiation streaming during maintenance planning.

Draft. Not approved for public release.
The only OFFICIAL COPY of this document is the on-line electronic version in ORNL's document management application.
Before using a printed copy, verify that it is the most current version.

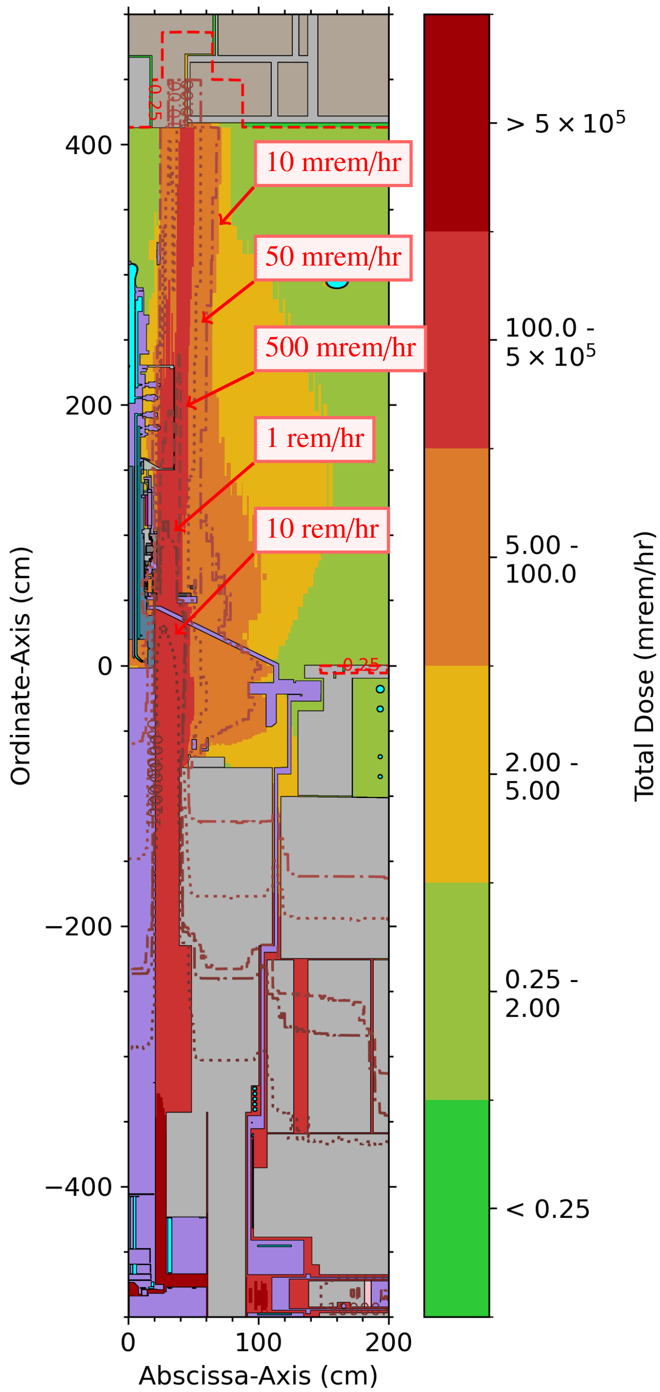

Figure 30. Cross section view of the discrete ordinates photon effective dose rate solution after 2 weeks of decay in the target drive room and STS target system for the third target segment removal configuration zoomed in on the downstream region of the target drive room.

5.4 CASE 4: MRA PIPE CUTTING

The results presented in this section pertain to the fourth configuration, where the hydrogen and water transfer pipes stemming from the MRA are prepared for removal by cutting. This configuration involves the removal of the MRA removable shield block, both core vessel tent hatches, three target segments, and the deployment of all three gamma gate arms. Additionally, the hatch in the target drive room ceiling is open to the high bay. To determine which scenario minimizes radiation exposure for pipe-cutting workers, two sub-configurations are evaluated: one with the hole caused by the removal of three target segments located on the downstream end of the target and another with the hole on the upstream end. The figures shown in this section confirm compliance with Requirement S.03.10.05-10942.

The contribution to the residual dose rates from photoneutrons are not included in the figures discussed in this section. Future analyses should consider the photoneutrons' contribution to the residual dose rates in the MRA pipe cutting configuration.

5.4.1 Case 4A: MRA Pipe Cutting with Downstream Target Segments Hole

A comparison between the discrete ordinates and Monte Carlo methods (described in Section 4.2.4) is performed for the sub-configuration with the hole on the downstream end. The errors associated with the Monte Carlo solutions show that the solutions are generally converged and are shown in Appendix F. All Monte Carlo solutions shown in this section are showing the dose rate plus 2 σ Monte Carlo transport uncertainty. The Monte Carlo solutions show the residual dose rate field from a combination of 80 out of 83 decay gamma sources. Due to the good agreement between the discrete ordinates solution, which has all decay gamma sources contributions, and the Monte Carlo solution, the remaining three decay gamma sources (PBW sources) are negligible.

The results show good agreement between the two methodologies, as illustrated in Figure 31. The dose rate map obtained from the Monte Carlo solution is limited to the TDR between the elevations from 360 cm to 885 cm above the proton beam. While the radiation and high-radiation areas are similar, differences are observed in the radiation buffer and controlled areas. Notably, the Monte Carlo solution yields a larger controlled area compared to the discrete ordinates solution. This discrepancy can be attributed to the better representation of backscatter effects in the Monte Carlo methodology, which more accurately captures the scattering of radiation off the ceiling. Another region where differences are evident is near the core vessel gamma blocker, as shown in Figure 32. These discrepancies arise from the distinct geometries used in each method: the voxelized geometry employed in the discrete ordinates solution versus the exact geometry used in the Monte Carlo solution. The Monte Carlo geometry more accurately captures the gaps around the core vessel gamma blocker and resolves the water connections in the target water crown.

Draft. Not approved for public release.
The only OFFICIAL COPY of this document is the on-line electronic version in ORNL's document management application.
Before using a printed copy, verify that it is the most current version.

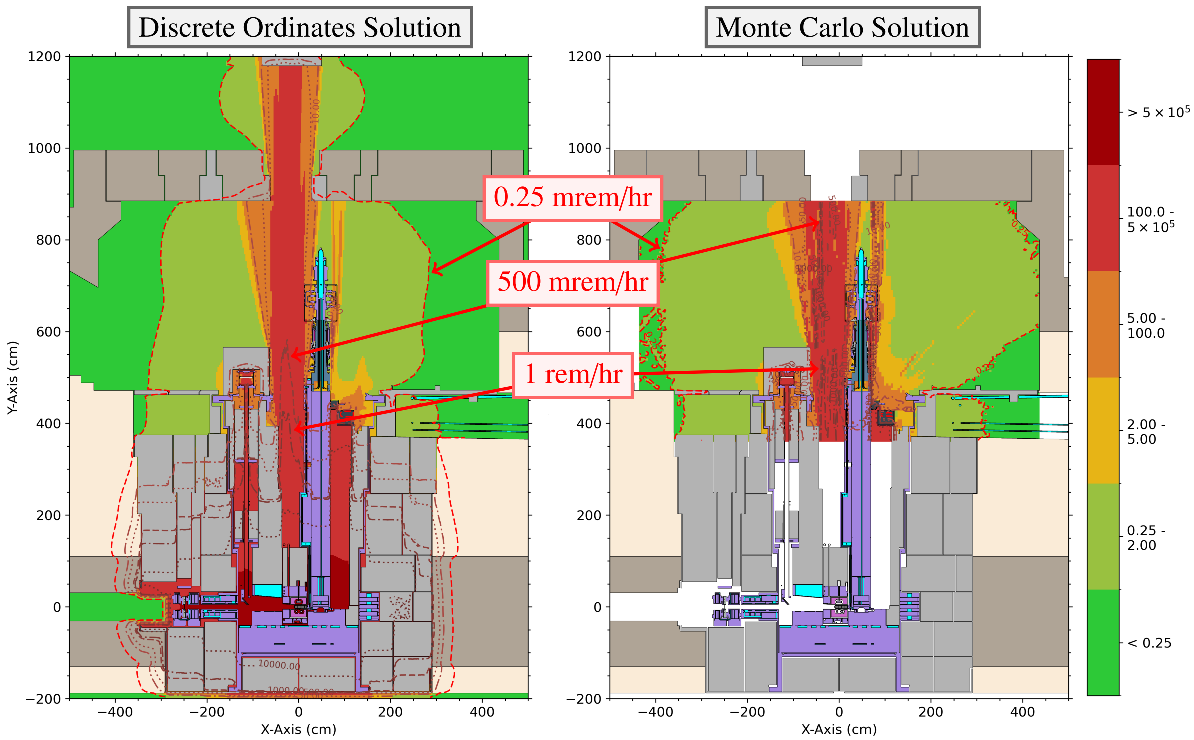

Figure 31. Cross section view along the proton beam of the photon effective dose rate after 2 weeks of decay in the target drive room and STS target system for the MRA pipe cutting configuration.

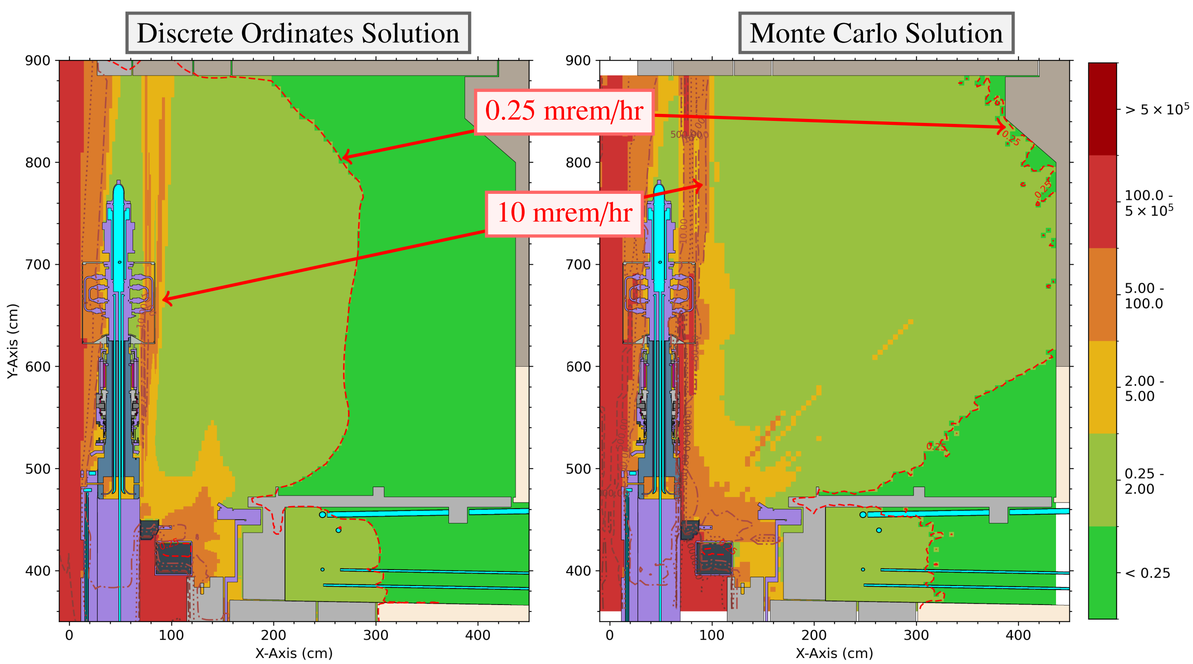

Figure 32. Cross section view along the proton beam of the photon effective dose rate after 2 weeks of decay in the target drive room and STS target system for the MRA pipe cutting configuration zoomed in on the region downstream of the target.

Draft. Not approved for public release.
The only OFFICIAL COPY of this document is the on-line electronic version in ORNL's document management application.
Before using a printed copy, verify that it is the most current version.

Figure 33 shows a plan view of the dose rate field for the MRA pipe-cutting configuration at an elevation of 1 m above the target drive room floor for both the discrete ordinates and Monte Carlo solutions. The solutions are in good agreement and show that the TDR is accessible for maintenance personnel. The radiation and high radiation areas in Figure 33 are centrally located around the open hole caused by the absence of the MRA removable shield block and do not extend more than 1 m from the hole boundary. The maximum dose rate in the figure is 1.3 rem/hr and is notated on the figure.

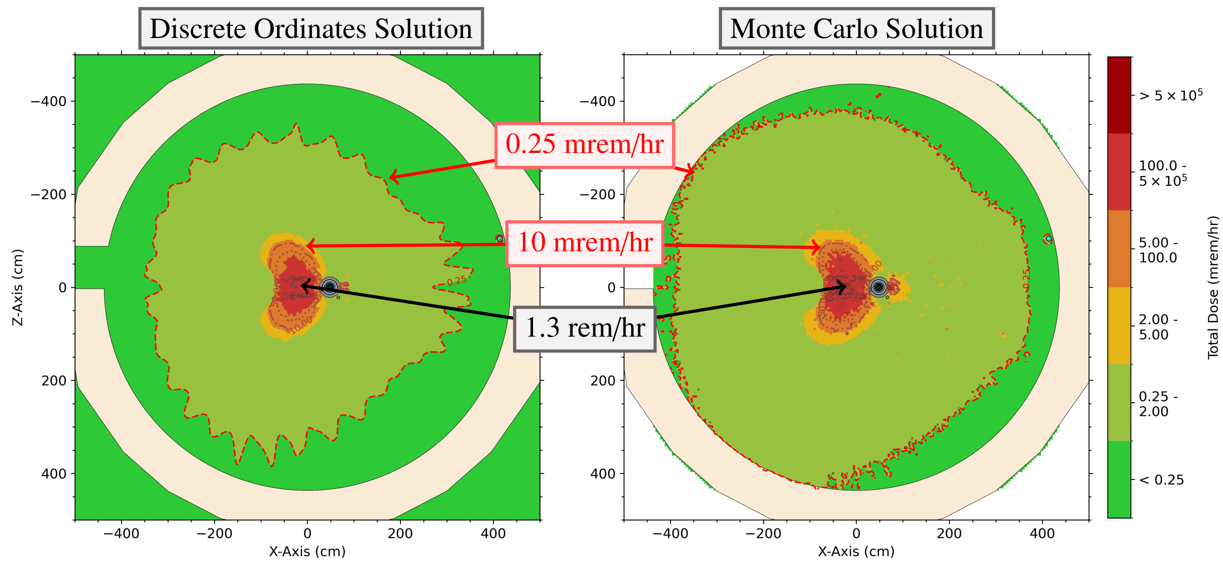

Figure 33. Plan view at an elevation of 1 m above the TDR floor of the photon effective dose rate after 2 weeks of decay in the target drive room and STS target system for the MRA pipe cutting configuration.

5.4.2 Case 4B: MRA Pipe Cutting with Upstream Target Segments Hole

Only the discrete ordinates method was used for Case 4B where the configuration is largely the same as Case 4A described in Section 5.4.2 except for the hole left by the removal of three target segments is rotated to be upstream of the target shaft. By rotating the hole, a larger gap between the MRA and target shaft is opened and allows much more radiation to stream through to the TDR. All of the figures in this section show both Case 4A & 4B for direct comparison of the placement of the hole left by the removal of the three target segments.

Figure 34 shows the decay gamma dose rates for both Cases 4A & 4B. All radiation dose rate categories upstream of the target shaft cover larger areas in Case 4B as compared to Case 4A due to the larger opening between the MRA and target shaft in Case 4B. The high bay area also saw increases in the radiation streaming into the area. With more radiation incident on the crane hook block in the high bay, the radiation buffer and controlled areas push out considerably in Case 4B when compared with Case 4A.

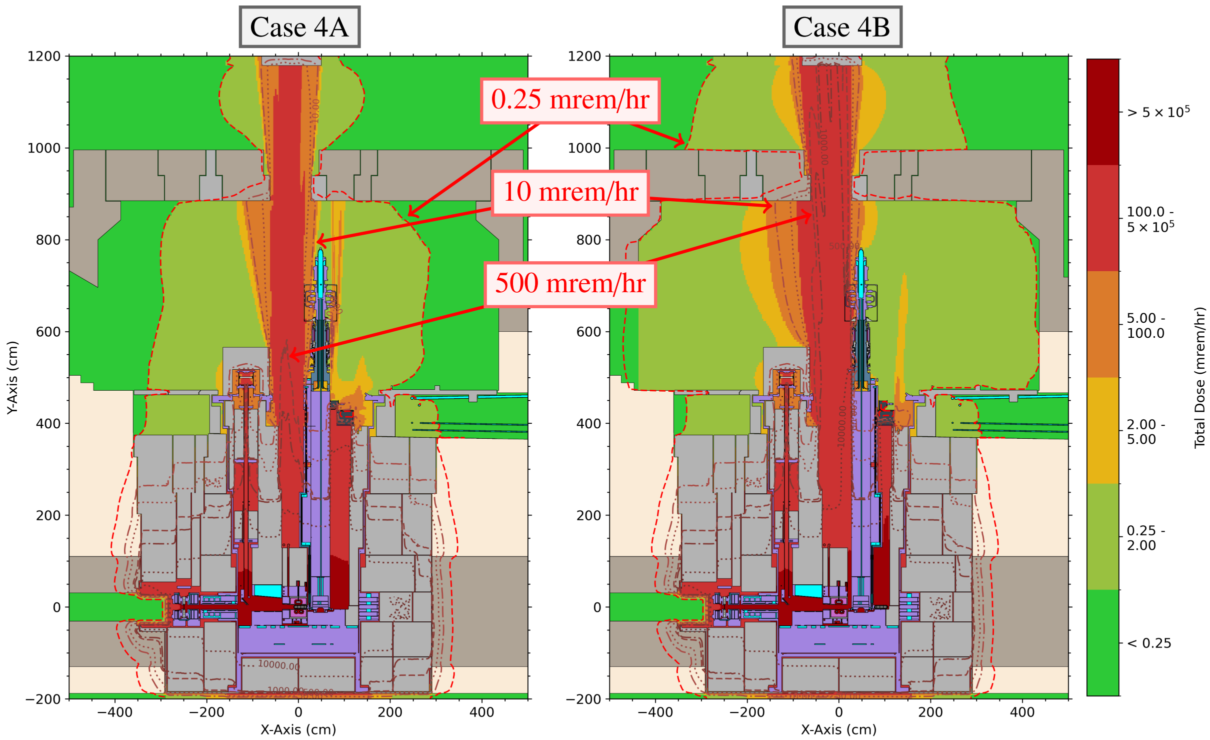

Figure 34. Cross section view along the proton beam of the photon effective dose rate after 2 weeks of decay in the target drive room and STS target system for the MRA pipe cutting configuration showing Cases 4A & 4B.

Figure 35 shows the downstream portion of the target drive room for both Cases 4A & 4B. Figure 35 for Case 4B shows that the 0.25 mrem/hr boundary extends out to the outer wall of the target drive room as compared to Case 4A where the boundary leaves around 1.5 m of space between it and the wall. However, the radiation buffer and radiation areas on the downstream side target shaft that reach to the ceiling in Case 4A are not present in Case 4B. Due to the absence of the target segment in Case 4A, the very hot sources in the bottom of the core vessel are free to stream up a relatively large opening before being collimated down to the gaps between the core vessel gamma gate and the target segments and shaft. The streaming up the large opening and then collimation down to small gaps near the top leads to strong radiation streaming into the target drive room. Case 4B mitigates this issue with the inclusion of the target segment. The target segment and in particular the segment's stave acts more as a shield than a source in Case 4B where the radiation is collimated much further down in the core vessel.

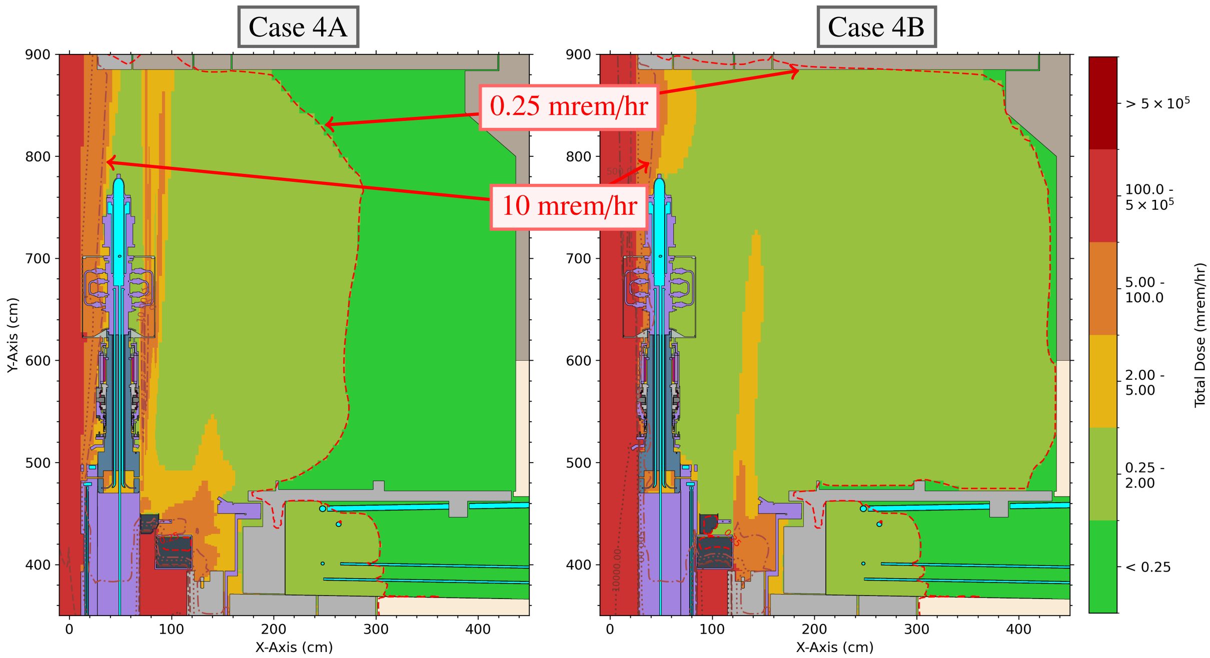

Figure 35. Cross section view along the proton beam of the photon effective dose rate after 2 weeks of decay in the target drive room and STS target system for the MRA pipe cutting configuration zoomed in on the region downstream of the target for both Cases 4A & 4B.

Figure 36 shows a detail view of the upstream portion of the target drive room with Cases 4A & 4B shown for direct comparison. The controlled area in Case 4B extends to the entrance of the TDR whereas is Case 4A, the controlled area begins approximately 1 m from the entrance to the TDR. The radiation buffer and radiation areas in Case 4B extend out past the TVP towards the entrance of the TDR.

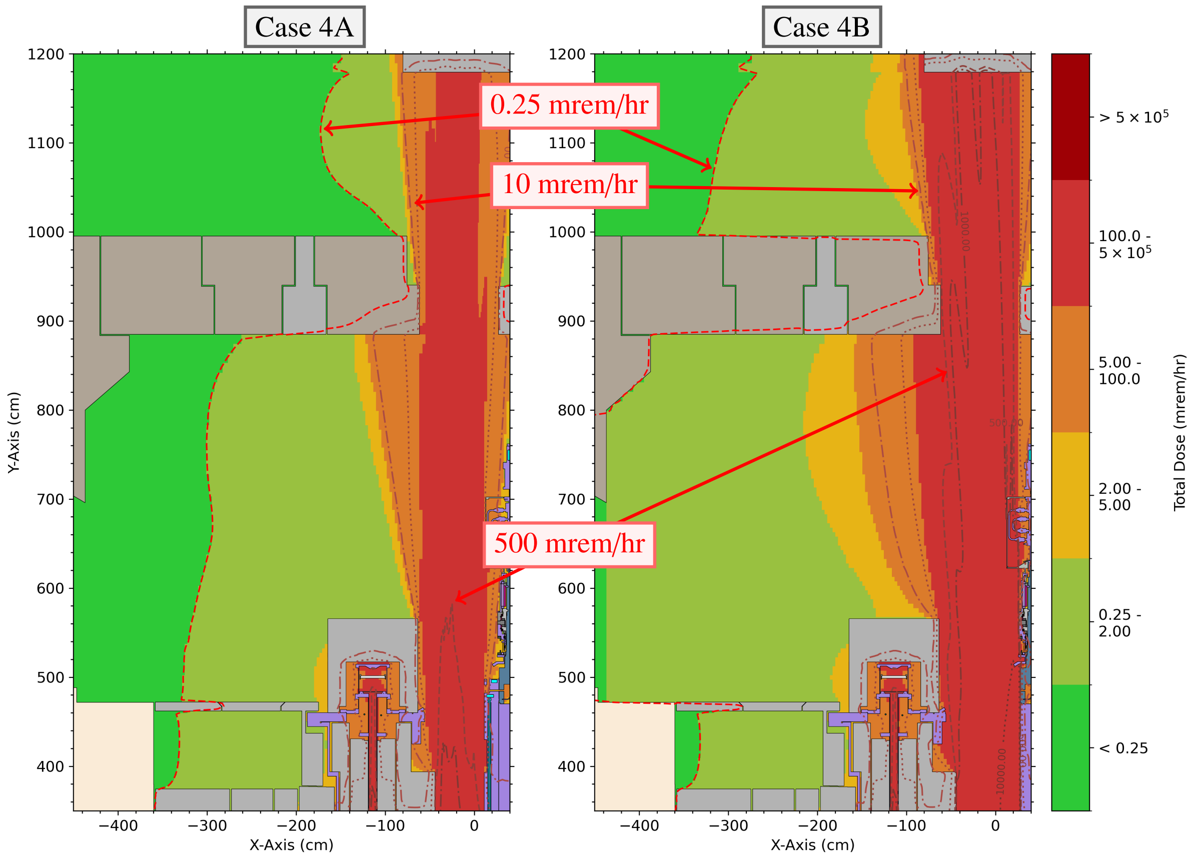

Figure 36. Cross section view along the proton beam of the photon effective dose rate after 2 weeks of decay in the target drive room and STS target system for the MRA pipe cutting configuration zoomed in on the region upstream of the target for Cases 4A & 4B.

Figure 37 shows an plan view of the TDR at an elevation of 1 m above the TDR floor for Cases 4A & 4B. Case 4B shows more prominent ray effects from the discrete ordinates methodology in the radiation buffer area and overall increase in the dose rate fields as compared to Case 4A. Figure 37 shows that entrance to the TDR is feasible in the MRA pipe-cutting configuration in either Case 4A or 4B.

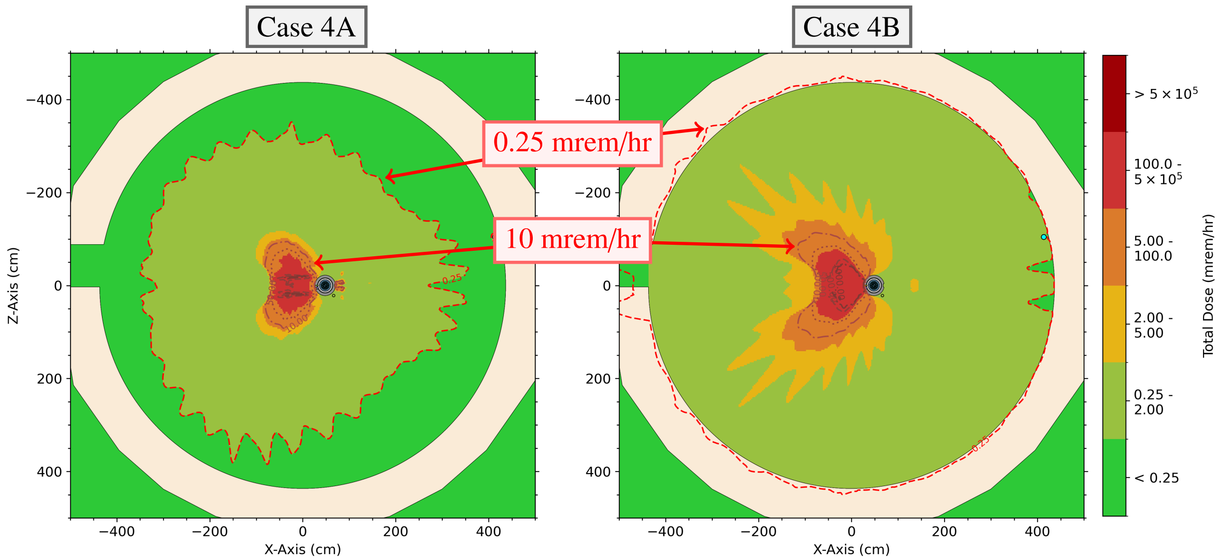

Figure 37. Plan view at an elevation of 1 m above the TDR floor of the photon effective dose rate after 2 weeks of decay in the target drive room and STS target system for the MRA pipe cutting configuration for Cases 4A & 4B.

5.5 CASE 5: MRA REMOVED

The discrete ordinates method was used for Case 5 where the configuration is largely the same as Case 4A described in Section 5.4.2 except for the MRA has been completely removed. The figures shown in this section confirm compliance with Requirement S.03.06-7125.

Figure 38 shows an overview of the residual gamma dose rate field for configuration 5, the MRA removed configuration. The dose rate fields in the TDR are overall much higher in this configuration as compared to the other configurations discussed in this section. The radiation area shown in orange in Figure 38 extends more than 2 m from the opening in the core vessel shielding and the high radiation area extends over the TVP. In the high bay, the radiation buffer area extends out 2 m from the center of the open hatch in the TDR roof. In the MRA removed configuration, the crane block is much lower than when compared with Cases 4A & 4B.

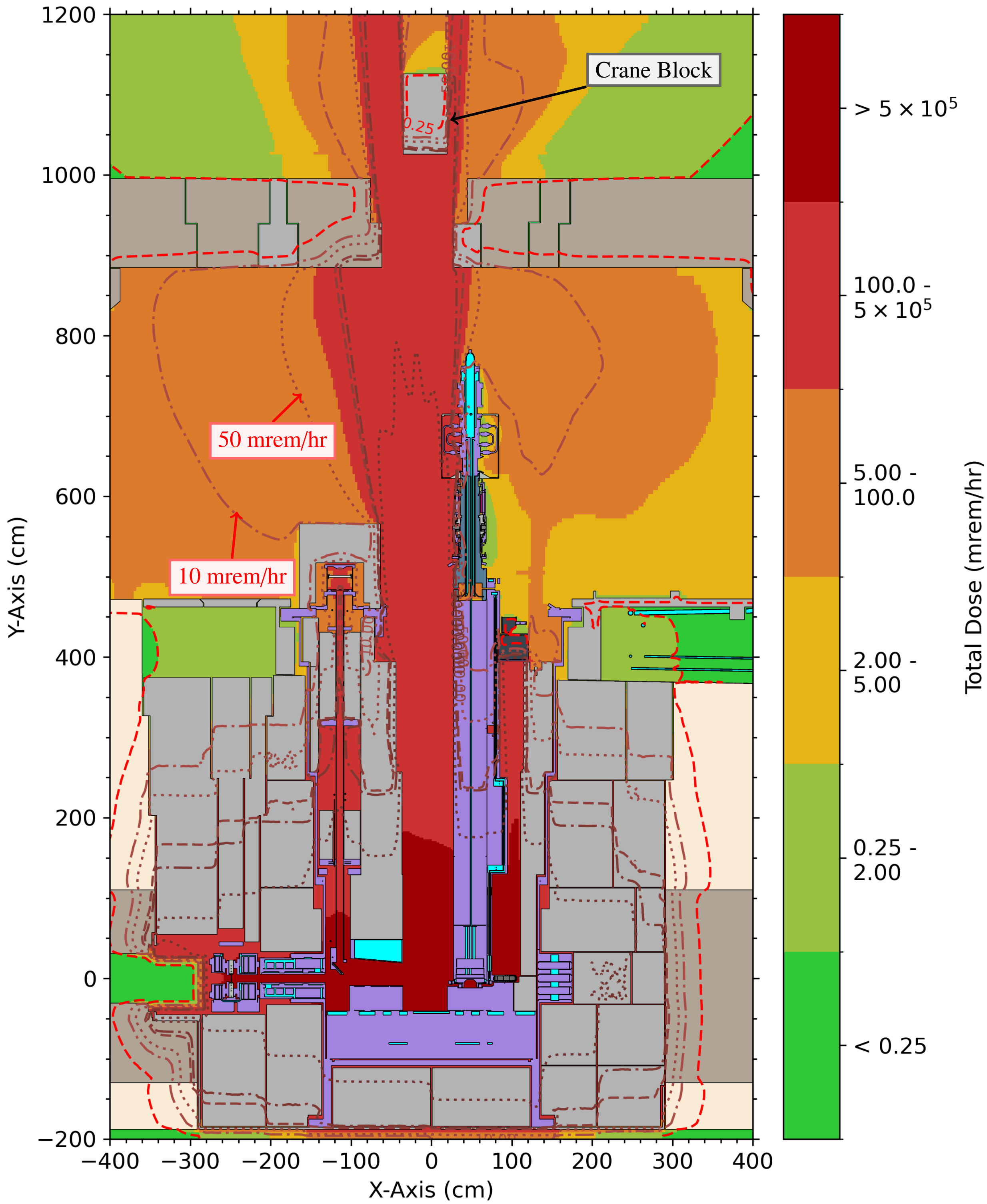

Figure 38. Cross section view along the proton beam after 2 weeks of decay in the target drive room for the MRA removed configuration.

Figure 39 shows the plan view of the TDR effective dose rates at an elevation of 1 m above the TDR floor. The radiation area shown in Figure 39 extends out to the walls of the TDR upstream of the target assembly. Figure 39 shows that entry into the TDR in this condition is feasible.

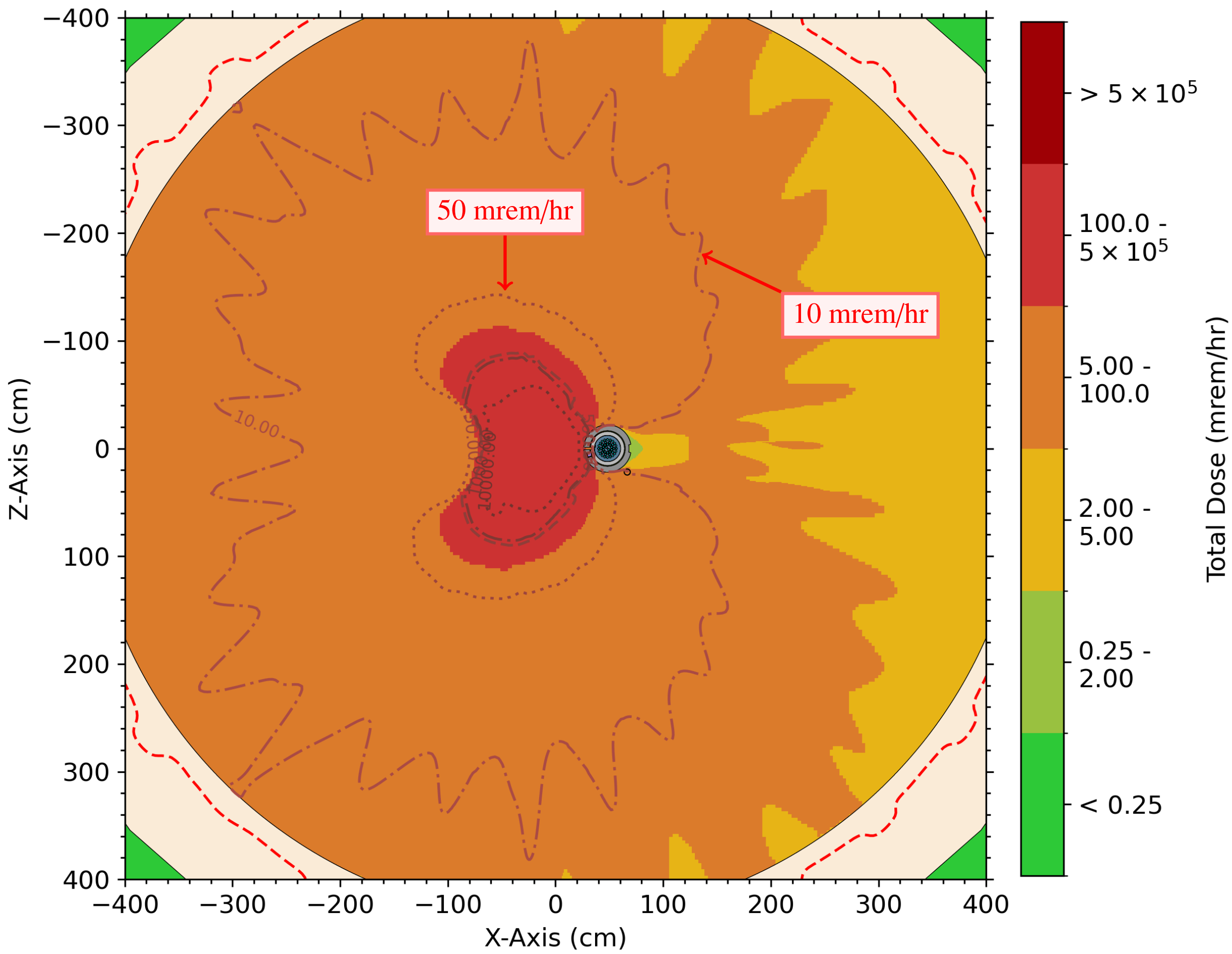

Figure 39. Plan view at an elevation of 1 m above the TDR floor of the photon effective dose rate after 2 weeks of decay in the target drive room and STS target system for the MRA removed configuration.

6 CONCLUSIONS

In conclusion, this report has presented a comprehensive analysis of various target segment and MRA removal sequences, providing detailed dose rate fields for each configuration. The results demonstrate compliance with the requirements outlined in Section 2, ensuring a solid foundation for the safe and efficient operation of the STS target system. For requirements that are still under evaluation, the dose rate fields presented in Section 5 offer valuable insights to support planning and confirmation of compliance. Ultimately, this report aims to inform the design of remote handling special equipment and the planning of corresponding operations, thereby contributing to the overall safety and efficiency of the STS target system.

7 REFERENCES

[1] T. M. Miller, T. C. McClanahan, W. de Wet, and I. Remec, "Second target station project bulk shielding design objectives and requirements," Tech. Rep. ORNL/LTR-2025/3772, 2025.

[2] A. Jacques and L. Bearden, "Second Target Station Requirements, Target Drive," Tech. Rep. S03020300-SRD10000-R02, Apr. 2026.

[3] C. Anton, H. Knott, L. Bearden, and M. Strong, "Second Target Station (STS): Vessel Systems Requirements," Tech. Rep. S03060000-SRD10000, Mar. 2025.

[4] *Requirement S.03.04-10944: MRA Utilities Dose Rate Requirement*, Second Target Station (STS) Project Std. [Online]. Available: https://sts-req.ornl.gov:8443/cb/issue/10944

[5] *Requirement S.03.10.04-10938–Personnel Safety (for target segment maintenance)*, Second Target Station Project Std. S.03.10.04-10 938. [Online]. Available: https://sts-req.ornl.gov:8443/cb/issue/10938

[6] *Requirement S.03.10.04-10943–Personnel Safety (for target drive maintenance)*, Second Target Station Project Std. [Online]. Available: https://sts-req.ornl.gov:8443/cb/issue/10943

[7] *Requirement S.03.10.05-10942–Personnel Safety (for MRA maintenance)*, Second Target Station Project Std. [Online]. Available: https://sts-req.ornl.gov:8443/cb/issue/10942

[8] *Requirement S.03.10.03-10940–Personnel Safety (for PBW or TVP) maintenance*, Second Target Station Project Std. [Online]. Available: https://sts-req.ornl.gov:8443/cb/issue/10940

[9] T. C. McClanahan and I. Remec, "Analysis of Second Target Station Target Removal Dose Rates," *Nuclear Science and Engineering*, vol. 200, no. 2, pp. 320–334, 2026. [Online]. Available: https://doi.org/10.1080/00295639.2025.2515656

[10] I. I. Popova, "An Updated Manual for CINDER2008 Codes and Data in the AARE Package," Tech. Rep. ORNL/TM-2018/926, Dec. 2018.

[11] S. W. Mosher, S. R. Johnson, A. M. Bevill, A. M. Ibrahim, C. R. Daily, T. M. Evans, J. C. Wagner, J. O. Johnson, and R. E. Grove, "ADVANTG–An Automated Variance Reduction Parameter Generator," Tech. Rep. ORNL/TM-2013/416, 2015.

[12] C. J. Werner, J. Armstrong, S. G. Mashnik, G. W. McKinney, F. B. Brown, M. E. Rising, G. E. McMath, J. S. Bull, C. Solomon, J. S. Hendricks, L. Casswell, A. Sood, D. B. Pelowitz, L. J. Cox, J. E. Sweezy, R. E. Prael, D. Dixon, C. J. Werner, T. E. Booth, R. A. Forester, A. Zukaitis, M. R. James, J. T. Goorley, C. Anderson, M. L. Fensin, H. G. Hughes, J. S. Elson, T. A. Wilcox, J. Favorite, J. W. Durkee, B. C. Kiedrowski, R. Martz, and R. C. Johns, "MCNP User's Manual Code Version 6.2," Tech. Rep. LA-UR-17-29981, Oct. 2017.

[13] M. Chadwick and et. al, "ENDF/B-VII.1 Nuclear Data for Science and Technology: Cross Sections, Covariances, Fission Product Yields and Decay Data," *Nuclear Data Sheets*, vol. 112, no. 12, pp. 2887 – 2996, 2011, special Issue on ENDF/B-VII.1 Library.

[14] I. K. Abu-Shumays, "Angular Quadratures for Imporved Transport Computations," Tech. Rep. B-T-3276, 1999.

[15] I. Popova, "Flux to Dose Conversion Factors," Tech. Rep. SNS-NFDD-NSD-TR-0001, R00, Mar. 2010.

[16] "Radiological Worker Training Study Guide," Tech. Rep. NRPD-SG-1007, Feb. 2023.

APPENDIX A. COMPUTER HARDWARE AND SOFTWARE

APPENDIX A. COMPUTER HARDWARE AND SOFTWARE

The Kryo and Saturn clusters were used in this analysis. The mcnp/mcnp6.2mod_20230411 module was used for MCNP® and advantg/3.2.0-HILO module was used for the ADVANTG package, and the AARE package was used for the activation.

Draft. Not approved for public release.
The only OFFICIAL COPY of this document is the on-line electronic version in ORNL's document management application.
Before using a printed copy, verify that it is the most current version.

APPENDIX B. LOCATION OF COMPUTATIONAL INPUT AND OUTPUT FILES

APPENDIX B. LOCATION OF COMPUTATIONAL INPUT AND OUTPUT FILES

The computational input and output files are located in the sts_archive located at:

/home/sts_archive/S.03.12_Neutronics/S.03.12.01_Neutronics_Analysis_Support/S03120100-TRT10015_STS_Target_MRA_Maintenance_Dose_Rates/Supporting_Data.tar.gz

This .tar.gz file contains the following three folders:

- Residual_Dose_Calculations
  - This folder contains the inputs and outputs for the residual dose calculations where the folders inside are marked by the configuration:
    - Case_1_Beam_Off_Walking_In/
    - Case_2_Beam_Off_Segment_Removed/
    - Case_3_Beam_Off_Two_Segments_Removed/
    - Case_4_MRA_Pipe_Cutting/
    - Case_5_MRA_Open_Pit/
  - Inside of each configuration folder is an ADVANTG and Photon_Sources directory, and for the fourth configuration, an ADVANTG, DENOVO_Only, Photon_Sources, and MCNP directory containing the respective inputs and outputs.
  - There are also Post_Processing directories that houses the Python script that was used to merge result files together.
- Generating_Decay_Gamma_Sources
  - This folder contains the inputs and outputs for generating the decay gamma sources with the protons-on-target source calculations:
    - ADVANTG/
      - This folder contains the ADVANTG calculations for each major component group for the protons-on-target calculations.
    - CINDER2008/
      - This folder contains the CINDER2008 calculations for each major component groups.
    - Generate_Final_Outp_Files/
      - This folder contains the script for producing the outp files generated from the protons-on-target calculations that are used in the CINDER2008 calculations. These outp files are generated using upper 95% confidence interval fluxes and high-energy reaction rates by the generate_final_outp_file.py script.
    - MCNP/
      - This folder contains the MCNP calculations for each major component group for the protons-on-target calculations.
    - Water_Neutron_Sources/
      - This folder contains the MCNP calculations for the major components where the water neutron sources contribute to the overall activation.
- Generating_Figures
  - This folder contains plotting scripts used to generate the figures in this document.
  - The script that generates all figures in this report is generate_plots.py

Draft. Not approved for public release.
The only OFFICIAL COPY of this document is the on-line electronic version in ORNL's document management application.
Before using a printed copy, verify that it is the most current version.

APPENDIX C. TECHNICAL REVIEW DOCUMENTATION

APPENDIX C. TECHNICAL REVIEW DOCUMENTATION

TECHNICAL REVIEW CHECKLIST

	Yes	No	N/A
Is the calculation well organized, legible, and complete?			
If excerpts from other sources are included in the calculation package, are the excerpts legible and properly referenced?			
Do the calculations cover the expressed purpose?			
Are all necessary elements included?			
Is the method used appropriate considering the purpose and type of analysis and the use and acceptability of the results (i.e. margin to limits)?			
Is the method in accordance with codes, standards, and regulatory requirements?			
Has the method been employed similarly elsewhere in industry?			
Are assumptions necessary to perform the analysis adequately described, justified, and reasonable?			
Are there any Unverified Assumptions (UVAs)?			
Were UVAs justified?			
Are the inputs sufficiently documented considering the purpose of the analysis?			
Is all the software used identified correctly (name, version, manual reference, OS, and compilers are documented)?			
Are the computer codes suitable for the present analysis?			
Does the model adequately represent the physical systems?			
Is the magnitude of the result reasonable?			
Are the directions of trends reasonable?			

Additional comments:

Technical Reviewer Date

ADVANCED REVIEW CHECKLIST

Method of Advanced Review used

____ In-Depth Calculation Review

____ Alternate Calculation

____ Qualification Test

Supporting Material: (Title, number of pages)

Independent Review Verification

	Yes	No
Did you perform the original calculation?		
Did you specify a single analytical approach?		
Did you rule out certain analytical considerations?		
Did you establish any input to the calculation being verified?		

Justification for any “Yes” to a question above:

Does the independent review support the calculation findings? What differences were observed?

Additional comments:

Reviewer Date

APPENDIX D. MATERIAL DEFINITION

APPENDIX D. MATERIAL DEFINITION

Table D.1. Para-H Material Definition

Nuclide	Mass Fraction	Atom Fraction
^{4}H	1.0000E+00	1.0000E+00
Density (g/cm^3)	0.0729194	

Table D.2. H2O 293K Material Definition

Nuclide	Mass Fraction	Atom Fraction
^{1}H	1.1190E-01	6.6659E-01
^{2}H	2.5720E-05	7.6667E-05
^{16}O	8.8772E-01	3.3321E-01
^{17}O	3.5865E-04	1.2667E-04
Density (g/cm^3)	1.0	

Table D.3. HD concrete Material Definition

Nuclide	Mass Fraction	Atom Fraction
^{1}H	3.7726E-03	1.0151E-01
^{16}O	3.2409E-01	5.4945E-01
^{23}Na	1.0033E-04	1.1834E-04
^{24}Mg	1.6261E-03	1.8384E-03
^{25}Mg	2.1445E-04	2.3274E-04
^{26}Mg	2.4553E-04	2.5625E-04
^{27}Al	5.3969E-03	5.4241E-03
^{28}Si	1.8100E-02	1.7544E-02
^{29}Si	9.5236E-04	8.9127E-04
^{30}Si	6.5017E-04	5.8822E-04

Draft. Not approved for public release.
The only OFFICIAL COPY of this document is the on-line electronic version in ORNL's document management application.
Before using a printed copy, verify that it is the most current version.

Table D.3 – continued from previous page

Nuclide	Mass Fraction	Atom Fraction
^{32}S	1.0697E-03	9.0731E-04
^{39}K	1.8501E-04	1.2876E-04
^{40}K	2.3807E-08	1.6154E-08
^{41}K	1.4036E-05	9.2923E-06
^{40}Ca	4.3534E-02	2.9541E-02
^{42}Ca	3.0507E-04	1.9716E-04
^{43}Ca	6.5171E-05	4.1140E-05
^{44}Ca	1.0304E-03	6.3568E-04
^{46}Ca	2.0656E-06	1.2189E-06
^{48}Ca	1.0077E-04	5.6986E-05
^{55}Mn	8.7910E-04	4.3393E-04
^{54}Fe	3.1877E-02	1.6026E-02
^{56}Fe	5.5139E-01	2.6732E-01
^{57}Fe	1.2755E-02	6.0750E-03
^{58}Fe	1.6434E-03	7.6924E-04
Density (g/cm^3)	3.84	

Table D.4. Ordinary concrete Material Definition

Nuclide	Mass Fraction	Atom Fraction
^{1}H	5.5571E-03	1.0357E-01
^{2}H	1.6661E-06	1.5537E-05
^{16}O	4.9801E-01	5.8481E-01
^{23}Na	1.7104E-02	1.3974E-02
^{24}Mg	1.9999E-03	1.5661E-03
^{25}Mg	2.6374E-04	1.9827E-04
^{26}Mg	3.0197E-04	2.1829E-04
^{27}Al	4.5753E-02	3.1850E-02

Draft. Not approved for public release.
The only OFFICIAL COPY of this document is the on-line electronic version in ORNL's document management application.
Before using a printed copy, verify that it is the most current version.

Table D.4 – continued from previous page

Nuclide	Mass Fraction	Atom Fraction
^{28}Si	2.8950E-01	1.9436E-01
^{29}Si	1.5232E-02	9.8739E-03
^{30}Si	1.0399E-02	6.5165E-03
^{32}S	1.2791E-03	7.5143E-04
^{39}K	1.7883E-02	8.6205E-03
^{40}K	2.3011E-06	1.0815E-06
^{41}K	1.3567E-03	6.2212E-04
^{40}Ca	8.0184E-02	3.7687E-02
^{42}Ca	5.6189E-04	2.5153E-04
^{43}Ca	1.2004E-04	5.2483E-05
^{44}Ca	1.8978E-03	8.1097E-04
^{46}Ca	3.8046E-06	1.5551E-06
^{48}Ca	1.8560E-04	7.2699E-05
^{54}Fe	7.0664E-04	2.4607E-04
^{56}Fe	1.1392E-02	3.8253E-03
^{57}Fe	2.6549E-04	8.7583E-05
^{58}Fe	3.6019E-05	1.1678E-05
Density (g/cm^3)	2.339	

Table D.5. Air Material Definition

Nuclide	Mass Fraction	Atom Fraction
^{1}H	1.8281E-03	2.5785E-02
^{2}H	5.4790E-07	3.8671E-06
^{4}He	6.7998E-07	2.4150E-06
^{0}C	1.2244E-04	1.4492E-04
^{14}N	7.4040E-01	7.5164E-01
^{15}N	2.9142E-03	2.7618E-03

Draft. Not approved for public release.
The only OFFICIAL COPY of this document is the on-line electronic version in ORNL's document management application.
Before using a printed copy, verify that it is the most current version.

Table D.5 – continued from previous page

Nuclide	Mass Fraction	Atom Fraction
^{16}O	2.4201E-01	2.1509E-01
^{17}O	9.7960E-05	8.1920E-05
^{38}Ar	7.6060E-06	2.8482E-06
^{40}Ar	1.2618E-02	4.4886E-03
^{78}Kr	9.2662E-09	1.6905E-09
^{80}Kr	6.1095E-08	1.0868E-08
^{82}Kr	3.2284E-07	5.6027E-08
^{84}Kr	1.6249E-06	2.7528E-07
^{86}Kr	5.0496E-07	8.3555E-08
^{124}Xe	3.6068E-10	4.1380E-11
^{126}Xe	3.4263E-10	3.8685E-11
^{128}Xe	7.4705E-09	8.3030E-10
^{129}Xe	1.0406E-07	1.1476E-08
^{130}Xe	1.6170E-08	1.7695E-09
^{131}Xe	8.4986E-08	9.2291E-09
^{132}Xe	1.0853E-07	1.1696E-08
^{134}Xe	4.2728E-08	4.5361E-09
^{136}Xe	3.6807E-08	3.8500E-09
Density (g/cm^3)	0.00121	

Table D.6. Inconel-718 Material Definition

Nuclide	Mass Fraction	Atom Fraction
^{10}B	1.1059E-05	6.3593E-05
^{11}B	4.8941E-05	2.5597E-04
^{0}C	8.0000E-04	3.8351E-03
^{27}Al	8.0000E-03	1.7072E-02
^{28}Si	3.2153E-03	6.6175E-03

Draft. Not approved for public release.
The only OFFICIAL COPY of this document is the on-line electronic version in ORNL's document management application.
Before using a printed copy, verify that it is the most current version.

Table D.6 – continued from previous page

Nuclide	Mass Fraction	Atom Fraction
^{29}Si	1.6918E-04	3.3617E-04
^{30}Si	1.1550E-04	2.2187E-04
^{31}P	1.5000E-04	2.7885E-04
^{32}S	1.4207E-04	2.5586E-04
^{33}S	1.1568E-06	2.0202E-06
^{34}S	6.7534E-06	1.1448E-05
^{36}S	1.6826E-08	2.6936E-08
^{46}Ti	9.1081E-04	1.1413E-03
^{47}Ti	8.3924E-04	1.0292E-03
^{48}Ti	8.4922E-03	1.0198E-02
^{49}Ti	6.3620E-04	7.4839E-04
^{50}Ti	6.2156E-04	7.1658E-04
^{50}Cr	8.7647E-03	1.0104E-02
^{52}Cr	1.7577E-01	1.9485E-01
^{53}Cr	2.0314E-02	2.2095E-02
^{54}Cr	5.1521E-03	5.4998E-03
^{55}Mn	3.5000E-03	3.6683E-03
^{54}Fe	6.7092E-03	7.1619E-03
^{56}Fe	1.0922E-01	1.1243E-01
^{57}Fe	2.5674E-03	2.5964E-03
^{58}Fe	3.4766E-04	3.4554E-04
^{59}Co	2.5000E-03	2.4426E-03
^{58}Ni	3.6959E-01	3.6732E-01
^{60}Ni	1.4727E-01	1.4149E-01
^{61}Ni	6.5085E-03	6.1505E-03
^{62}Ni	2.1091E-02	1.9610E-02
^{64}Ni	5.5448E-03	4.9942E-03
^{63}Cu	2.0544E-03	1.8797E-03
^{65}Cu	9.4562E-04	8.3860E-04
^{93}Nb	5.4500E-02	3.3777E-02

Draft. Not approved for public release.
The only OFFICIAL COPY of this document is the on-line electronic version in ORNL's document management application.
Before using a printed copy, verify that it is the most current version.

Table D.6 – continued from previous page

Nuclide	Mass Fraction	Atom Fraction
^{92}Mo	4.6693E-03	2.9253E-03
^{94}Mo	2.9814E-03	1.8281E-03
^{95}Mo	5.1906E-03	3.1491E-03
^{96}Mo	5.5025E-03	3.3036E-03
^{97}Mo	3.1867E-03	1.8934E-03
^{98}Mo	8.1464E-03	4.7910E-03
^{100}Mo	3.3231E-03	1.9152E-03
^{181}Ta	5.0000E-04	1.5910E-04
Density (g/cm^3)	8.19	

Table D.7. Zinc Selenide Material Definition

Nuclide	Mass Fraction	Atom Fraction
^{64}Zn	2.1369E-01	2.4129E-01
^{66}Zn	1.2772E-01	1.3984E-01
^{67}Zn	1.9012E-02	2.0505E-02
^{68}Zn	8.9486E-02	9.5099E-02
^{70}Zn	3.0555E-03	3.1543E-03
^{74}Se	4.5581E-03	4.4510E-03
^{76}Se	4.9284E-02	4.6860E-02
^{77}Se	4.0661E-02	3.8158E-02
^{78}Se	1.2832E-01	1.1888E-01
^{80}Se	2.7468E-01	2.4810E-01
^{82}Se	4.9545E-02	4.3660E-02
Density (g/cm^3)	5.27	

Draft. Not approved for public release.
The only OFFICIAL COPY of this document is the on-line electronic version in ORNL's document management application.
Before using a printed copy, verify that it is the most current version.

Table D.8. Al 5052-O Material Definition

Nuclide	Mass Fraction	Atom Fraction
^{24}Mg	2.1826E-02	2.4613E-02
^{25}Mg	2.8784E-03	3.1159E-03
^{26}Mg	3.2956E-03	3.4306E-03
^{27}Al	9.5900E-01	9.6134E-01
^{28}Si	2.2967E-03	2.2204E-03
^{29}Si	1.2084E-04	1.1280E-04
^{30}Si	8.2497E-05	7.4443E-05
^{50}Cr	1.4608E-04	7.9107E-05
^{52}Cr	2.9295E-03	1.5255E-03
^{53}Cr	3.3858E-04	1.7298E-04
^{54}Cr	8.5868E-05	4.3058E-05
^{55}Mn	1.0000E-03	4.9233E-04
^{54}Fe	2.2582E-04	1.1323E-04
^{56}Fe	3.6759E-03	1.7775E-03
^{57}Fe	8.6412E-05	4.1051E-05
^{58}Fe	1.1701E-05	5.4629E-06
^{63}Cu	6.8479E-04	2.9433E-04
^{65}Cu	3.1521E-04	1.3131E-04
^{64}Zn	4.7190E-04	1.9965E-04
^{66}Zn	2.8204E-04	1.1571E-04
^{67}Zn	4.1984E-05	1.6967E-05
^{68}Zn	1.9761E-04	7.8690E-05
^{70}Zn	6.7476E-06	2.6100E-06
Density (g/cm^3)	2.68	

Table D.9. Beryllium Material Definition

Nuclide	Mass Fraction	Atom Fraction
^{6}Li	3.8068E-06	5.7596E-06
^{7}Li	5.4060E-05	7.0124E-05
^{9}Be	9.8503E-01	9.9471E-01
^{10}B	1.5608E-06	1.4186E-06
^{11}B	6.9076E-06	5.7101E-06
^{0}C	9.5117E-04	7.2071E-04
^{16}O	6.1391E-03	3.4930E-03
^{17}O	2.4854E-06	1.3306E-06
^{24}Mg	4.0007E-04	1.5180E-04
^{25}Mg	5.2761E-05	1.9218E-05
^{26}Mg	6.0408E-05	2.1159E-05
^{27}Al	6.4155E-04	2.1639E-04
^{28}Si	3.5362E-04	1.1503E-04
^{29}Si	1.8606E-05	5.8438E-06
^{30}Si	1.2702E-05	3.8567E-06
^{54}Fe	4.7084E-05	7.9441E-06
^{56}Fe	7.6647E-04	1.2471E-04
^{57}Fe	1.8018E-05	2.8800E-06
^{58}Fe	2.4399E-06	3.8328E-07
^{103}Rh	2.7292E-04	2.4136E-05
^{107}Ag	1.9123E-04	1.6280E-05
^{109}Ag	1.8100E-04	1.5125E-05
^{106}Cd	3.1430E-07	2.7008E-08
^{108}Cd	2.2801E-07	1.9230E-08
^{110}Cd	3.2590E-06	2.6987E-07
^{111}Cd	3.3703E-06	2.7657E-07
^{112}Cd	6.4108E-06	5.2137E-07
^{113}Cd	3.2756E-06	2.6403E-07

Draft. Not approved for public release.
The only OFFICIAL COPY of this document is the on-line electronic version in ORNL's document management application.
Before using a printed copy, verify that it is the most current version.

Table D.9 – continued from previous page

Nuclide	Mass Fraction	Atom Fraction
^{114}Cd	7.7693E-06	6.2076E-07
^{116}Cd	2.0610E-06	1.6183E-07
^{113}In	4.1028E-06	3.3071E-07
^{115}In	9.3155E-05	7.3782E-06
^{142}Nd	4.6057E-04	2.9537E-05
^{143}Nd	2.0804E-04	1.3249E-05
^{144}Nd	4.0869E-04	2.5845E-05
^{145}Nd	1.4352E-04	9.0135E-06
^{146}Nd	2.9947E-04	1.8678E-05
^{148}Nd	1.0060E-04	6.1897E-06
^{150}Nd	1.0018E-04	6.0815E-06
^{144}Sm	4.7125E-07	2.9801E-08
^{147}Sm	2.3491E-06	1.4551E-07
^{148}Sm	1.7733E-06	1.0911E-07
^{149}Sm	2.1952E-06	1.3415E-07
^{150}Sm	1.1801E-06	7.1640E-08
^{152}Sm	4.3347E-06	2.5967E-07
^{154}Sm	3.7351E-06	2.2084E-07
^{151}Eu	9.4735E-06	5.7127E-07
^{153}Eu	1.0478E-05	6.2359E-07
^{152}Gd	3.9667E-09	2.3763E-10
^{154}Gd	4.3806E-08	2.5901E-09
^{155}Gd	2.9934E-07	1.7584E-08
^{156}Gd	4.1668E-07	2.4321E-08
^{157}Gd	3.2062E-07	1.8594E-08
^{158}Gd	5.1213E-07	2.9513E-08
^{160}Gd	4.5641E-07	2.5972E-08
^{156}Dy	5.5191E-08	3.2213E-09
^{158}Dy	9.4828E-08	5.4647E-09
^{160}Dy	2.3543E-06	1.3397E-07

Table D.9 – continued from previous page

Nuclide	Mass Fraction	Atom Fraction
^{161}Dy	1.9214E-05	1.0866E-06
^{162}Dy	2.6074E-05	1.4654E-06
^{163}Dy	2.5639E-05	1.4321E-06
^{164}Dy	2.9282E-05	1.6256E-06
^{162}Er	8.2284E-07	4.6246E-08
^{164}Er	9.5945E-06	5.3266E-07
^{166}Er	2.0322E-04	1.1146E-05
^{167}Er	1.3956E-04	7.6087E-06
^{168}Er	1.6562E-04	8.9757E-06
^{170}Er	9.2627E-05	4.9606E-06
^{169}Tm	2.8158E-04	1.5169E-05
^{175}Lu	7.2313E-04	3.7619E-05
^{176}Lu	1.9337E-05	1.0003E-06
^{174}Hf	3.7713E-07	1.9732E-08
^{176}Hf	1.2540E-05	6.4866E-07
^{177}Hf	4.4598E-05	2.2938E-06
^{178}Hf	6.5781E-05	3.3643E-06
^{179}Hf	3.3027E-05	1.6797E-06
^{180}Hf	8.5540E-05	4.3262E-06
^{191}Ir	8.7890E-05	4.1887E-06
^{193}Ir	1.4929E-04	7.0412E-06
^{197}Au	3.4086E-04	1.5749E-05
^{196}Hg	4.7456E-07	2.2039E-08
^{198}Hg	3.1865E-05	1.4649E-06
^{199}Hg	5.4189E-05	2.4786E-06
^{200}Hg	7.4575E-05	3.3940E-06
^{201}Hg	4.2763E-05	1.9365E-06
^{202}Hg	9.7364E-05	4.3872E-06
^{204}Hg	2.2623E-05	1.0094E-06
^{234}U	1.7031E-09	6.6227E-11

Table D.9 – continued from previous page

Nuclide	Mass Fraction	Atom Fraction
^{235}U	2.2819E-07	8.8352E-09
^{238}U	3.1848E-05	1.2176E-06
Density (g/cm^3)	1.82922	

Table D.10. Steel A36 Material Definition

Nuclide	Mass Fraction	Atom Fraction
^{0}C	2.6000E-03	1.1921E-02
^{28}Si	3.6747E-03	7.2333E-03
^{29}Si	1.9335E-04	3.6746E-04
^{30}Si	1.3200E-04	2.4251E-04
^{31}P	4.0000E-04	7.1119E-04
^{32}S	4.7358E-04	8.1572E-04
^{33}S	3.8560E-06	6.4405E-06
^{34}S	2.2511E-05	3.6496E-05
^{36}S	5.6085E-08	8.5874E-08
^{55}Mn	1.2000E-02	1.2029E-02
^{54}Fe	5.5214E-02	5.6371E-02
^{56}Fe	8.9880E-01	8.8491E-01
^{57}Fe	2.1128E-02	2.0436E-02
^{58}Fe	2.8611E-03	2.7197E-03
^{59}Co	5.0000E-04	4.6723E-04
^{63}Cu	1.3696E-03	1.1985E-03
^{65}Cu	6.3042E-04	5.3471E-04
Density (g/cm^3)	7.85	

Table D.11. Steel A572 Material Definition

Nuclide	Mass Fraction	Atom Fraction
^{0}C	2.3000E-03	1.0554E-02
^{28}Si	3.6748E-03	7.2394E-03
^{29}Si	1.9335E-04	3.6777E-04
^{30}Si	1.3200E-04	2.4272E-04
^{31}P	4.0001E-04	7.1179E-04
^{32}S	4.7357E-04	8.1638E-04
^{33}S	3.8560E-06	6.4458E-06
^{34}S	2.2511E-05	3.6526E-05
^{36}S	5.6085E-08	8.5944E-08
^{55}Mn	1.3501E-02	1.3544E-02
^{54}Fe	5.5287E-02	5.6492E-02
^{56}Fe	8.9949E-01	8.8631E-01
^{57}Fe	2.1157E-02	2.0480E-02
^{58}Fe	2.8649E-03	2.7256E-03
^{59}Co	5.0000E-04	4.6761E-04
Density (g/cm^3)	7.8	

Table D.12. Copper Material Definition

Nuclide	Mass Fraction	Atom Fraction
^{16}O	4.9865E-06	1.9810E-05
^{17}O	2.0187E-09	7.5462E-09
^{31}P	3.0000E-06	6.1547E-06
^{32}S	1.4207E-05	2.8237E-05
^{33}S	1.1568E-07	2.2295E-07
^{34}S	6.7534E-07	1.2634E-06
^{36}S	1.6826E-09	2.9727E-09

Draft. Not approved for public release.
The only OFFICIAL COPY of this document is the on-line electronic version in ORNL's document management application.
Before using a printed copy, verify that it is the most current version.

Table D.12 – continued from previous page

Nuclide	Mass Fraction	Atom Fraction
^{55}Mn	5.0000E-07	5.7833E-07
^{54}Fe	5.6456E-07	6.6509E-07
^{56}Fe	9.1902E-06	1.0440E-05
^{57}Fe	2.1604E-07	2.4112E-07
^{58}Fe	2.9255E-08	3.2089E-08
^{58}Ni	6.7198E-06	7.3704E-06
^{60}Ni	2.6776E-06	2.8391E-06
^{61}Ni	1.1834E-07	1.2342E-07
^{62}Ni	3.8349E-07	3.9350E-07
^{64}Ni	1.0082E-07	1.0022E-07
^{63}Cu	6.8473E-01	6.9142E-01
^{65}Cu	3.1518E-01	3.0847E-01
^{64}Zn	4.7177E-07	4.6893E-07
^{66}Zn	2.8196E-07	2.7178E-07
^{67}Zn	4.1973E-08	3.9852E-08
^{68}Zn	1.9756E-07	1.8482E-07
^{70}Zn	6.7458E-09	6.1303E-09
^{75}As	5.0000E-06	4.2408E-06
^{74}Se	2.4997E-08	2.1488E-08
^{76}Se	2.7028E-07	2.2623E-07
^{77}Se	2.2299E-07	1.8422E-07
^{78}Se	7.0369E-07	5.7389E-07
^{80}Se	1.5064E-06	1.1978E-06
^{82}Se	2.7171E-07	2.1077E-07
^{107}Ag	1.2844E-05	7.6345E-06
^{109}Ag	1.2156E-05	7.0929E-06
^{106}Cd	1.1777E-08	7.0663E-09
^{108}Cd	8.5432E-09	5.0311E-09
^{110}Cd	1.2211E-07	7.0603E-08
^{111}Cd	1.2628E-07	7.2355E-08

Table D.12 – continued from previous page

Nuclide	Mass Fraction	Atom Fraction
^{112}Cd	2.4021E-07	1.3641E-07
^{113}Cd	1.2274E-07	6.9081E-08
^{114}Cd	2.9111E-07	1.6241E-07
^{116}Cd	7.7228E-08	4.2340E-08
^{112}Sn	1.8288E-08	1.0385E-08
^{114}Sn	1.2666E-08	7.0662E-09
^{115}Sn	6.5820E-09	3.6400E-09
^{116}Sn	2.8392E-07	1.5566E-07
^{117}Sn	1.5126E-07	8.2220E-08
^{118}Sn	4.8110E-07	2.5930E-07
^{119}Sn	1.7208E-07	9.1964E-08
^{120}Sn	6.5815E-07	3.4880E-07
^{122}Sn	9.5092E-08	4.9569E-08
^{124}Sn	1.2087E-07	6.1988E-08
^{121}Sb	2.2723E-06	1.1943E-06
^{123}Sb	1.7277E-06	8.9327E-07
^{120}Te	1.6914E-09	8.9638E-10
^{122}Te	4.8722E-08	2.5397E-08
^{123}Te	1.7145E-08	8.8644E-09
^{124}Te	9.2052E-08	4.7210E-08
^{125}Te	1.3841E-07	7.0416E-08
^{126}Te	3.7178E-07	1.8764E-07
^{128}Te	6.3630E-07	3.1612E-07
^{130}Te	6.9391E-07	3.3943E-07
^{204}Pb	6.8905E-08	2.1466E-08
^{206}Pb	1.1978E-06	3.6953E-07
^{207}Pb	1.1037E-06	3.3885E-07
^{208}Pb	2.6296E-06	8.0344E-07
^{209}Bi	1.0000E-06	3.0407E-07

Draft. Not approved for public release.
The only OFFICIAL COPY of this document is the on-line electronic version in ORNL's document management application.
Before using a printed copy, verify that it is the most current version.

Table D.12 – continued from previous page

Nuclide	Mass Fraction	Atom Fraction
Density (g/cm^3)	7.144	

Table D.13. Inconel-625 Material Definition

Nuclide	Mass Fraction	Atom Fraction
^{0}C	9.8998E-04	4.8513E-03
^{27}Al	3.9600E-03	8.6386E-03
^{28}Si	4.5474E-03	9.5671E-03
^{29}Si	2.3927E-04	4.8602E-04
^{30}Si	1.6334E-04	3.2076E-04
^{31}P	1.4800E-04	2.8125E-04
^{32}S	1.4017E-04	2.5805E-04
^{33}S	1.1413E-06	2.0374E-06
^{34}S	6.6631E-06	1.1546E-05
^{36}S	1.6601E-08	2.7167E-08
^{46}Ti	3.1355E-04	4.0162E-04
^{47}Ti	2.8891E-04	3.6219E-04
^{48}Ti	2.9235E-03	3.5887E-03
^{49}Ti	2.1902E-04	2.6336E-04
^{50}Ti	2.1398E-04	2.5217E-04
^{50}Cr	8.9735E-03	1.0575E-02
^{52}Cr	1.7996E-01	2.0393E-01
^{53}Cr	2.0798E-02	2.3124E-02
^{54}Cr	5.2748E-03	5.7559E-03
^{55}Mn	4.9500E-03	5.3033E-03
^{54}Fe	2.7942E-03	3.0490E-03
^{56}Fe	4.5485E-02	4.7863E-02
^{57}Fe	1.0692E-03	1.1054E-03

Draft. Not approved for public release.
The only OFFICIAL COPY of this document is the on-line electronic version in ORNL's document management application.
Before using a printed copy, verify that it is the most current version.

Table D.13 – continued from previous page

Nuclide	Mass Fraction	Atom Fraction
^{58}Fe	1.4479E-04	1.4710E-04
^{59}Co	9.8990E-03	9.8866E-03
^{58}Ni	3.8975E-01	3.9596E-01
^{60}Ni	1.5530E-01	1.5252E-01
^{61}Ni	6.8635E-03	6.6301E-03
^{62}Ni	2.2242E-02	2.1140E-02
^{64}Ni	5.8473E-03	5.3837E-03
^{93}Nb	3.6500E-02	2.3124E-02
^{92}Mo	1.2734E-02	8.1553E-03
^{94}Mo	8.1309E-03	5.0964E-03
^{95}Mo	1.4156E-02	8.7792E-03
^{96}Mo	1.5007E-02	9.2099E-03
^{97}Mo	8.6907E-03	5.2786E-03
^{98}Mo	2.2217E-02	1.3357E-02
^{100}Mo	9.0630E-03	5.3393E-03
Density (g/cm^3)	8.44	

Table D.14. Invar Material Definition

Nuclide	Mass Fraction	Atom Fraction
^{0}C	1.4827E-03	6.9470E-03
^{28}Si	3.6748E-03	7.3922E-03
^{29}Si	1.9335E-04	3.7553E-04
^{30}Si	1.3200E-04	2.4784E-04
^{31}P	2.5001E-04	4.5426E-04
^{32}S	2.3679E-04	4.1680E-04
^{33}S	1.9280E-06	3.2909E-06
^{34}S	1.1255E-05	1.8648E-05

Draft. Not approved for public release.
The only OFFICIAL COPY of this document is the on-line electronic version in ORNL's document management application.
Before using a printed copy, verify that it is the most current version.

Table D.14 – continued from previous page

Nuclide	Mass Fraction	Atom Fraction
^{36}S	2.8043E-08	4.3879E-08
^{50}Cr	1.0435E-04	1.1758E-04
^{52}Cr	2.0926E-03	2.2673E-03
^{53}Cr	2.4185E-04	2.5710E-04
^{54}Cr	6.1337E-05	6.3997E-05
^{55}Mn	6.0002E-03	6.1466E-03
^{54}Fe	3.5031E-02	3.6550E-02
^{56}Fe	5.7025E-01	5.7375E-01
^{57}Fe	1.3405E-02	1.3251E-02
^{58}Fe	1.8153E-03	1.7634E-03
^{59}Co	5.0002E-03	4.7749E-03
^{58}Ni	2.4192E-01	2.3500E-01
^{60}Ni	9.6397E-02	9.0522E-02
^{61}Ni	4.2603E-03	3.9349E-03
^{62}Ni	1.3806E-02	1.2546E-02
^{64}Ni	3.6295E-03	3.1952E-03
Density (g/cm^3)	8.05	

Table D.15. Lead Material Definition

Nuclide	Mass Fraction	Atom Fraction
^{54}Fe	1.1290E-06	4.3362E-06
^{56}Fe	1.8378E-05	6.8067E-05
^{57}Fe	4.3202E-07	1.5720E-06
^{58}Fe	5.8502E-08	2.0920E-07
^{58}Ni	6.7192E-06	2.4027E-05
^{60}Ni	2.6774E-06	9.2552E-06
^{61}Ni	1.1833E-07	4.0232E-07

Draft. Not approved for public release.
The only OFFICIAL COPY of this document is the on-line electronic version in ORNL's document management application.
Before using a printed copy, verify that it is the most current version.

Table D.15 – continued from previous page

Nuclide	Mass Fraction	Atom Fraction
^{62}Ni	3.8345E-07	1.2827E-06
^{64}Ni	1.0081E-07	3.2669E-07
^{63}Cu	2.0542E-05	6.7625E-05
^{65}Cu	9.4555E-06	3.0170E-05
^{64}Zn	2.3593E-06	7.6455E-06
^{66}Zn	1.4101E-06	4.4311E-06
^{67}Zn	2.0990E-07	6.4973E-07
^{68}Zn	9.8799E-07	3.0133E-06
^{70}Zn	3.3735E-08	9.9946E-08
^{75}As	9.9992E-06	2.7649E-05
^{107}Ag	2.5686E-05	4.9776E-05
^{109}Ag	2.4310E-05	4.6244E-05
^{106}Cd	1.1776E-07	2.3035E-07
^{108}Cd	8.5426E-08	1.6401E-07
^{110}Cd	1.2210E-06	2.3016E-06
^{111}Cd	1.2628E-06	2.3589E-06
^{112}Cd	2.4019E-06	4.4467E-06
^{113}Cd	1.2273E-06	2.2520E-06
^{114}Cd	2.9109E-06	5.2943E-06
^{116}Cd	7.7222E-07	1.3803E-06
^{112}Sn	9.1432E-08	1.6927E-07
^{114}Sn	6.3322E-08	1.1517E-07
^{115}Sn	3.2907E-08	5.9330E-08
^{116}Sn	1.4195E-06	2.5373E-06
^{117}Sn	7.5625E-07	1.3402E-06
^{118}Sn	2.4053E-06	4.2264E-06
^{119}Sn	8.6033E-07	1.4990E-06
^{120}Sn	3.2905E-06	5.6853E-06
^{122}Sn	4.7542E-07	8.0794E-07
^{124}Sn	6.0429E-07	1.0104E-06

Table D.15 – continued from previous page

Nuclide	Mass Fraction	Atom Fraction
^{121}Sb	5.6804E-06	9.7333E-06
^{123}Sb	4.3190E-06	7.2801E-06
^{204}Pb	1.3775E-02	1.3990E-02
^{206}Pb	2.3945E-01	2.4083E-01
^{207}Pb	2.2064E-01	2.2085E-01
^{208}Pb	5.2568E-01	5.2363E-01
^{209}Bi	2.9998E-04	2.9737E-04
Density (g/cm^3)	11.34	

Table D.16. 17-4 PH condition A SS Material Definition

Nuclide	Mass Fraction	Atom Fraction
^{0}C	3.5000E-04	1.6103E-03
^{28}Si	4.5934E-03	9.0733E-03
^{29}Si	2.4169E-04	4.6093E-04
^{30}Si	1.6500E-04	3.0420E-04
^{31}P	2.0001E-04	3.5684E-04
^{32}S	1.4207E-04	2.4556E-04
^{33}S	1.1568E-06	1.9389E-06
^{34}S	6.7533E-06	1.0987E-05
^{36}S	1.6825E-08	2.5851E-08
^{50}Cr	6.8033E-03	7.5274E-03
^{52}Cr	1.3643E-01	1.4516E-01
^{53}Cr	1.5768E-02	1.6460E-02
^{54}Cr	3.9991E-03	4.0972E-03
^{55}Mn	5.0001E-03	5.0296E-03
^{54}Fe	4.1850E-02	4.2876E-02
^{56}Fe	6.8126E-01	6.7307E-01

Table D.16 – continued from previous page

Nuclide	Mass Fraction	Atom Fraction
^{57}Fe	1.6015E-02	1.5544E-02
^{58}Fe	2.1686E-03	2.0686E-03
^{59}Co	2.0001E-03	1.8755E-03
^{58}Ni	2.6880E-02	2.5639E-02
^{60}Ni	1.0711E-02	9.8763E-03
^{61}Ni	4.7336E-04	4.2931E-04
^{62}Ni	1.5340E-03	1.3688E-03
^{64}Ni	4.0327E-04	3.4860E-04
^{63}Cu	2.7392E-02	2.4055E-02
^{65}Cu	1.2609E-02	1.0732E-02
^{93}Nb	3.0001E-03	1.7845E-03
Density (g/cm^3)	7.78	

Table D.17. SS-316 Material Definition

Nuclide	Mass Fraction	Atom Fraction
^{0}C	7.9073E-04	3.6489E-03
^{28}Si	9.1866E-03	1.8200E-02
^{29}Si	4.8336E-04	9.2456E-04
^{30}Si	3.2999E-04	6.1020E-04
^{31}P	4.5000E-04	8.0525E-04
^{32}S	2.8415E-04	4.9259E-04
^{33}S	2.3136E-06	3.8892E-06
^{34}S	1.3507E-05	2.2040E-05
^{36}S	3.3651E-08	5.1857E-08
^{50}Cr	7.5126E-03	8.3368E-03
^{52}Cr	1.5066E-01	1.6077E-01
^{53}Cr	1.7412E-02	1.8229E-02

Draft. Not approved for public release.
The only OFFICIAL COPY of this document is the on-line electronic version in ORNL's document management application.
Before using a printed copy, verify that it is the most current version.

Table D.17 – continued from previous page

Nuclide	Mass Fraction	Atom Fraction
^{54}Cr	4.4161E-03	4.5378E-03
^{55}Mn	2.0000E-02	2.0178E-02
^{54}Fe	3.4802E-02	3.5761E-02
^{56}Fe	5.6653E-01	5.6137E-01
^{57}Fe	1.3318E-02	1.2965E-02
^{58}Fe	1.8034E-03	1.7253E-03
^{59}Co	2.0000E-03	1.8810E-03
^{58}Ni	9.4077E-02	9.0002E-02
^{60}Ni	3.7486E-02	3.4668E-02
^{61}Ni	1.6567E-03	1.5070E-03
^{62}Ni	5.3688E-03	4.8051E-03
^{64}Ni	1.4114E-03	1.2237E-03
^{92}Mo	4.2448E-03	2.5599E-03
^{94}Mo	2.7103E-03	1.5997E-03
^{95}Mo	4.7187E-03	2.7558E-03
^{96}Mo	5.0023E-03	2.8910E-03
^{97}Mo	2.8970E-03	1.6569E-03
^{98}Mo	7.4059E-03	4.1926E-03
^{100}Mo	3.0210E-03	1.6760E-03
Density (g/cm^3)	8.0	

Table D.18. SS-316L Material Definition

Nuclide	Mass Fraction	Atom Fraction
^{0}C	2.9652E-04	1.3708E-03
^{28}Si	9.1866E-03	1.8232E-02
^{29}Si	4.8336E-04	9.2621E-04
^{30}Si	3.2999E-04	6.1129E-04

Draft. Not approved for public release.
The only OFFICIAL COPY of this document is the on-line electronic version in ORNL's document management application.
Before using a printed copy, verify that it is the most current version.

Table D.18 – continued from previous page

Nuclide	Mass Fraction	Atom Fraction
^{31}P	4.5000E-04	8.0669E-04
^{32}S	2.8415E-04	4.9347E-04
^{33}S	2.3136E-06	3.8962E-06
^{34}S	1.3507E-05	2.2079E-05
^{36}S	3.3651E-08	5.1949E-08
^{50}Cr	7.5126E-03	8.3517E-03
^{52}Cr	1.5066E-01	1.6106E-01
^{53}Cr	1.7412E-02	1.8262E-02
^{54}Cr	4.4161E-03	4.5459E-03
^{55}Mn	2.0000E-02	2.0214E-02
^{54}Fe	3.4830E-02	3.5854E-02
^{56}Fe	5.6699E-01	5.6283E-01
^{57}Fe	1.3328E-02	1.2998E-02
^{58}Fe	1.8049E-03	1.7299E-03
^{59}Co	2.0000E-03	1.8843E-03
^{58}Ni	9.4077E-02	9.0163E-02
^{60}Ni	3.7486E-02	3.4730E-02
^{61}Ni	1.6567E-03	1.5097E-03
^{62}Ni	5.3688E-03	4.8137E-03
^{64}Ni	1.4114E-03	1.2259E-03
^{92}Mo	4.2448E-03	2.5645E-03
^{94}Mo	2.7103E-03	1.6026E-03
^{95}Mo	4.7187E-03	2.7607E-03
^{96}Mo	5.0023E-03	2.8961E-03
^{97}Mo	2.8970E-03	1.6599E-03
^{98}Mo	7.4059E-03	4.2001E-03
^{100}Mo	3.0210E-03	1.6790E-03
Density (g/cm^3)	8.0	

Table D.19. Ta max impurities Material Definition

Nuclide	Mass Fraction	Atom Fraction
^{1}H	1.4999E-05	2.6692E-03
^{2}H	3.4474E-09	3.0698E-07
^{0}C	9.8854E-05	1.4761E-03
^{14}N	9.9622E-05	1.2760E-03
^{15}N	3.8987E-07	4.6615E-06
^{16}O	1.4961E-04	1.6776E-03
^{17}O	6.0569E-08	6.3904E-07
^{28}Si	4.5938E-05	2.9450E-04
^{29}Si	2.4171E-06	1.4961E-05
^{30}Si	1.6501E-06	9.8735E-06
^{46}Ti	7.9210E-06	3.0915E-05
^{47}Ti	7.2986E-06	2.7880E-05
^{48}Ti	7.3854E-05	2.7625E-04
^{49}Ti	5.5328E-06	2.0273E-05
^{50}Ti	5.4055E-06	1.9411E-05
^{54}Fe	5.6463E-06	1.8774E-05
^{56}Fe	9.1913E-05	2.9471E-04
^{57}Fe	2.1606E-06	6.8062E-06
^{58}Fe	2.9257E-07	9.0576E-07
^{58}Ni	6.7206E-05	2.0805E-04
^{60}Ni	2.6779E-05	8.0140E-05
^{61}Ni	1.1835E-06	3.4837E-06
^{62}Ni	3.8353E-06	1.1107E-05
^{64}Ni	1.0083E-06	2.8289E-06
^{93}Nb	1.0001E-03	1.9307E-03
^{92}Mo	2.8302E-05	5.5230E-05
^{94}Mo	1.8071E-05	3.4514E-05
^{95}Mo	3.1462E-05	5.9456E-05

Draft. Not approved for public release.
The only OFFICIAL COPY of this document is the on-line electronic version in ORNL's document management application.
Before using a printed copy, verify that it is the most current version.

Table D.19 – continued from previous page

Nuclide	Mass Fraction	Atom Fraction
^{96}Mo	3.3353E-05	6.2373E-05
^{97}Mo	1.9315E-05	3.5748E-05
^{98}Mo	4.9378E-05	9.0454E-05
^{100}Mo	2.0142E-05	3.6159E-05
^{181}Ta	9.9759E-01	9.8878E-01
^{180}W	5.8736E-07	5.8541E-07
^{182}W	1.3115E-04	1.2928E-04
^{183}W	7.1211E-05	6.9810E-05
^{184}W	1.5331E-04	1.4947E-04
^{186}W	1.4380E-04	1.3869E-04
Density (g/cm^3)	16.65	

Table D.20. W max impurities Material Definition

Nuclide	Mass Fraction	Atom Fraction
^{0}C	9.8843E-05	1.5059E-03
^{14}N	9.9611E-05	1.3017E-03
^{15}N	3.8982E-07	4.7555E-06
^{16}O	9.9730E-05	1.1409E-03
^{17}O	4.0374E-08	4.3461E-07
^{28}Si	9.1867E-05	6.0087E-04
^{29}Si	4.8336E-06	3.0525E-05
^{30}Si	3.2999E-06	2.0146E-05
^{54}Fe	5.6456E-06	1.9153E-05
^{56}Fe	9.1903E-05	3.0065E-04
^{57}Fe	2.1604E-06	6.9435E-06
^{58}Fe	2.9254E-07	9.2402E-07
^{58}Ni	6.7198E-05	2.1225E-04

Table D.20 – continued from previous page

Nuclide	Mass Fraction	Atom Fraction
^{60}Ni	2.6776E-05	8.1756E-05
^{61}Ni	1.1834E-06	3.5540E-06
^{62}Ni	3.8348E-06	1.1331E-05
^{64}Ni	1.0082E-06	2.8859E-06
^{180}W	1.1739E-03	1.1937E-03
^{182}W	2.6211E-01	2.6361E-01
^{183}W	1.4232E-01	1.4235E-01
^{184}W	3.0640E-01	3.0480E-01
^{186}W	2.8739E-01	2.8281E-01
Density (g/cm^3)	19.25	

Table D.21. Steel 1018 Material Definition

Nuclide	Mass Fraction	Atom Fraction
^{0}C	2.0000E-03	9.2240E-03
^{31}P	4.0001E-04	7.1539E-04
^{32}S	4.7357E-04	8.2051E-04
^{33}S	3.8560E-06	6.4783E-06
^{34}S	2.2511E-05	3.6711E-05
^{36}S	5.6085E-08	8.6379E-08
^{55}Mn	9.0003E-03	9.0750E-03
^{54}Fe	5.5784E-02	5.7288E-02
^{56}Fe	9.0808E-01	8.9930E-01
^{57}Fe	2.1347E-02	2.0769E-02
^{58}Fe	2.8906E-03	2.7639E-03
Density (g/cm^3)	7.87	

Draft. Not approved for public release.
The only OFFICIAL COPY of this document is the on-line electronic version in ORNL's document management application.
Before using a printed copy, verify that it is the most current version.

Table D.22. Al ASTM B247-M-20 Material Definition

Nuclide	Mass Fraction	Atom Fraction
^{24}Mg	9.3540E-03	1.0623E-02
^{25}Mg	1.2336E-03	1.3449E-03
^{26}Mg	1.4124E-03	1.4807E-03
^{27}Al	9.6000E-01	9.6919E-01
^{28}Si	7.3493E-03	7.1557E-03
^{29}Si	3.8669E-04	3.6352E-04
^{30}Si	2.6399E-04	2.3991E-04
^{46}Ti	1.1880E-04	7.0422E-05
^{47}Ti	1.0947E-04	6.3511E-05
^{48}Ti	1.1077E-03	6.2930E-04
^{49}Ti	8.2983E-05	4.6181E-05
^{50}Ti	8.1073E-05	4.4217E-05
^{50}Cr	1.4608E-04	7.9670E-05
^{52}Cr	2.9295E-03	1.5364E-03
^{53}Cr	3.3858E-04	1.7421E-04
^{54}Cr	8.5868E-05	4.3365E-05
^{55}Mn	1.5000E-03	7.4374E-04
^{54}Fe	3.9519E-04	1.9957E-04
^{56}Fe	6.4331E-03	3.1329E-03
^{57}Fe	1.5123E-04	7.2354E-05
^{58}Fe	2.0478E-05	9.6286E-06
^{63}Cu	2.7392E-03	1.1857E-03
^{65}Cu	1.2608E-03	5.2896E-04
^{64}Zn	1.1794E-03	5.0254E-04
^{66}Zn	7.0491E-04	2.9126E-04
^{67}Zn	1.0493E-04	4.2707E-05
^{68}Zn	4.9390E-04	1.9807E-04
^{70}Zn	1.6864E-05	6.5695E-06

Draft. Not approved for public release.
The only OFFICIAL COPY of this document is the on-line electronic version in ORNL's document management application.
Before using a printed copy, verify that it is the most current version.

Table D.22 – continued from previous page

Nuclide	Mass Fraction	Atom Fraction
Density (g/cm^3)	2.7	

Table D.23. Graphite Material Definition

Nuclide	Mass Fraction	Atom Fraction
^{10}B	1.8431E-07	2.2109E-07
^{11}B	8.1569E-07	8.8991E-07
^{0}C	1.0000E+00	1.0000E+00
Density (g/cm^3)	1.7	

Table D.24. Copper Chromium Zirconium Material Definition

Nuclide	Mass Fraction	Atom Fraction
^{28}Si	9.1867E-04	2.0801E-03
^{29}Si	4.8336E-05	1.0567E-04
^{30}Si	3.2999E-05	6.9741E-05
^{50}Cr	5.0084E-04	6.3523E-04
^{52}Cr	1.0044E-02	1.2250E-02
^{53}Cr	1.1608E-03	1.3890E-03
^{54}Cr	2.9440E-04	3.4576E-04
^{54}Fe	4.5164E-05	5.3042E-05
^{56}Fe	7.3521E-04	8.3265E-04
^{57}Fe	1.7283E-05	1.9229E-05
^{58}Fe	2.3404E-06	2.5591E-06
^{63}Cu	6.7329E-01	6.7776E-01
^{65}Cu	3.0991E-01	3.0237E-01
^{90}Zr	1.5212E-03	1.0718E-03

Draft. Not approved for public release.
The only OFFICIAL COPY of this document is the on-line electronic version in ORNL's document management application.
Before using a printed copy, verify that it is the most current version.

Table D.24 – continued from previous page

Nuclide	Mass Fraction	Atom Fraction
^{91}Zr	3.3543E-04	2.3374E-04
^{92}Zr	5.1834E-04	3.5728E-04
^{94}Zr	5.3673E-04	3.6207E-04
^{96}Zr	8.8314E-05	5.8332E-05
Density (g/cm^3)	8.89	

Table D.25. PPE Type Oil Material Definition

Nuclide	Mass Fraction	Atom Fraction
^{1}H	6.7097E-02	4.7053E-01
^{2}H	1.5422E-05	5.4118E-05
^{0}C	7.9974E-01	4.7059E-01
^{16}O	1.3280E-01	5.8681E-02
^{17}O	3.4380E-04	1.4294E-04
Density (g/cm^3)	1.166	

Table D.26. EPDM Material Definition

Nuclide	Mass Fraction	Atom Fraction
^{1}H	1.4111E-01	6.6190E-01
^{2}H	3.2435E-05	7.6127E-05
^{0}C	8.5886E-01	3.3803E-01
Density (g/cm^3)	0.9	

Table D.27. Steel 1040 ASTM A830 Material Definition

Nuclide	Mass Fraction	Atom Fraction
^{0}C	4.4000E-03	2.0123E-02
^{31}P	3.0001E-04	5.3206E-04
^{32}S	2.8415E-04	4.8819E-04
^{33}S	2.3136E-06	3.8545E-06
^{34}S	1.3507E-05	2.1843E-05
^{36}S	3.3651E-08	5.1394E-08
^{55}Mn	9.0003E-03	8.9991E-03
^{54}Fe	5.5665E-02	5.6688E-02
^{56}Fe	9.0565E-01	8.8939E-01
^{57}Fe	2.1301E-02	2.0551E-02
^{58}Fe	2.8845E-03	2.7350E-03
^{59}Co	5.0000E-04	4.6604E-04
Density (g/cm^3)	7.85	

Table D.28. Steel 4130 ASTM A829 Material Definition

Nuclide	Mass Fraction	Atom Fraction
^{0}C	3.3000E-03	1.5104E-02
^{28}Si	3.2154E-03	6.3180E-03
^{29}Si	1.6918E-04	3.2096E-04
^{30}Si	1.1550E-04	2.1183E-04
^{31}P	3.0001E-04	5.3246E-04
^{32}S	3.7886E-04	6.5140E-04
^{33}S	3.0848E-06	5.1432E-06
^{34}S	1.8009E-05	2.9145E-05
^{36}S	4.4868E-08	6.8576E-08
^{50}Cr	4.5912E-04	5.0532E-04

Draft. Not approved for public release.
The only OFFICIAL COPY of this document is the on-line electronic version in ORNL's document management application.
Before using a printed copy, verify that it is the most current version.

Table D.28 – continued from previous page

Nuclide	Mass Fraction	Atom Fraction
^{52}Cr	9.2073E-03	9.7446E-03
^{53}Cr	1.0641E-03	1.1050E-03
^{54}Cr	2.6988E-04	2.7505E-04
^{55}Mn	6.0002E-03	6.0039E-03
^{54}Fe	5.4931E-02	5.5983E-02
^{56}Fe	8.9370E-01	8.7832E-01
^{57}Fe	2.1020E-02	2.0296E-02
^{58}Fe	2.8464E-03	2.7010E-03
^{92}Mo	3.5374E-04	2.1158E-04
^{94}Mo	2.2586E-04	1.3222E-04
^{95}Mo	3.9323E-04	2.2777E-04
^{96}Mo	4.1686E-04	2.3894E-04
^{97}Mo	2.4141E-04	1.3695E-04
^{98}Mo	6.1716E-04	3.4652E-04
^{100}Mo	2.5175E-04	1.3852E-04
^{59}Co	5.0000E-04	4.6639E-04
Density (g/cm^3)	7.85	

Table D.29. Steel 4340 ASTM A829 Material Definition

Nuclide	Mass Fraction	Atom Fraction
^{0}C	4.3000E-03	1.9635E-02
^{28}Si	3.2154E-03	6.3034E-03
^{29}Si	1.6918E-04	3.2022E-04
^{30}Si	1.1550E-04	2.1134E-04
^{31}P	3.0001E-04	5.3122E-04
^{32}S	3.7886E-04	6.4990E-04
^{33}S	3.0848E-06	5.1313E-06

Draft. Not approved for public release.
The only OFFICIAL COPY of this document is the on-line electronic version in ORNL's document management application.
Before using a printed copy, verify that it is the most current version.

Table D.29 – continued from previous page

Nuclide	Mass Fraction	Atom Fraction
^{34}S	1.8009E-05	2.9078E-05
^{36}S	4.4868E-08	6.8418E-08
^{50}Cr	3.7565E-04	4.1249E-04
^{52}Cr	7.5332E-03	7.9545E-03
^{53}Cr	8.7065E-04	9.0197E-04
^{54}Cr	2.2081E-04	2.2452E-04
^{55}Mn	8.0003E-03	7.9867E-03
^{54}Fe	5.3661E-02	5.4562E-02
^{56}Fe	8.7402E-01	8.5699E-01
^{57}Fe	2.0534E-02	1.9780E-02
^{58}Fe	2.7806E-03	2.6324E-03
^{59}Co	5.0003E-04	4.6534E-04
^{58}Ni	1.3440E-02	1.2723E-02
^{60}Ni	5.3554E-03	4.9009E-03
^{61}Ni	2.3668E-04	2.1304E-04
^{62}Ni	7.6699E-04	6.7926E-04
^{64}Ni	2.0164E-04	1.7299E-04
^{92}Mo	4.2449E-04	2.5331E-04
^{94}Mo	2.7103E-04	1.5830E-04
^{95}Mo	4.7187E-04	2.7269E-04
^{96}Mo	5.0023E-04	2.8607E-04
^{97}Mo	2.8970E-04	1.6396E-04
^{98}Mo	7.4059E-04	4.1487E-04
^{100}Mo	3.0211E-04	1.6584E-04
Density (g/cm^3)	7.85	

Draft. Not approved for public release.
The only OFFICIAL COPY of this document is the on-line electronic version in ORNL's document management application.
Before using a printed copy, verify that it is the most current version.

Table D.30. Steel 8620 ASTM A829 Material Definition

Nuclide	Mass Fraction	Atom Fraction
^{0}C	2.3000E-03	1.0572E-02
^{28}Si	3.2154E-03	6.3449E-03
^{29}Si	1.6918E-04	3.2233E-04
^{30}Si	1.1550E-04	2.1273E-04
^{31}P	3.0001E-04	5.3473E-04
^{32}S	3.7886E-04	6.5418E-04
^{33}S	3.0848E-06	5.1651E-06
^{34}S	1.8009E-05	2.9269E-05
^{36}S	4.4868E-08	6.8868E-08
^{50}Cr	2.5043E-04	2.7680E-04
^{52}Cr	5.0221E-03	5.3379E-03
^{53}Cr	5.8044E-04	6.0527E-04
^{54}Cr	1.4721E-04	1.5067E-04
^{55}Mn	9.0003E-03	9.0442E-03
^{54}Fe	5.4649E-02	5.5932E-02
^{56}Fe	8.9011E-01	8.7851E-01
^{57}Fe	2.0912E-02	2.0277E-02
^{58}Fe	2.8318E-03	2.6985E-03
^{59}Co	5.0003E-04	4.6841E-04
^{58}Ni	4.7040E-03	4.4824E-03
^{60}Ni	1.8744E-03	1.7266E-03
^{61}Ni	8.2838E-05	7.5055E-05
^{62}Ni	2.6845E-04	2.3931E-04
^{64}Ni	7.0573E-05	6.0945E-05
^{92}Mo	3.5374E-04	2.1248E-04
^{94}Mo	2.2586E-04	1.3278E-04
^{95}Mo	3.9323E-04	2.2874E-04
^{96}Mo	4.1686E-04	2.3996E-04

Table D.30 – continued from previous page

Nuclide	Mass Fraction	Atom Fraction
^{97}Mo	2.4141E-04	1.3753E-04
^{98}Mo	6.1716E-04	3.4800E-04
^{100}Mo	2.5175E-04	1.3911E-04
Density (g/cm^3)	7.85	

Table D.31. Steel 9310 AMS 6265R Material Definition

Nuclide	Mass Fraction	Atom Fraction
^{10}B	1.8432E-06	1.0210E-05
^{11}B	8.1572E-06	4.1096E-05
^{0}C	1.3000E-03	6.0032E-03
^{28}Si	3.2154E-03	6.3747E-03
^{29}Si	1.6918E-04	3.2384E-04
^{30}Si	1.1550E-04	2.1373E-04
^{31}P	1.5001E-04	2.6862E-04
^{32}S	1.4207E-04	2.4647E-04
^{33}S	1.1568E-06	1.9460E-06
^{34}S	6.7533E-06	1.1027E-05
^{36}S	1.6825E-08	2.5946E-08
^{50}Cr	5.8434E-04	6.4890E-04
^{52}Cr	1.1718E-02	1.2514E-02
^{53}Cr	1.3544E-03	1.4189E-03
^{54}Cr	3.4348E-04	3.5320E-04
^{55}Mn	7.0002E-03	7.0674E-03
^{54}Fe	5.2667E-02	5.4156E-02
^{56}Fe	8.5784E-01	8.5063E-01
^{57}Fe	2.0154E-02	1.9633E-02
^{58}Fe	2.7291E-03	2.6128E-03

Table D.31 – continued from previous page

Nuclide	Mass Fraction	Atom Fraction
^{59}Co	5.0003E-04	4.7061E-04
^{58}Ni	2.3520E-02	2.2517E-02
^{60}Ni	9.3719E-03	8.6735E-03
^{61}Ni	4.1419E-04	3.7703E-04
^{62}Ni	1.3422E-03	1.2021E-03
^{64}Ni	3.5286E-04	3.0615E-04
^{63}Cu	2.3968E-03	2.1125E-03
^{65}Cu	1.1033E-03	9.4247E-04
^{92}Mo	2.1224E-04	1.2809E-04
^{94}Mo	1.3552E-04	8.0044E-05
^{95}Mo	2.3594E-04	1.3789E-04
^{96}Mo	2.5012E-04	1.4465E-04
^{97}Mo	1.4485E-04	8.2905E-05
^{98}Mo	3.7029E-04	2.0978E-04
^{100}Mo	1.5105E-04	8.3859E-05
Density (g/cm^3)	7.85	

Table D.32. Silicon Carbide Material Definition

Nuclide	Mass Fraction	Atom Fraction
^{0}C	2.9955E-01	4.9999E-01
^{28}Si	6.4348E-01	4.6112E-01
^{29}Si	3.3857E-02	2.3425E-02
^{30}Si	2.3114E-02	1.5460E-02
Density (g/cm^3)	3.21	

Draft. Not approved for public release.
The only OFFICIAL COPY of this document is the on-line electronic version in ORNL's document management application.
Before using a printed copy, verify that it is the most current version.

Table D.33. Corning 7980 fused silica Material Definition

Nuclide	Mass Fraction	Atom Fraction
^{16}O	5.3112E-01	6.6499E-01
^{17}O	1.4432E-03	1.7003E-03
^{28}Si	4.2942E-01	3.0739E-01
^{29}Si	2.2594E-02	1.5615E-02
^{30}Si	1.5425E-02	1.0306E-02
Density (g/cm^3)	2.2	

Table D.34. Invar 20K Material Definition

Nuclide	Mass Fraction	Atom Fraction
^{0}C	1.4827E-03	6.9470E-03
^{28}Si	3.6748E-03	7.3922E-03
^{29}Si	1.9335E-04	3.7553E-04
^{30}Si	1.3200E-04	2.4784E-04
^{31}P	2.5001E-04	4.5426E-04
^{32}S	2.3679E-04	4.1680E-04
^{33}S	1.9280E-06	3.2909E-06
^{34}S	1.1255E-05	1.8648E-05
^{36}S	2.8043E-08	4.3879E-08
^{50}Cr	1.0435E-04	1.1758E-04
^{52}Cr	2.0926E-03	2.2673E-03
^{53}Cr	2.4185E-04	2.5710E-04
^{54}Cr	6.1337E-05	6.3997E-05
^{55}Mn	6.0002E-03	6.1466E-03
^{54}Fe	3.5031E-02	3.6550E-02
^{56}Fe	5.7025E-01	5.7375E-01
^{57}Fe	1.3405E-02	1.3251E-02

Draft. Not approved for public release.
The only OFFICIAL COPY of this document is the on-line electronic version in ORNL's document management application.
Before using a printed copy, verify that it is the most current version.

Table D.34 – continued from previous page

Nuclide	Mass Fraction	Atom Fraction
^{58}Fe	1.8153E-03	1.7634E-03
^{59}Co	5.0002E-03	4.7749E-03
^{58}Ni	2.4192E-01	2.3500E-01
^{60}Ni	9.6397E-02	9.0522E-02
^{61}Ni	4.2603E-03	3.9349E-03
^{62}Ni	1.3806E-02	1.2546E-02
^{64}Ni	3.6295E-03	3.1952E-03
Density (g/cm^3)	8.051	

Table D.35. Al-6061 20K Material Definition

Nuclide	Mass Fraction	Atom Fraction
^{24}Mg	9.3540E-03	1.0623E-02
^{25}Mg	1.2336E-03	1.3449E-03
^{26}Mg	1.4124E-03	1.4807E-03
^{27}Al	9.6000E-01	9.6919E-01
^{28}Si	7.3493E-03	7.1557E-03
^{29}Si	3.8669E-04	3.6352E-04
^{30}Si	2.6399E-04	2.3991E-04
^{46}Ti	1.1880E-04	7.0422E-05
^{47}Ti	1.0947E-04	6.3511E-05
^{48}Ti	1.1077E-03	6.2930E-04
^{49}Ti	8.2983E-05	4.6181E-05
^{50}Ti	8.1073E-05	4.4217E-05
^{50}Cr	1.4608E-04	7.9670E-05
^{52}Cr	2.9295E-03	1.5364E-03
^{53}Cr	3.3858E-04	1.7421E-04
^{54}Cr	8.5868E-05	4.3365E-05

Table D.35 – continued from previous page

Nuclide	Mass Fraction	Atom Fraction
^{55}Mn	1.5000E-03	7.4374E-04
^{54}Fe	3.9519E-04	1.9957E-04
^{56}Fe	6.4331E-03	3.1329E-03
^{57}Fe	1.5123E-04	7.2354E-05
^{58}Fe	2.0478E-05	9.6286E-06
^{63}Cu	2.7392E-03	1.1857E-03
^{65}Cu	1.2608E-03	5.2896E-04
^{64}Zn	1.1794E-03	5.0254E-04
^{66}Zn	7.0491E-04	2.9126E-04
^{67}Zn	1.0493E-04	4.2707E-05
^{68}Zn	4.9390E-04	1.9807E-04
^{70}Zn	1.6864E-05	6.5695E-06
Density (g/cm^3)	2.7	

Table D.36. SS-416 Material Definition

Nuclide	Mass Fraction	Atom Fraction
^{0}C	1.5000E-03	6.7882E-03
^{28}Si	9.1869E-03	1.7849E-02
^{29}Si	4.8338E-04	9.0673E-04
^{30}Si	3.3000E-04	5.9842E-04
^{31}P	6.0002E-04	1.0529E-03
^{32}S	1.4207E-03	2.4153E-03
^{33}S	1.1568E-05	1.9070E-05
^{34}S	6.7533E-05	1.0807E-04
^{36}S	1.6825E-07	2.5427E-07
^{50}Cr	5.8433E-03	6.3591E-03
^{52}Cr	1.1718E-01	1.2263E-01

Draft. Not approved for public release.
The only OFFICIAL COPY of this document is the on-line electronic version in ORNL's document management application.
Before using a printed copy, verify that it is the most current version.

Table D.36 – continued from previous page

Nuclide	Mass Fraction	Atom Fraction
^{53}Cr	1.3543E-02	1.3905E-02
^{54}Cr	3.4348E-03	3.4613E-03
^{55}Mn	1.2500E-02	1.2368E-02
^{54}Fe	4.6965E-02	4.7327E-02
^{56}Fe	7.6452E-01	7.4293E-01
^{57}Fe	1.7972E-02	1.7157E-02
^{58}Fe	2.4337E-03	2.2833E-03
^{59}Co	2.0001E-03	1.8447E-03
Density (g/cm^3)	7.7	

Table D.37. N2 Material Definition

Nuclide	Mass Fraction	Atom Fraction
^{14}N	9.9610E-01	9.9636E-01
^{15}N	3.8982E-03	3.6400E-03
Density (g/cm^3)	0.0035418	

Table D.38. NdFeB Magnets (with Ni coating) Material Definition

Nuclide	Mass Fraction	Atom Fraction
^{10}B	1.1432E-03	7.4866E-03
^{11}B	5.0595E-03	3.0135E-02
^{27}Al	3.6796E-03	8.9423E-03
^{54}Fe	3.7404E-02	4.5470E-02
^{56}Fe	6.0888E-01	7.1378E-01
^{57}Fe	1.4313E-02	1.6484E-02
^{58}Fe	1.9382E-03	2.1938E-03

Draft. Not approved for public release.
The only OFFICIAL COPY of this document is the on-line electronic version in ORNL's document management application.
Before using a printed copy, verify that it is the most current version.

Table D.38 – continued from previous page

Nuclide	Mass Fraction	Atom Fraction
^{59}Co	1.6821E-02	1.8716E-02
^{58}Ni	1.5471E-02	1.7511E-02
^{60}Ni	6.1648E-03	6.7451E-03
^{61}Ni	2.7245E-04	2.9320E-04
^{62}Ni	8.8291E-04	9.3486E-04
^{64}Ni	2.3211E-04	2.3808E-04
^{63}Cu	7.9192E-04	8.2517E-04
^{65}Cu	3.6452E-04	3.6814E-04
^{64}Zn	9.9193E-05	1.0174E-04
^{66}Zn	5.9286E-05	5.8967E-05
^{67}Zn	8.8251E-06	8.6464E-06
^{68}Zn	4.1539E-05	4.0100E-05
^{70}Zn	1.4184E-06	1.3301E-06
^{112}Sn	9.6130E-07	5.6329E-07
^{114}Sn	6.6576E-07	3.8327E-07
^{115}Sn	3.4598E-07	1.9744E-07
^{116}Sn	1.4924E-05	8.4435E-06
^{117}Sn	7.9511E-06	4.4599E-06
^{118}Sn	2.5289E-05	1.4065E-05
^{119}Sn	9.0454E-06	4.9883E-06
^{120}Sn	3.4595E-05	1.8920E-05
^{122}Sn	4.9985E-06	2.6887E-06
^{124}Sn	6.3534E-06	3.3623E-06
^{141}Pr	2.8280E-02	1.3160E-02
^{142}Nd	6.4511E-02	2.9809E-02
^{143}Nd	2.9139E-02	1.3370E-02
^{144}Nd	5.7244E-02	2.6083E-02
^{145}Nd	2.0102E-02	9.0961E-03
^{146}Nd	4.1945E-02	1.8850E-02
^{148}Nd	1.4091E-02	6.2467E-03

Draft. Not approved for public release.
The only OFFICIAL COPY of this document is the on-line electronic version in ORNL's document management application.
Before using a printed copy, verify that it is the most current version.

Table D.38 – continued from previous page

Nuclide	Mass Fraction	Atom Fraction
^{150}Nd	1.4032E-02	6.1371E-03
^{152}Gd	2.0313E-06	8.7676E-07
^{154}Gd	2.2433E-05	9.5567E-06
^{155}Gd	1.5329E-04	6.4880E-05
^{156}Gd	2.1338E-04	8.9736E-05
^{157}Gd	1.6419E-04	6.8606E-05
^{158}Gd	2.6226E-04	1.0889E-04
^{160}Gd	2.3372E-04	9.5830E-05
^{159}Tb	1.2616E-03	5.2052E-04
^{156}Dy	7.8522E-06	3.3022E-06
^{158}Dy	1.3492E-05	5.6019E-06
^{160}Dy	3.3495E-04	1.3733E-04
^{161}Dy	2.7336E-03	1.1138E-03
^{162}Dy	3.7096E-03	1.5022E-03
^{163}Dy	3.6477E-03	1.4681E-03
^{164}Dy	4.1660E-03	1.6664E-03
Density (g/cm^3)	7.5	

Draft. Not approved for public release.
The only OFFICIAL COPY of this document is the on-line electronic version in ORNL's document management application.
Before using a printed copy, verify that it is the most current version.

APPENDIX E. DOSE CONVERSION FACTORS

APPENDIX E. DOSE CONVERSION FACTORS

Table E.1. Photon flux to dose conversion factors [15]

Energy (MeV)	**DCF (mrem hr^{-1} (γ/cm^2/sec)$^{-1}$)**
1.0000E-02	1.7466E-05
1.5000E-02	4.5153E-05
2.0000E-02	7.3786E-05
3.0000E-02	1.0798E-04
4.0000E-02	1.2170E-04
5.0000E-02	1.2861E-04
6.0000E-02	1.3608E-04
8.0000E-02	1.5838E-04
1.0000E-01	1.8618E-04
1.5000E-01	2.7084E-04
2.0000E-01	3.6147E-04
3.0000E-01	5.4300E-04
4.0000E-01	7.1850E-04
5.0000E-01	8.8764E-04
6.0000E-01	1.0469E-03
8.0000E-01	1.3417E-03
1.0000E+00	1.6140E-03
1.5000E+00	2.2104E-03
2.0000E+00	2.6963E-03
3.0000E+00	3.5587E-03
4.0000E+00	4.3255E-03
5.0000E+00	5.0405E-03
6.0000E+00	5.7554E-03
8.0000E+00	7.1709E-03
1.0000E+01	8.5536E-03
1.5000E+01	1.0080E-02
2.0000E+01	1.1880E-02

Draft. Not approved for public release.
The only OFFICIAL COPY of this document is the on-line electronic version in ORNL's document management application.
Before using a printed copy, verify that it is the most current version.

Table E.1 – continued from previous page

Energy (MeV)	**DCF (mrem hr^{-1} (γ/cm^2/sec)$^{-1}$)**
3.0000E+01	1.4760E-02
4.0000E+01	1.6920E-02
5.0000E+01	1.8720E-02
1.0000E+02	2.3760E-02
2.0000E+02	2.7720E-02
5.0000E+02	3.1680E-02
1.0000E+03	3.3480E-02
2.0000E+03	3.4560E-02
5.0000E+03	3.5640E-02
1.0000E+04	3.6360E-02

APPENDIX F. MONTE CARLO DOSE RATE UNCERTAINTY FIGURES

APPENDIX F. MONTE CARLO DOSE RATE UNCERTAINTY FIGURES

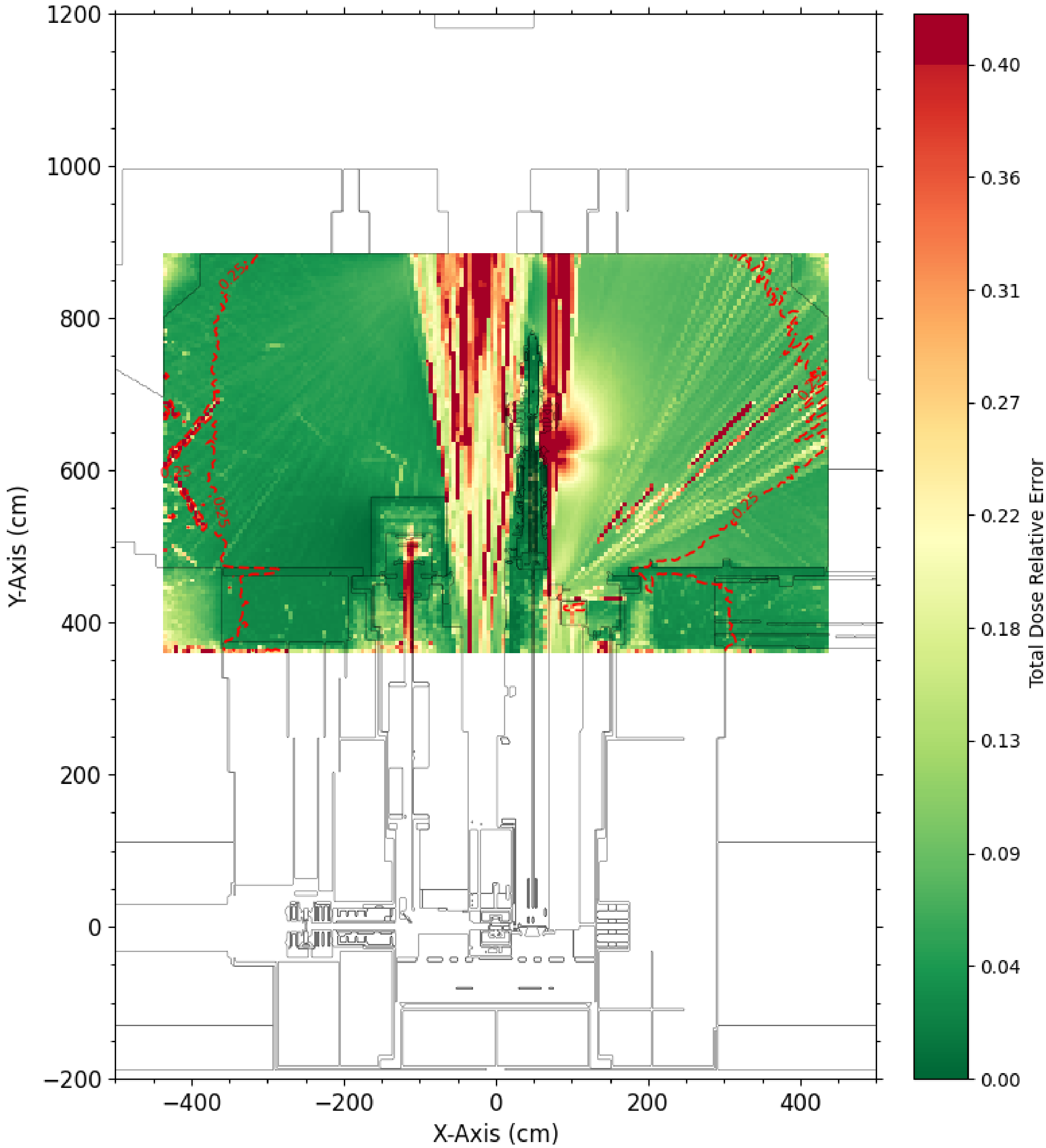

Figure F.1. Cross section view along the proton beam of the photon effective dose rate relative errors from the Monte Carlo solution after 2 weeks of decay in the target drive room and STS target system for the MRA pipe cutting configuration.

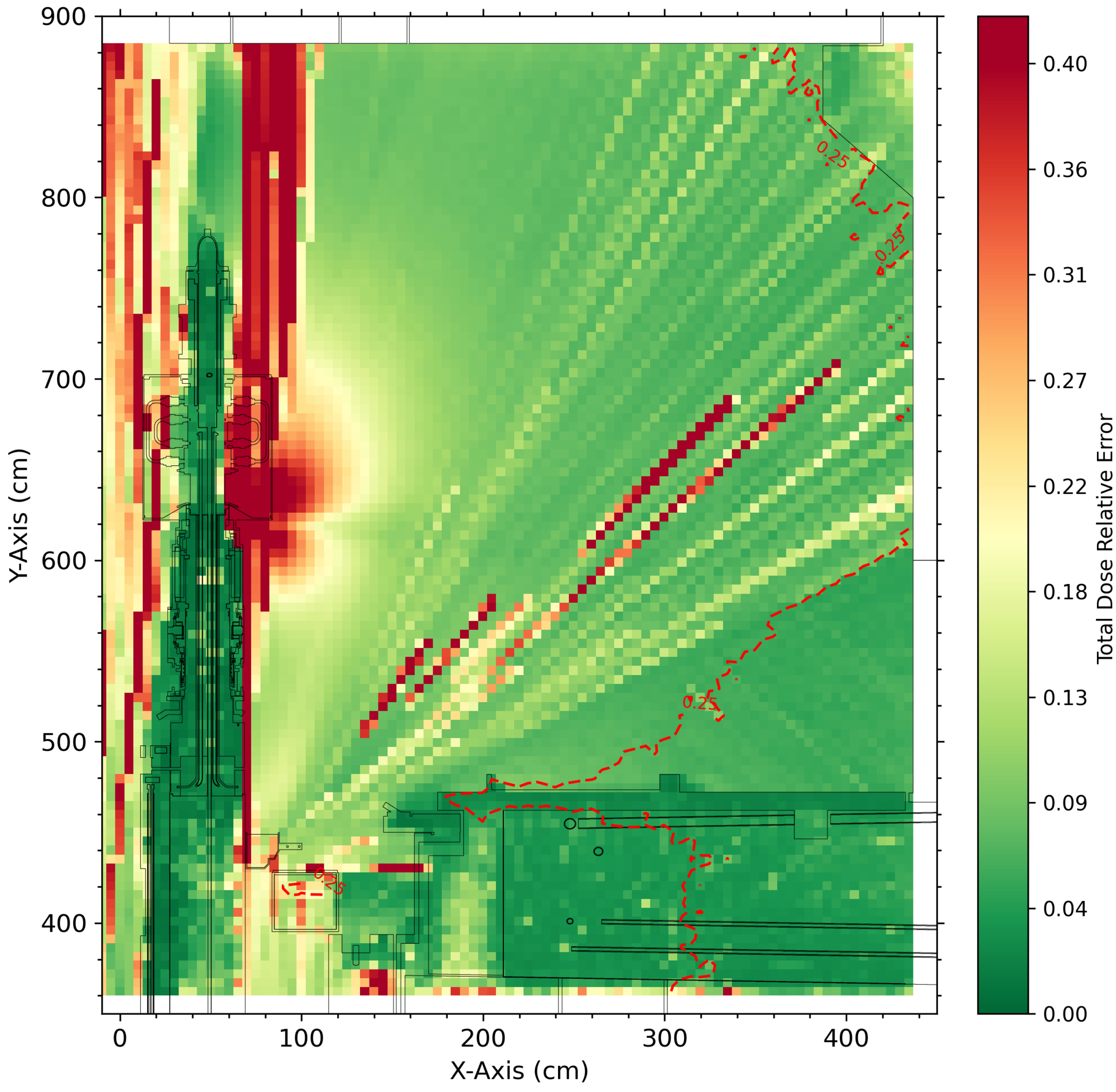

Figure F.2. Cross section view along the proton beam of the photon effective dose rate relative error from the Monte Carlo solution after 2 weeks of decay in the target drive room and STS target system for the MRA pipe cutting configuration zoomed in on the region downstream of the target.

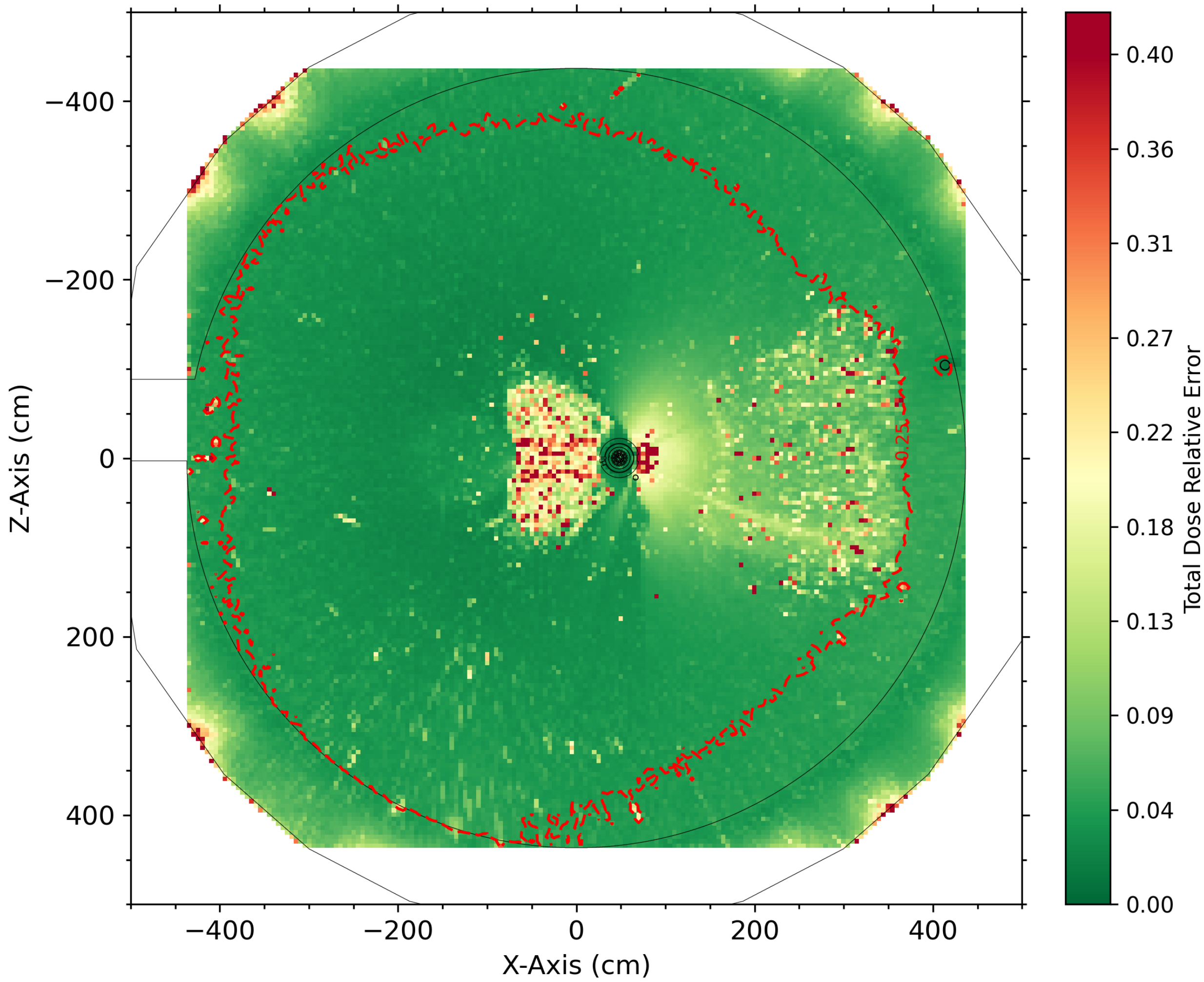

Figure F.3. Plan view at an elevation of 1 m above the TDR floor of the photon effective dose rate relative errors from the Monte Carlo solution after 2 weeks of decay in the target drive room and STS target system for the MRA pipe cutting configuration.